AN ABSTRACT OF THE DISSERTATION OF

Maria T Kavanaugh for the degree of Doctor of Philosophy in Oceanography presented on September 12, 2012.

Title: Dynamic Seascapes: A Quantitative Framework for Scaling Pelagic Ecology and Biogeochemistry

Abstract approved: _____

Ricardo M Letelier

Understanding and modeling microbial responses and feedbacks to climate change is hampered by a lack of a framework in the pelagic environment by which to link local mechanism to large scale patterns. Where terrestrial ecology draws from landscape theory and practice to address issues of scale, the pelagic seascape concept is still in its infancy. We have applied the patch mosaic paradigm of landscape ecology to the study of the seasonal and interannual variability of the North Pacific to facilitate comparative analysis between pelagic ecosystems and provide spatiotemporal context for eulerian time-series studies. Using multivariate, 13-year climatologies of sea surface temperature, photosynthetically active radiation, and chlorophyll a derived from remote sensing observations, we classified hierarchical seascapes at monthly and interannual scales. These dynamic, objectively-determined seascapes offer improved hydrographic coherence relative to oceanic regions with subjectively defined and static boundaries (Chapter 2) and represent unique biogeochemical functioning (Chapter 2) and microbial communities (Chapter3). Furthermore they provide consilience between satellite studies and *in situ* observations (Chapter 4) and allow for objective comparison of ecosystem forcing (Chapters, 4 and 5).

In Chapter 2, we rigorously tested the assumption that satellite-derived seascapes describe regions of biogeochemical coherence. The seasonal cycle of the North Pacific was characterized at three levels of spatiotemporal hierarchy and broader relevance of monthly – resolved seascapes was assessed through analysis of variance (ANOVA) and multiple linear regression (MLR) analyses of nutrient, primary productivity, and pCO_2 data. Distinct nutrient and primary productivity regimes were well-characterized in the coarsest two levels of hierarchy (ANOVA, $R^2 = 0.5\text{-}0.7$). Finer scale partitioning was more relevant for pCO_2. MLR analyses revealed differential forcing on pCO_2 across seascapes and hierarchical levels and a 33 % reduction in mean model error with increased partitioning (from 18.5 µatm to 12.0 µatm pCO_2).

In Chapter 3 we verified the seascapes with *in situ* collections of microbial abundance and structure. Flow cytometry data was collected from two long term time series and several cruises spanning thousand kilometers of the NE Pacific; these data allowed us to quantify spatiotemporal patterns. In addition, multiple response permutation analysis revealed differences in community structure across discrete seascapes, in terms of both absolute and relative abundances. Principal component analysis of the assemblage supported seascape divisions and revealed structure along environmental gradients with strong associations with chlorophyll a and sea surface temperature and, to a lesser extent, with mixed layer depth and mean photosynthetically active radiation in the mixed layer. Differences of assemblage structure between seascapes and strength of environmental forcing were strong in the subarctic and transition zones, but less pronounced in the subtropics, suggesting satellite-detected changes in bulk properties that may be associated with local physiology or interannual shifts in seascape boundaries.

Base on the work presented in Chapter 4, we discovered that interannual shifts in the boundaries of a transition seascape and two distinct oligotrophic subtropical seascapes affect the

variability observed at benchmark time series Station ALOHA; the latter two seascapes oscillate in their contributions to the expansion of the entire subtropics. On interannual scales, *in situ* phytoplankton abundance (as measured by chl-a), net primary productivity (NPP), and the relative abundance of eukaryotic phytoplankton and *Synechococcus* sp. increased during periods of encroachment by the transition seascape. Conversely, the relative abundance of *Prochlorococcus* increased and chl –a and NPP decreased when the highly oligotrophic seascape encroached on Station ALOHA. The dynamic range (~6 million km^2) of subtropical expansion is born almost entirely by the transition zone - resulting in a transfer of ~1.2 Pg of total primary C production between a system primed for export production and one dominated by the microbial loop.

In Chapter 5, we investigated multiple factors that contribute to the effectiveness of the biological pump in the transition seascape. Near-continuous measurements of net primary production (NPP), net community production (NCP) and several ecophysiological variables were collected in across subarctic, transition, and subtropical seascapes of the Northeast Pacific during August and September of 2008. Mesoscale processes and shifts in community structure contributed to high export efficiency in the subtropical seascape; the convergence of assemblage structure, high biomass, moderate NPP: NCP and high NCP contributed to biologically mediated air-sea exchange in the transition seascape. Furthermore, NPP and NCP were strongly spatially coupled in both the transition ($r_{1, 39}$ =0.70; $p<0.0001$) and subtropical seascapes ($r_{1, 45}$= 0.68, $p<0.0001$), suggesting the possibility for empirical modeling efforts.

This dissertation provides a first step to characterize the seascape variability in the NE Pacific and to understand the modulation of primary and export production in a critical transition region. The multivariate seascape approach described here provides spatiotemporal context for *in situ* studies and allows objective comparisons of systems' responses to climatic forcing. An

integrated ocean observing system will require insight from *in situ* observations and experiments, ecosystem models, and satellite remote sensing. The results highlighted in this dissertation suggest that the pelagic seascape framework, through its capacity to scale both context and mechanism, may serve as an important and unifying component of such an observing system.

Dynamic Seascapes:
A Quantitative Framework for Scaling Pelagic Ecology and Biogeochemistry

by
Maria T. Kavanaugh

A DISSERTATION

submitted to

Oregon State University

in partial fulfillment of
the requirements for the
degree of

Doctor of Philosophy

Presented September 12, 2012
Commencement June 2013

Doctor of Philosophy dissertation of Maria T. Kavanaugh presented on September 12, 2012.

APPROVED:

_____

Major Professor, representing Oceanography

_____

Dean of the College of Earth Ocean and Atmospheric Sciences

_____

Dean of the Graduate School

I understand that my dissertation will become part of the permanent collection of Oregon State University libraries. My signature below authorizes release of my dissertation to any reader upon request.

_____

Maria T. Kavanaugh, Author

ACKNOWLEDGEMENTS

Thanks to my advisor, Ricardo Letelier, for his enthusiasm, encouragement, and support for my dissertation research over the last 6 years. Ricardo also gave me an enormous amount of freedom in the last couple years of my dissertation, which made it possible for me to develop as an independent researcher. I look forward to all of our future collaborations, cruises, and adventures.

Thanks also to a great and supportive dissertation committee, including Curt Davis, Burke Hales, Yvette Spitz, Evelyn Sherr, Lisa Madsen, and Kerry McPhail. You all rolled up your proverbial sleeves to help me finish this behemoth of a dissertation. My only regret is that I didn't work more closely with some of you.

My time at Oregon State has been made enjoyable by having a great extended lab family over the course of the dissertation, including Sam Laney, Angel White, Marnie Jo Zirbel, Amanda Whitmire, Katy-Watkins Brandt, Morgaine McKibben, Amanda Ashe, Roberto Venegas, Jasmine Nahorniak, Curt Vandetta, Nick Tufallario, Joe Jennings and recently, Rosie Gradoville and Brian Burkhardt. Our group constantly facilitated study sessions, journal groups, and science lunches where ideas, newly hatched or more polished, were always encouraged. Importantly, there were also many capable hands and hearts for toddler wrangling- which was essential for this new mother to transition between diapers to scientific discourse.

From our group morphed a network of incredible women, sisters in science and play. We have witnessed marriages, births, illness and deaths. I have been in constant awe of Dr. Angel White and her wife, Jen de-Vries, Rinpoches both of them, precious teachers of how to live a rich and balanced life. The Zirbelliots, Whitmires, Watkins-Brandts and Nahorniaks continue to teach me about what it means to be a parent, person and a scientist.

These women served as my inspiration to help other women navigate the waters of academic science from which the ATPinBEESS project arose. I am incredibly grateful that I met Barb Lachenbruch, Lisa Ganio, Louisa Hooven and Sarah Close and got to work more closely with Kate Boersma. Particularly, I am grateful for the example of how diverse perspectives and modalities of thinking can result in an incredibly positive collaboration.

I thank my office mates through the years- Aaron Hartz, Wiley Evans, Amanda Kaltenberg , Brandon Briggs, and Amy Smith for the great conversations in the Bio-Oce ghetto that Weniger provided. Thank you especially to Brie Lindsey- her incredible capacity to explain complex biophysical interactions as well as her generous spirit is truly inspiring. Big thanks to all in the Prahl Lab, including Fred Prahl, Margaret Sparrow, Matt Wolhowe and Russ Desiderio, for providing lively conversation and laughter. Thanks also to Charlie Miller, Pat Wheeler, Hal Batchelder, George Waldbusser, Kelly Benoit-Bird and Rick Colwell for insight about science and life (big or small) . Finally, this degree would not have been possible without the assistance and encouragement of several COAS staff members, especially Robert Allan, Lori Hartline, and Mary Hitch who always had a way to frame troublesome things in a positive light.

I was fortunate to meet and maintain friendships with several people during my master's degree who continued to provide incredible support through my PhD process. Bruce Menge and the Lub-Menge lab were my "go-to-for-all-things-ecological" and gave a safe haven when I simply missed the sights and sounds of the shore. Spencer Wood and Sarah Thompson have been unceasing in their encouragement –reminding me often of why we wish to do what we do. Kate Boersma, Rocky Parker and Mike Bogan were incredible friends and never ceased in their support, even though we were rarely in the same town simultaneously. The Grorud-Colvert, McLeod, and Born families shared meals, many happy times, and much wisdom regarding balancing work and family.

Thanks to Deirdre Lockwood, Steve Emerson and Paul Quay of the University of Washington School of Oceanography for allowing me to be the token biologist (and Beaver) on a cruise full of Husky geochemists. Much gratitude is extended to Marie Robert and the staff scientists at the Canadian Institute for Ocean Sciences for all their patient training and friendship during adventures on the Line P cruises. The crew of the CCGS John P.Tully deserves special recognition for putting up with my engineering shenanigans, creative knots, and country of origin.

Enormous thanks goes to my family for always encouraging me to follow my curiosity. My parents and siblings have always been supportive of this endeavor and a lifetime of learning. My thoughtful and loving partner, Kale Haggard, has been a rock of stability over the past years as I have traveled around the world to meetings and cruises, struggled through proposal deadlines and dissertation writing, and transitioned into the challenging but incredibly rewarding life of parenting. Finally, I have so much gratitude for my son, Walden, who has made every day since his arrival nearly 3 years ago full of light, life and joy, providing a daily dose of much-welcomed perspective and purpose.

CONTRIBUTION OF AUTHORS

DR. RICARDO M. LETELIER gave valuable advice in the design, implementation, and editing of this dissertation, and provided financial support in the form of research assistantships during several terms between 2011 and 2012. Dr. Letelier is a co-author of Chapters 2, 3, 4 and 5.

BURKE HALES contributed to the intellectual development of Chapters 2, 4, and 5 and financial support during 2012. He is a co-author of Chapters 2, 4 and 5.

CURT DAVIS contributed to the intellectual development of Chapters 2 and 4 and provided a keen editorial eye to the entire dissertation. He is a co-author of Chapters 2 and 4.

ANGELIQUE WHITE, YVETTE SPITZ and MARTIN SARACENO contributed to editing and to the conceptualization of Chapters 2 and 4. They are co-authors on Chapters 2 and 4.The original code for PRSOM and HAC was provided by Dr. Saraceno.

DR. EVELYN SHERR helped conceptualize Chapter 3, provided lab space and analytical facilities, and contributed immensely to improving the writing on the entire dissertation. She is a co-author on Chapter 3.

DEIRDRE LOCKWOOD, STEVE EMERSON and PAUL QUAY provided cruise platforms and data contained within Chapter 5. They are co-authors on the resultant publication.

TABLE OF CONTENTS

TABLE OF CONTENTS (CONTINUED)

LIST OF FIGURES

LIST OF FIGURES (Continued)

LIST OF TABLES

LIST OF TABLES (Continued)

LIST OF TABLES (Continued)

DEDICATION

This dissertation is dedicated to my son Walden who brings immense joy and purpose to my life.

Dynamic Seascapes:
A Quantitative Framework for Scaling Pelagic Ecology and Biogeochemistry

CHAPTER 1: General Introduction

Progress in ecology and biogeochemistry is dependent on the combination of species-level information such as distribution and richness with regional and global information on primary productivity, nutrient cycles and climate (Turner et al., 2003). Investigators must therefore take a multi-scale, interdisciplinary approach to understanding systems responses and feedbacks to environmental variability, including climate change. In the marine realm, large-scale advective processes and diffuse boundaries create challenges in identifying distinct systems and subsystems; these distinctions allow us to compare study units and scale-up observations within them appropriately and objectively. To this aim, my dissertation embeds local ecological and biogeochemical observations and experiments with seascape analyses of system boundaries, structure, and function.

The necessity of a formal pelagic seascape concept

Marine ecosystems are arguably the largest on the planet and are responsible for approximately half of the global primary production (Field et al., 1998; Behrenfeld et al., 2001) and over 80% of the fish that humans consume (Pauly et al., 2005). Communities of plankton and nekton suspended in the surface ocean provide these ecological services. The microbial assemblages drive elemental cycles in the pelagic environment and contribute to the transfer of gases between the atmosphere and the deep ocean (Emerson et al., 1997; Monahan and Denman, 2004). Here we follow the convention of Sherr and

Sherr (2000) who define the term microbes to encompass all unicellular plankton including eukaryote and prokaryotes, autotrophic and heterotrophic cells, as well as viruses. Scenarios for climate change suggest that the oceans will experience shifts in sea surface temperature (Behrenfeld et al., 2006; Polovina et al., 2008, 2011) and carbon chemistry (Dore et al., 2009; Feely et al., 2008; Doney et al., 2009), which may have profound impacts on the structure and function of surface microbial communities (Liu et al., 2010).

The pelagic ocean is a complex system in which pattern and process interact to provide feedbacks on multiple scales of spatial, temporal, and biological organization (Lubchenco and Petes, 2010, Doney et al., 2012). Non-linearities are common in biogeochemical (e.g. Gruber, 2011; Hales et al., 2012), biophysical (e.g. Hsieh et al., 2005) and trophic (Litzow and Ciannelli, 2007, Brander et al., 2010) interactions. Spatial heterogeneity is ubiquitous and occurs at all scales observed (Steele, 1991; Levin and Whitfield, 1994; Mitchell et al., 2008). Unlike landscapes, which are relatively fixed in space, seascapes are embedded in a dynamic, advective ocean. Understanding and modeling pelagic ecosystem responses and feedbacks to environmental perturbation is therefore hampered by the lack of an objective framework to (1) scale microbial processes to ocean basins (2) define how temporal and spatial scaling of microbial habitats may change regionally, and (3) place the ‘snapshots’ of data collected in a typical oceanographic research expedition into a regional context. Terrestrial and coastal ecology draws from landscape ecology theory to address issues of spatiotemporal context, i.e. scale, sampling bias, and edge effects (Turner, 2005). Seascape ecology can

provide the spatial and temporal context necessary to link oceanographic observations and models to climate change studies.

Landscapes are loosely defined as self-organized systems shaped by the local topography (Wiens 1976; Turner et al., 2001; Turner, 2005) and are conceptualized and analyzed as mosaics of discrete patches (Forman 1995; Turner et al., 2001). Models describe the varying composition and shapes of different adjacent habitats (Forman and Godron, 1981) as well as the composite dynamics of individual patches and their interactions at adjacent hierarchical levels (Wu and Loucks, 1995). The landscape concept has informed our understanding of the controls on biodiversity and system responses to climate change or change in land-use strategies, and the application of ecosystem management practices among other far-reaching topics (Turner et al., 2005). Just as terrestrial ecosystems are parsed into landscapes, the global ocean can be viewed as a mosaic of distinct ecosystems, or *seascapes*, composed of unique combinations of physical, biological and chemical elements.

Seascape ecology, like its terrestrial counterpart, seeks to define the relationships between variable ecosystem pattern and function (Karl and Letelier, 2009). Like landscapes, the grain (smallest unit of resolution) and domain (spatiotemporal extent) of seascapes are dependent on the pattern and process of interest. From a biogeochemical perspective, the seascape concept can be evoked to describe patterns and processes that range in scale from microbial interactions on sinking particles to functioning of entire oceanic basins (Karl and Letelier, 2009). In this context, a useful seascape framework is one in which the biology, physical forcing, and spatiotemporal patterns co-vary in a mechanistic and quantifiably distinct fashion at multiple scales.

For landscape ecologists, hierarchy theory has provided a means to scale up from the grain and down from the domain (Wu and Loucks, 1995; Wu 1999). Hierarchy in mathematical terms is a partially ordered set, a collection of parts with ordered relationships inside a whole (Simon, 1973). Hierarchical levels are populated by entities whose properties characterize the level in question. Investigators of complex systems often think of hierarchies when they embed regional models within global scale models (Schneider and Dickinson, 1974; Ghil and Robertson, 2000) or conduct nested surveys of species abundances and richness (Schoch et al, 2006) in order to identify whether organismal to global scale patterns are coherent and what may drive this coherence. The focus of hierarchies within landscape ecology has historically been one of aggregates within different spatial scales (Wiens, 1989, O'Neill, 1992; Wu 2002; but see Gillson, 2009). However, because of the added role of advection, the intrinsic scaling hierarchy for seascape ecology is one of nested spatial and temporal scales and thus requires synoptic time series for both classification and evaluation of would be seascapes.

A quantitative seascape framework can link regional oceanography to both global patterns and local mechanisms. Synoptic time series such as those derived from satellite algorithms of chlorophyll a (chl-a; Gregg et al., 2005) or net primary production (NPP) (Behrenfeld et al., 2006) and coupled ocean-atmosphere models (Boyd and Doney, 2002; Sarmiento et al., 2004) reveal strong regional differences in responses of pelagic ecosystems to climate change. These differences suggest that some regions of the world's oceans are more sensitive to perturbation than other areas. However, at least for oligotrophic gyres, the interannual patterns observed from space (Behrenfeld et al., 2006; Polovina et al., 2008) do not appear to match with those derived from *in situ* observations

(Corno et al., 2007; Lomas et al., 2011). The mismatch may be in part due to the dynamic nature of the upper ocean, which complicates objective delineation of spatially coherent and persistent regions to track responses or recovery through time (Hardman-Mountford et al., 2008). For this reason, despite a recent call for ecosystem comparison (Murawski et al., 2010), there have been few quantitative comparative analyses to understand the underlying mechanisms of responses and feedbacks of pelagic ecosystems to environmental variability.

Seascape classification

A classification is a spatio-temporal segmentation of the world that, in its ideal form, has consistent principles, mutually exclusive classes, and complete systems (Bowker and Leigh Star, 1999). In other words, all descriptors or parts of a classified unit must have similar origins or organizing principles, be necessary for complete description of the unit, and can only be attributable to a single unit-- conditions that rarely exist outside of the ideal. In practice, a classification scheme should order a large array of ecosystem components so that differences and similarities are more apparent and understood, while preserving as much information as possible. If the goal is to reduce error in empirical or semi-empirical models (Hales et al., 2012), calculate fluxes for box models (Cole, 2005), or define objective extents by which to extrapolate local observations, the theoretical underpinnings of classification may not matter as long as the method is objective and the results reasonable, repeatable, and refutable. However, the classification of seascapes may require further justification. We recognize that boundaries that delineate ecosystems

and the hierarchical organization of ecosystems may be formed by exogenous (Gleason, 1939) or endogenous (Clements 1916, 1936) natural forces. For seascapes, the former includes substantial contributions by turbulence and circulation (Richardson, 1922; Mitchell et al., 2008). Thus, like landscapes, the classification of seascapes should allow for non-linear and dynamic biophysical interactions of the system at multiple hierarchical scales and reveal discontinuities that are relevant to the scale of the organism or population (Lidecker, 2008).

Early attempts to classify pelagic microbial patterns are apparent in Mary Somerville's Physical Geography (1858):

"the waters of the ocean also derive their colour from animacules of the infusorial kind, vegetable substances, and minute particles of matter… rapid transitions take place…..from aquamarine to olive-green, from purity to opacity. The appearances are not delusive, but constant as to place and colour…"

These early observations based on ocean color informed many contemporary classification efforts that have been based, at least in part, on synoptic satellite-derived measurements (Platt and Sathyendranath, 1998; Longhurst et al., 1995; Longhurst 1998, 2007; Hooker et al., 2000). Of these, the most comprehensive approach combining geography, ocean color, and biogeochemistry can arguably be attributed to Longhurst (1998, 2007). This framework used chl-*a* from the Coastal Zone Color Scanner, ship-based climatologies of nutrients, euphotic depth and several physical variables describing water column stratification. Although static, rectilinear, and subjectively chosen, these provinces have been instrumental in understanding changes in fishery and zooplankton

distributions (Beaugrand et al., 2000) and optimizing biogeochemical models, particularly satellite primary productivity algorithms (Siegel et al., 2001).

Recent efforts have recognized that the constancy inferred by Somerville and delineated by Longhurst does not adequately characterize dynamic ocean ecosystems (Hardman-Mountford et al., 2008). Some studies have inferred seasonal dynamics for coastal regions- with discontinuous but dynamic boundaries (Saraceno et al., 2006; Devred et al., 2008) or by explicitly including spatiotemporal forcing in their assessments (Hales et al., 2012). Others have classified on a global scale using objective clustering (Oliver and Irwin, 2008; Irwin and Oliver, 2009) or expert information (Spalding et al., 2012). The latter study (Spalding et al., 2012) used a synthesis of existing taxonomic surveys of primarily multicellular organisms to subjectively define boundaries; while informed by oceanographic data, it ignored ecosystem dynamics and processes. Thus, how open ocean ecosystems, in their extent, delineation, and functioning, respond to seasonal and interannual variability has yet to be rigorously assessed with both biogeochemical and assemblage-level data. Moreover, most previous efforts have focused on a single scale. Conversely, ocean seascapes, like landscapes, may be comprised of a hierarchy of scales and processes that occur at those scales.

Dissertation research

In this dissertation, I evaluate the application of the hierarchical patch mosaic paradigm from landscape ecology to the study of the seasonal and interannual variability of the North Pacific in order to facilitate comparative analysis between pelagic ecosystems and

provide spatiotemporal context for Eulerian time-series studies. Using multivariate, 13-year time-series of sea surface temperature, photosynthetically active radiation, and chlorophyll a, we classified hierarchical seascapes at monthly and interannual scales. Results of this effort demonstrate that dynamic, objectively determined seascapes offer improved hydrographic coherence relative to oceanic regions with subjectively defined and static boundaries (Chapter 2) and represent unique biogeochemical functioning (Chapter 2) and microbial communities (Chapter3). This work additionally connects satellite studies and *in situ* observations (Chapter 4) and allows for objective comparison of ecosystem forcing (Chapters 2- 5).

Because physical and chemical limitations determine the biological nature of pelagic systems, the underlying assumption is that seascape analogs derived from satellite ocean color are also distinct in their ecology and biogeochemistry (Platt and Sathyendranath, 1999). In Chapter 2, I introduce the seascape concept, the classification method, and test the assumption of biogeochemical coherence using within- and between-seascape analysis of nutrient, primary productivity, and pCO_2 data. Because of the strong, complex coupling of phytoplankton to physical forcing at multiple scales (Jassby and Platt, 1976; Steele, 1992; Belgrano et al., 2004; Hsieh et al., 2005), I chose a neural network classifier that is robust to nonlinear interactions, maintains underlying biophysical distributions, and allows for hierarchical organization (Saraceno et al., 2006; Hales et al., 2012). After briefly describing the algorithm, I characterize the seasonal dynamics of the North Pacific, and rigorously test assumptions of within-seascape coherence using spatial and general inferential statistics. Finally, I evaluate the

improvement gained by seasonally evolving seascapes compared to seasonally static provinces (Longhurst, 1998).

Chapter 3 is devoted to the assessment of the organismal relevance of satellite – derived seascapes by verifying the seascapes with *in situ* collections of microbial abundance and structure. Flow cytometry (Yentsch et al, 1983; Olsen et al., 1991) enumerates and identifies phytoplankton and bacterioplankton cells through fluorescence and scattering properties. While identified groups are taxonomically coarse, the cell is the unit of natural selection for microbes (Levin et al., 2001); flow cytometry allows seascape assessment at the scale of cells to assemblages. Flow cytometry data was collected from two long term time-series programs and several opportunistic cruises spanning several thousand kilometers of the NE Pacific and spatiotemporal patterns were quantified across both assemblage- and seascape-driven gradients.

In Chapter 4, I present a modified method that allows for dynamic seascape boundaries on interannual scales, focusing on expansion and contraction of seascapes, what may drive these patterns, and the resultant effects on seascape functioning. Seascape functioning was assessed using *in situ* data from Station ALOHA (A Long-term Oligotrophic Habitat Assessment, 22.75 N, 158 W) as well as satellite-derived measurements in subtropical and transition zone seascapes. I discuss potential ramifications of shifts in ocean-region surface area from a system primed for carbon export to one dominated by the microbial loop.

I used a seascape approach in Chapter 5 to investigate the spatial variability of factors that contribute to the functioning of the biological pump in the Northeast Pacific.

Near-continuous measurements of net primary production (NPP), net community production (NCP) and several ecophysiological variables were collected across subarctic, transition, and subtropical seascapes during August and September of 2008. In this context, seascapes allowed for objective comparison of different forcing and dynamics, elucidating underlying potential mechanisms behind biologically mediated air-sea CO_2 exchange.

Finally, in Chapter 6, I briefly synthesize the results of the previous chapters by discussing the utility of the seascape concept to advance ecological theory, improve ecosystem models, and optimize ocean-observing programs. Ocean time series are limited in spatiotemporal coverage, satellites are limited to seeing the surface, and models are limited in their complexity. Thus, an integrated ocean observing system that incorporates all three will be necessary. The seascape framework, through its capacity to scale both context and mechanism, may serve as an important and unifying component of such an observing system.

"Perception operates only upon difference. All receipt of information is necessarily the receipt of news of difference." Bateson, G. (1979).

CHAPTER 2: Towards a quantitative framework for pelagic seascape ecology

2. 1 ABSTRACT

We applied the patch mosaic paradigm of landscape ecology to the study of the seasonal variability of the North Pacific to facilitate comparative analysis between pelagic ecosystems and provide spatiotemporal context for eulerian time-series studies. Using multivariate, 13-year climatologies of sea surface temperature (SST), photosynthetically active radiation (PAR), and chlorophyll a (Chl-a), we classified monthly-resolved hierarchical seascapes. These dynamic, objectively determined seascapes offer improved hydrographic coherence when compared to oceanic regions with subjectively defined and static boundaries.

To test the assumption that seascapes represent distinct biogeochemical functioning systems, we evaluated differences between seascapes using *in situ* distributions of nutrients, NPP and pCO_2. To do this we applied analysis of variance and multiple linear regression to analyze nutrient, net primary productivity (NPP), and pCO_2 data for the same regions. Distinct nutrient and primary productivity models characterized distributions well in the first two levels of hierarchy (R^2 = 0.5-0.7). Finer scale partitioning was more relevant for pCO_2. Multiple linear regression analyses revealed differential forcing on pCO_2 across seascapes and hierarchical levels and a 33 % reduction in mean model error with increased partitioning (from 18.5 µatm to 12.0 µatm pCO_2). Furthermore, the empirical influence of seasonality was minor across seascapes at all hierarchical levels, suggesting that seascape partitioning minimizes the effect of non-hydrographic variables. As part of the emerging field of pelagic seascape ecology, this

effort provides an improved means of monitoring and interpreting oceanographic biophysical dynamics and an objective, quantitative basis by which to scale data from local experiments and observations to global biogeochemical cycles.

2.2. INTRODUCTION

2.2.1. The necessity of a formal pelagic seascape concept

The pelagic ocean is a complex system in which pattern and process interact and provide feedbacks on multiple scales of spatial, temporal, and biological organization (Lubchenco and Petes, 2010, Doney et al., 2012). Non-linearities are common in biogeochemical (e.g. Gruber, 2011; Hales et al., 2012), biophysical (e.g. Hsieh et al., 2005) and trophic (Litzow and Ciannelli, 2007, Brander et al., 2010) interactions. Furthermore, spatial heterogeneity is ubiquitous and occurs at all scales observed (Steele, 1991; Levin and Whitfield, 1994; Mitchell et al., 2008). Understanding and modeling pelagic ecosystem responses and feedbacks to environmental perturbation is therefore hampered by the lack of an objective framework to (1) scale local processes to ocean basins (2) define how temporal and spatial scaling of habitats may change regionally, and (3) place the 'snapshots' of data collected in a typical oceanographic research expedition into a regional context. Terrestrial ecologists look to landscape ecology to address issues of context and scale (Turner, 2001); however, there has been little formal application of a seascape concept to open ocean systems.

A quantitative seascape framework can link regional oceanography to both global patterns and local mechanisms (Karl and Letelier, 2009). Synoptic time series such as those derived from satellite algorithms of chlorophyll a (chl-a; Gregg et al., 2005) or net primary production (NPP) (Behrenfeld et al., 2006) and coupled ocean-atmosphere models (Boyd and Doney, 2002; Sarmiento et al., 2004) reveal strong regional differences in responses of pelagic ecosystems to climate change. These differences suggest that some regions of the world's oceans are more sensitive to perturbation than

other areas. However, the dynamic nature of the upper ocean complicates objective delineation of spatially coherent and persistent regions to track responses or recovery through time (Hardman-Mountford et al., 2008). For this reason, despite the recent call to action (Murawski et al., 2010), there have been few quantitative comparative analyses to understand the underlying mechanisms of responses and feedbacks of pelagic ecosystems to environmental variability.

Pelagic biogeography based on ocean color can be traced as far back as Somerville (1858); however, the most comprehensive approach combining geography, ocean color, and biogeochemistry can arguably be attributed to Longhurst (1998, 2007). The Longhurst framework used chl-a from the Coastal Zone Color Scanner, ship-based climatologies of nutrients, euphotic depth and several physical variables describing water column stratification. Although static, rectilinear, and subjectively chosen, these provinces have been instrumental in understanding changes in fishery and zooplankton distributions (Beaugrand et al., 2000) and optimizing biogeochemical models, particularly satellite primary productivity algorithms (Siegel et al., 2001). More recent efforts have used the maturing satellite data record to classify regions of biophysical coherence for coastal (Saraceno et al., 2006; Devred et al., 2008; Hales et al., 2012) and open ocean regions (Oliver and Irwin, 2008). The majority of these efforts have been temporally static and at a single spatial scale.

Because physical and chemical limitations determine the biological nature of pelagic systems, the underlying assumption is that seascape analogs derived from satellite ocean color are also distinct in their ecology and biogeochemistry (Platt and Sathyendranath, 1999). We have classified satellite-derived attributes in a spatial and temporally specific

fashion and explicitly test the hypothesis that coherent regions as identified with satellite data represent distinct regions of ecosystem functioning. To do this first, we extended the methods presented by Saraceno et al., 2006 and Hales et al., 2012 to resolve the intra-annual evolution of seascapes in the open North Pacific based on a 13-year climatology of satellite observations. Second, we explicitly apply the concept of patch hierarchy (Wu and Loucks, 1995) to classify basin and gyre seascapes using the same domain. Finally, we test the assumption that seascapes represent areas of distinct biogeochemical function by evaluating differences between seascapes using independent *in situ* distributions of nutrients, NPP and pCO_2. With this framework we are able to address the following questions:

How does a hierarchical seascape framework represent the seasonal and spatial dynamics of the North Pacific?

Do hierarchical seascapes describe significant variation in surface biogeochemical patterns, and if so, at what hierarchical level?

Do seascapes describe regions that differ in their biogeochemical functioning?

2.2.2. Study Area

The North Pacific is a dynamic ocean region in which includes the oligotrophic and subarctic gyres that are separated by the broad North Pacific current, NPC (Figure 2.1). In the western basin, the circulation strength and sharp gradients are driven by inputs from the strong Kuroshio (~3 km hr^{-1}) and Oyashio currents. In the east, the NPC

broadens and slows (~0.5 km hr^{-1}), bifurcating off the coast of British Columbia coast to form the Alaska and California Currents and the subarctic and subtropical gyres. The subarctic / subtropical transition zone from the Kuroshio extension into the eastern subarctic gyre is the largest sink region for atmospheric carbon dioxide in the North Pacific (Takahashi et al. 2009). Here, while biological uptake of dissolved inorganic carbon (DIC) tends to counteract the warming effect in the summer; the bulk of the drawdown has been attributed to winter cooling and the resultant increase in solubility of CO_2 in seawater (Takahashi et al., 2002).

Superimposed on the physical boundaries described above, seasonal and latitudinal changes in surface temperature (SST) and photosynthetically active radiation (PAR) contribute to defining the seascapes in which ecological assemblages develop and persist. The domain (120-240º W, 15-65º N) was chosen in order to highlight the open ocean variability by minimizing the influence of extreme values associated with ice-edge responses in the northern latitudes and tropical instability waves that pulse along the equator in the southern portion of the North Pacific subtropical gyre (Evans et al., 2009).

2.3. METHODS

2.3.1. Satellite data and processing

As a first step, we characterize in our classification scheme lower trophic level dynamics using only variables available via satellite, namely chl-a, light and temperature. We used archived monthly averages and 8-day composites of the latest processing of satellite data provided by the Ocean Productivity Group (*www.science.oregonstate.edu/ocean.productivity*), as used in their primary productivity

algorithms. These data have been cloud-filled which results in reduced variability at seascape boundaries associated with patchy cloud cover (Kavanaugh unpubl. data). We downloaded Level 3, 18 km binned, 8-day composites and monthly averages of SeaWiFS (R2010) chl-a, PAR, and Advanced Very High Radiometer sea surface temperature (AVHRR SST); the 18 km data were subsequently binned into ¼ degree pixels. The SeaWiFs (SW) data record extends from 1998-2010 albeit with episodic gaps during 2008-2010 due to sensor failure. Where missing, SW chl-a and PAR were interpolated using the comparable MODIS (R2012) product. Linear regression was conducted at each pixel using the eight-day composite of each sensor for each month over the years 2003-2010. Predicted SW chl did not vary more than 25% from actual SW chl-a (usually less than 10%) and predicted PAR varied less than 10% from actual SW PAR. The predicted 8-day composite was then used to fill gaps in the real SeaWiFs 8-day composites; monthly averages were computed from the combined product. Chl-a values >8 mg m^{-3} were masked to minimize the effect of coastal variability and maximize variability in the open ocean. The chl-a field was $\log_{10}$-transformed. All three fields were normalized (to a scale of-1 to1) prior to classification, where the maximum value would be 1, minimum -1 and median=0 if the variable was normally distributed.

2.3.2. Hierarchical classification of seascapes

Because of the strong, complex, coupling of phytoplankton to physical forcing at cellular (Jassby and Platt, 1976), local/community (Steele, 1992; Belgrano et al., 2004) and mesoscales, we chose a classifier that was robust to nonlinear interactions and maintained underlying biophysical distributions. In brief, we used a probabilistic self-organizing map

(PRSOM, Anouar et al., 1998) combined with a hierarchical agglomerative classification (HAC, Jain and Dubes, 1988) to achieve a non-linear, topology-preserving data reduction. SOMs have been used in oceanography to classify regions (Richardson et al., 2003; Saraceno et al., 2006), define regions of mechanistic coherence in predictive pCO2 models (Hales et al., 2012), and to find drivers of net primary productivity (Lachkar and Gruber, 2012). As with most SOM methods, PRSOM uses a deformable neuronal net to maintain data similarities and topological order between clusters. The PRSOM, however, introduces a probabilistic formalism; clusters are produced by approximating the probability density function with a mixture of normal distributions and optimization based on a maximum likelihood function (Anouar et al., 1998).

Monthly climatological grids were vectorized and concatenated to allow classification of space and time simultaneously. The PRSOM reduced the 3-variable (SST, PAR, chl-a) spatiotemporal data set onto a 15×15 neuron map resulting in 225 classes, each with its own 3-D weight based on the maximum likelihood estimation. The neuron map size and shape was chosen to maximize sensitivity to mesoscale processes while preventing underpopulated nodes (defined as less than 500 pixels). The 3-D weights were then further reduced using a hierarchical agglomerative clustering (HAC) with Ward linkages (Ward, 1963). This linkage method uses combinatorial, euclidian distances that conserve the original data space with sequential linkages (McCune et al., 2002). Euclidian distances here are equivalent to within-group and total sum of squares (GSS and TSS, respectively). An objective function (I, information remaining) was determined a priori to determine total number of seascapes:

$$(I) = (TSS\text{-}GSS)/TSS \quad \text{(McCune et al., 2002)}$$

where TSS=GSS when all seascapes (S) are fused into one.

To define seascapes at emergent scales by which we would evaluate the differences in biogeochemistry, we examined stepwise agglomerations of seascape classes (C), which resulted in local, rapid shifts in I. This was evaluated by comparing the shift in objective function to that which would occur under a random spatial structure where increased class size would add (1/C) information. We then determined whether the proportional shift was greater (aggregated) or less (dispersed) than unity:

$$\text{aggregation index} = 1-[(I_{C(data)} - I_{C-1(random)}) / I_{C(random)} - I_{C-1(random)})]$$

2.3.3.Verification of satellite-derived classes

To conduct parametric post hoc summaries, we accounted for autocorrelation and anisotropy in our remote sensing dataset and resampled at data densities that were statistically independent. Correlation, ρ, and number of pixel pairs, Np, at a given distance (d) and azimuth (a) were calculated with the original $\log_{10}$-transformed chl-a data for each seascape as a function of 10 km binned distance and 45-degree binned direction. A correction factor ($\theta_{(d,a)}$) for each distance-azimuth bin was calculated where:

$$\theta_{(d,a)} = (1-\rho_{(d,a)})/(1+\rho_{(d,a)})$$ (Fortin and Dale, 2005).

The extent of seascapes was determined in the four cardinal directions and autocorrelation was calculated over either 1000 km or 0.6×least-extent, whichever distance was shorter. Because data tended to be positively correlated at local and

mesoscales and anticorrelated at larger scales, this limit resulted in a smaller effective sample size and therefore a more conservative estimate of seascape differences.

The correction factor was then weighted by the number of pixels pairs, $Np_{(d,a)}$ to obtain a "global" correction factor:

$$\theta = \Sigma[\theta_{(d,a)} * Np_{(d,a)}] / \Sigma Np_{(d,a)} \text{ where } 0 < \theta < 1.$$

The global correction factor was then applied to the total number of pixels in a sample N to obtain the effective sample size, N' for each seascape*month interaction:

$$N' = \theta * N$$

N' multivariate pixels were subsequently randomly selected for statistical comparison to test whether provinces result in different multivariate means. N' was calculated for each month*seascape; all three fields were randomly resampled at the N' level.

2.3.4. Evaluation of biogeochemistry

Differences of biogeochemical factors and processes among seascapes and the relative importance of seascapes compared to space and time were determined by evaluating archived nutrient concentrations, net primary productivity (NPP) and pCO_2 data. Surface concentrations of nitrate (NO_3), phosphate (PO_4) and silicate (SiO_2) were downloaded from open ocean stations (N >12000) archived in the World Ocean Database, WOD; data were subsequently binned into the nearest 1x1 degree pixel and monthly means were calculated (final N=3985). Climatological net primary productivity, NPP, was determined using monthly climatologies (1998-2010) of the updated carbon-based primary production model (Westberry et al., 2008) made available by the Ocean Productivity

group (http://www.science.oregonstate.edu/ocean.productivity/). NPP is reported for the same month*pixel density as nutrient data. Monthly climatological pCO_2 data were downloaded from the Lamont-Doherty Earth Observatory database (http://cdiac.ornl.gov/oceans/), and evaluated at the density reported by Takahashi et al., 2009.

2.3.5. Comparison to Longhurst provinces

The North Pacific is represented by nine Longhurst regions that are seasonally static: Bering Sea, Subarctic East, Subarctic West, Kuroshio, Polar Front, Subtropical West, Subtropical Gyre, and the Alaska and California Current Systems (Longhurst, 1998, 2006). Polygons delineating these regions were downloaded (http://www.vliz.be) and gridded to a 0.25-degree surface. The Alaska Current province did not have sufficient data density; thus comparisons were made among the remaining eight provinces to emergent seascapes.

2.3.6. Statistical Analysis

All statistics were performed using JMP v 8.2 (© SAS Institute, Cary NC). Satellite-derived seascape, nutrient and pCO_2 data were grouped according to seascapes and month. Summary statistics are reported for satellite data after month-wise decorrelation at all scales and at the dominant scale for *in situ* data. Nested analyses of variance (n ANOVA) were conducted to determine the relative importance of different hierarchical levels or space and time within a single hierarchical level on nutrients, nutrient ratios, and pCO_2.

While the relative efficiency of a classification scheme can be determined using the R^2 of an ANOVA output, this metric is biased toward increased number of classes, which may provide less descriptive capacity. In order to determine the relative efficiency of our partitioning to the Longhurst scheme, we compared the F-statistic of classification schemes for chl-a, nutrient concentrations and NPP within and across months thus allowing efficiency to be determined across variables that were included in one, the other, and neither (but inferred by both) classification scheme. We took this comparison one step further and asked which framework resulted in a greater reduction in NPP predictive model error. NPP predictive models were based on multiple linear regression of satellite-derived temperature, chl-a, PAR, and two non-hydrographic variables that modeled effects of space and season. Season was modeled by fitting a sine function to month of year (season=sine (month/4)) and space was modeled as a function of the interaction of latitude and longitude, with the longitude function representing degrees from the dateline. Finally to determine the relative importance of different biophysical interactions across seascapes, a multiple linear regression model was built to determine the effect of SST, chl-a, and nutrients on pCO_2 within seascapes. The resulting coefficients for all multiple linear regression analyses were scaled by their dynamic ranges (centered on mean), so that effect sizes could be determined between parameters and across seascapes and scales.

2.4. RESULTS

The PRSOM-HAC combination resulted in optimized clusters that accounted for approximately 90% of variance in climatological means of satellite-derived chl-a, SST, and PAR (Table 2.1). There were three distinct local maxima in the objective function (Figure 2.2a) from which we derived three levels of nestedness (Figure 2.1b). While month-wise spatial decorrelation resulted in a reduction of ~80% of the data, seascapes were still significantly different for all variables considered and at all scales (Tukey-Kramer, HSD; $p<0.05$), with the exception of chl-a between two clusters at the finest resolution (Table 2.1).

In general, seasonal variation within seascapes contributed much less variation than that between seascapes (Table 2.2: $F_{seascape} < F_{season\ [seascape]}$). Increased resolution to eight seascapes resulted in small, but significant, addition of variance explained for chl-a and SST, but a larger increase in variance of PAR explained. Thus nesting eight seascapes within three seascapes resulted in the characterization of the seasonal cycle of insolation, warming and biological response for the North Pacific (Table 2.3).

2.4.1. Spatiotemporal hierarchical patterns

2.4.1.1. First-level dynamics

At the basin scale, three distinct seascapes were classified that generally describe the known divisions between the subarctic, transition and subtropical regions (Figures 2.1b, 2.2). All three areas are present year round, with the transition zone approximating the division between the transition zone chlorophyll front (TZCF, Polovina et al., 2001) and the subarctic front. The Kuroshio extension is evident in February and the eastern north Pacific bifurcation becomes evident in May. Most of the seasonal dynamics, however, are limited to latitudinal variation in the location of the transition zone.

2.4.1.2. Second-level dynamics

At the second level of hierarchy, eight total seascapes were classified (Figure 2.2b, Figure 2.4) that generally described basin scale seasonality. Three seascapes each arose from the subtropics and subarctic whereas two seascapes resulted from division of the transition zone. Note that the number of seascapes found in each month is different and that a given seascape usually occupied a shifted geographical region as the time of year varied. Since the methodology distributed the seascapes in space and time in order to minimize the within-seascape variance of the variables considered, it was possible to follow the same composite properties by following a given seascape in time. Seascapes were nominally identified based on dominant season, geographic region and/or trophic status based on mean chl-a concentration, specifically: 1) Summer subtropical (Su-ST); 2) Winter subtropical (W-ST); 3) Oligotrophic boundary (OB); 4) Winter transition (W-

TR); 5) Summer transition (Su-TR); 6) Mesotrophic boundary (MB); 7) Winter subarctic (W-SA); 8) Summer subarctic (Su-SA).

In January, latitudinal variations in light separated the four winter seascapes: W-SA, MB, W-TR, and W-ST, with only minimal expression of Su-TR present in the extreme southeast part of the study region (Figure 2.4). February marked the expression of the Kuroshio extension with high chl-a in seascape W-TR and differentiation of regions abutting the North Pacific current, while the OB seascape expanded eastward, bifurcating W-ST into northern and southern components. In March, high chl-a water from the Oyashio current and the Sea of Japan was entrained in the subarctic front, illustrated by the cross-basin expansion of the Su-SA and MB seascapes, while W-TR and W-ST disappeared. April marked the onset of a spring transition with abrupt shifts in seascape identity: The W-SA seascape, which persisted Jan-Mar, disappeared entirely and was replaced by Su-SA. May, June, and July were similar to April, distinguished primarily by the northeastward expansion of Su-ST and the N-S broadening of MB north and south along the North American continent. During this time, the interface between the two boundary seascapes tended to follow the seasonal migration of the transition zone chlorophyll front. During August, the Su-SA zone was replaced by the MB seascape, while the Su-TR zone became constricted by the expansion of MB from the north and the OB from the south. September was similar to August, although the fall transition began then with the first hints of the W-ST encroaching from the southwest and the W-SA in patches within the Alaska Gyre and in the SW along the boundary of the Oyashio and Kuroshio. The fall transition was most clearly expressed in October, with the Tr-SA zone retreating from the open SA towards the continents, the first break in the cross-basin

expanse of Meso-BND since February, and the first widespread appearance of the three winter zones.

The progression of seascapes found in our analysis gives a new perspective on seasonality in the North Pacific. On a basin scale, winter appears to consist of three months spanning November – January, and is defined by the full cross-basin expression of W-ST and W-SA seascapes. Summer, defined by the cross-basin extent of the Su-TR and OB zones, accompanied by the expansion of Su-ST to the south and Su-SA persists for five months (April –August). Fall, defined by the first absence of defined summer or boundary zones, and first appearance of winter zones, is most clearly expressed in October, although hints of transition are evident in September at higher latitudes. The spring transition, defined by the first cross-basin appearance of the boundary seascapes and the first appearance of the Su-ST and Su-SA zones, is most clearly defined in March, although changes from winter conditions are evident in February.

2.4.1.3. Third level dynamics

Fourteen seascapes emerged at the finest hierarchical level. These seascapes were nominally identified by their relative [chl-a] and were indexed SS1 to SS14 (Figure 2.2b, Figure 2.5). Increasing hierarchical resolution from eight to fourteen seascapes did not affect the boundaries of the two subtropical seascapes (Su- and W-ST= SS1 and SS2 respectively), however, the remaining six seascapes each split.

In general, the resultant seascapes represented increased spatial variability in the subtropics and seasonal opposites at higher latitudes. The OB split into two distinct subseascapes, SS3 and SS4, both present for all but two months of the OB duration

(March- September vs. February- Oct). The W-TR split into two distinct subseascapes (SS5 and SS6) marked primarily by latitudinal differences in temperature and light. The Su-TR split into two seascapes (SS7 and SS9) that seasonally represented marginal ecosystems (e.g. the California Current). From the sixth seascape (MB), distinctions arose associated with the spring (SS8) and fall (SS12) transition in the subarctic with seascapes that identify the Kuroshio extension in February and April and the California current in early spring and late autumn. The seventh seascape (W-SA) split (SS10 and SS11) to include a higher chl-a region (SS11) apparent in the subarctic in October that shrinks to align with the boundary regions in the winter. Finally, the division of the Su-SA seascapes allowed for the slightly different dynamics of the eastern (SS 13) and western subarctic gyres (SS14).

2.4.2. In situ data evaluation

Here we tested the hypothesis that seascapes represent an optimized framework for describing biogeochemical distributions. Indeed, a significant portion of variance in nutrient concentrations is explained by seascapes. Because nesting was unbalanced (Su-ST and W-ST in two hierarchical levels), effects could not directly be translated into percent of model explained; however, the relative effect of nesting levels was determined by examining the F-statistics (Table 2.4). In most cases, the greatest amount of variance was explained by the coarsest level of hierarchy with the nested variable explaining less variance (Table 2.4, nANOVA F-stat (SS3)>> F-stat (SS8[SS3]> F-stat(SS14[SS8, SS3])). The exception to this was the N:P ratio where the SS3> SS14> SS8 and pCO_2 where SS14>SS3>SS8. This result (and the comparatively low total variance explained,

R^2 = 0.26) suggests that local processes and interactions are important in shaping pCO_2 concentrations although little change in explanatory power was added when considering continuous factors within seascapes (Table 2.4). This result contrasted with the NPP predictive model where continuous seasonal variability within seascapes contributed substantially to variance explained (Table 2.4). The large seasonality effect was driven primarily by changes in available solar radiation in the MB and W-SA seascapes. Given that the seasonality effect on nutrients and nutrient ratios were small (F=5-29) compared to between seascapes (F=74-168) this suggests that while the basic attributes of the system (nutrients, light, temperature) were not changing, perhaps the efficiency of phytoplankton's ability to utilize light changed with increased insolation.

We also examined the relative importance of continuous spatiotemporal variability within seascapes by considering individual hierarchical levels (Table 2.7). As may be expected from Table 2.4, the greatest amount of variation explained occurred at Level 3 (Table 2.7, R^2= 0.41). Furthermore, as determined by their F-statistics, other than a large interaction of space and time within seascapes at the coarsest hierarchical level, continuous variability within seascapes contributed much less than that between seascapes. Biogeochemical patterns tended to coincide with basin scale variation in temperature and salinity, with lowest nutrient concentrations and highest pCO_2 in Su-ST and highest (lowest) in Su-SA. There were, however, a few notable exceptions. Within the subtropics, nitrogen was not different between seascapes but P increased from Su-ST to OB (Su-ST<W-ST<OB, $p<0.05$ Tukey-Kramer HSD test) leading to low N:Si and N:P in SS3 compared to other subtropical seascapes and its northern neighbor (N:P : OB< W-ST=Su-ST<W-TR; $p<0.05$ All pairs, Tukey-Kramer multiple comparisons). pCO_2 also had a

local minima in the transition zone with values comparable to the cool, high chl-a Su-SA (W-TR=Su-SA <W-ST=MB=Su-TR<OB=W-ST<Su-ST).

2.4.3. *Seasonal seascape and Longhurst comparison*

Through comparison of F-statistics (Table 2.8), we examined the efficiency of the different classification schemes for capturing the spatial variability throughout the year of: [chl-a] (included explicitly in the PRSOM classification), surface PO_4 (included in explicitly in the Longhurst classes) and NPP (included in neither but implied by both through choice of classifying parameters). Within and across all months, PRSOM-based classification was more efficient at capturing variability in chl-a, perhaps not surprising given that chl-a was an input for the PRSOM. Within months, with the exception of March, PRSOM-derived seascapes explained more variability of NPP than did the Longhurst provinces (Table 2.8); on average, between-group variability for PRSOM was 35% higher than for Longhurst (F=47.6 compared to F=30.9). For phosphate within months, PRSOM-derived provinces resulted in greater between-group (province or seascape respectively) variability for most months considered, on average 20-40% increase the F-statistic, depending on whether averages were weighted by within-month sampling density or not.

For multiple linear regression models predicting NPP, parsing into multiple regions resulted in approximately 20% reduction in model root mean square error (RMSE: Table 2.9) with only a modest additional improvement if empirical dependence on seasonality and spatial variability within seascapes were added. Partitioning into eight seasonally evolving seascapes resulted in greater error reduction than when the domain was

partitioned into the eight static Longhurst provinces (log10-transformed RMSE = 0.117 and 0.113 mg C m^{-2} compared to 0.121 and 0.117 mg C m^{-2}). While the effect of seasonality was high in the subarctic for both classification schemes, the effect sizes of seasonality were on average two-fold higher for the Longhurst provinces (Table 2.9).

2.4.4. Biophysical forcing of pCO_2

The biophysical forcing on pCO_2 varied as a function of seascape and hierarchy as revealed by comparative multiple linear regression analysis (Table 2.10 Figure 2.6). In preliminary analyses, chl-a was found to be a stronger predictor of pCO_2 than was NPP when both were included in the model; the latter was therefore not included in subsequent analyses. With the exception of one seascape in the second level, seasonality was a relatively minor effect on pCO_2 across all hierarchical levels. Furthermore, substantial variation in North Pacific pCO_2 was explained by constraining mechanistic variables with seascape spatiotemporal boundaries (Table 2.10). The multiple linear regression analysis explained up to 88% and typically >60% of the variability. Correlations (after weighting for sample density within each seascape) averaged 0.68 for the coarsest level, 0.73 for level 2 and 0.70 for level 3. Root mean square error of the multiple linear regression model was also reduced with finer resolution. Across seascapes, pixel weighted mean RMSE (+/- SE) decreased from 18.5 µatm (basin) to 15.3 (+/-1.6) µatm at the Level 1 to 12.4 (+/-1.1) µatm at Level 2 to 12 (+/-0.8) µtam at Level 3.

In the subtropics, at the coarsest scale, pCO_2 decreased as a function of increased chl-a, cooling, and wintertime processes not related to cooling. pCO_2 also increased with decreased salinity in this region. With increased resolution (Level 2), the negative salinity

effect appeared to be driven by dynamics in OB with positive associations of salinity in both Su-ST and W-ST). The OB was unique also due to its strong contribution by chl-a to decreased pCO_2.

Across the transition zone, chl-a had the strongest effect on pCO_2 (Table 2.9, Figure 2.6). SST was not a significant factor in this region when changes in salinity were included. The chl-a effect significantly outpaced the warming effect in this region for the first 2 levels of hierarchy, however, the relative effects in the third level may not be resolved in many regions due to decreased sample size.

In the subarctic, physical mixing appeared to be the dominant factor with strong positive salinity effects, both in W-SA and Su-SA. While chl-a was a significant driver of pCO_2 in the subarctic, its effect was dwarfed by the mixing signal of salinity and cooling signal of SST in all but the MB seascape.

2.5. DISCUSSION

Because of the challenges in working in an advective environment and with organisms that exhibit patchy distributions on multiple scales, seascape ecology requires a sound theoretical framework for analyzing spatiotemporal patterns in the structure of phytoplankton assemblages and the biogeochemical function they provide (Karl and Letelier, 2009). The distinct seascapes in the North Pacific described here are validated by three lines of evidence: 1) hierarchically organized seascapes generally follow known patterns of circulation and characterize the seasonality of the North Pacific; 2) seascapes represent distinct surface nutrient and primary productivity regimes; 3) seascapes represent distinct biophysical interactions that are relevant to predicting both NPP and the relative importance of different forcing factors on pCO_2. The framework that we present meets or exceeds the high standards set by Longhurst. These seascapes are objectively-derived, and allow for evaluation of mean seasonal (this study) and interannual (Chapter 4) variability.

2.5.1. Scaling rules

In the Northeast Pacific, at least sixteen different programs ranging in duration from ~ 4-6 years to 6 decades have investigated the local to regional response of hydrography, biogeochemistry, plankton distributions and higher trophic level dynamics to climate forcing (Batchelder and Powell, 2002). Scaling these processes up requires an understanding of how the system is organized in space and time. As systems self-organize and reorganize, regional heterogeneity may provide spatiotemporal refugia (Levin, 1976), which could allow species and/or functions to persist for a sufficient

period of time and locally shift the dynamics of source-sink relationships (Mouquet et al., 2006) or the scale-specific response to perturbation. However, the nesting of gyre-scale patterns within basin seascapes suggests that scaling of local mechanism to global seascapes is feasible.

The North Pacific is a dynamic basin with several seasonally distinct features that exhibit a spatiotemporal hierarchy. Our seascape classification allowed visualization of the onset of the Kuroshio extension, the Oyashio bloom and entrainment into the subarctic frontal current, and the seasonal and meridional changes in the transition region between the oligotrophic subtropical and the productive subarctic gyres (Figure 2.2-2.4). The dynamics of these transition zones were also apparent with higher order clustering, as were heightened seasonality in the subarctic and transition regions (Figures 2.3 and 2.4). Importantly, our classification allowed for non-linear interaction between attributes and allowed for hierarchical organization and seasonal movement of seascapes within the hierarchy. Classifications that use different sensors, attributes, assumptions of linearity, or dispersed organizational structure will result in division of different state space and thus, the spatiotemporal location of seascapes and their boundaries. To some degree, the choice of classification depends on the question of interest; however, much can be learned about the organization of the system by comparing different methodologies and should be pursued in future efforts. As suggested by previous studies (Devred et al., 2008; Hales et al., 2012), seasonally evolving boundaries characterize the dynamics of marine systems better than static, rectilinear boundaries.

2.5.2. Biogeochemical distributions

The seasonal cycle of nutrients, nutrient ratios, and NPP in the North Pacific is well described by the boundaries of satellite-derived seascapes suggesting that seascapes demarcate natural boundaries in nutrient availability and nutrient use efficiency. Differences between seascapes accounted for a large amount of variance in both nutrient concentrations and nutrient ratios; seascape differences were also more important than both spatial and temporal variation within seascapes. While nutrient concentrations across seascapes followed patterns expected based on satellite chl a data, distinct minima in N:P and N:Si occurred in oligotrophic boundary seascape. This region is well documented to have persistent, albeit modest rates of N_2-fixation overlain by irregular summer-fall blooms of diazotrophs (Karl et al., 2012 Wilson et al., 2008, White et al., 2007). The net effect of this activity is high P and Si utilization in surface waters and a subsurface excess of N relative to P in an area extending southward from the TZCF into the subtropics (Deutsch et al., 2001). Accordingly, tracking the spatial and temporal migration of the OB might be analogous to tracking the optimal habitat for specific diazotrophs that would be selectively favored in low N: P or N: Si environments, including diazotrophic symbionts in diatoms (Venrick, 1974; Villareal, 1991).

Although circulation and biological effects on surface biogeochemical distributions could not be separated, the results suggest that these properties have a seasonally evolving biogeographic signature; whether this is associated with shifts in phytoplankton biogeography (Weber and Deutsch, 2010) remains to be seen. We did not explicitly include phytoplankton assemblage information in our study, nor have we addressed

interannual variation in seascape boundaries. Linking the seasonal and interannual dynamics of seascapes and their shifting boundaries to shifts in phytoplankton diversity and biogeochemical pattern remains a logical next step.

2.5.3. Understanding regional drivers of NPP and pCO_2

One of the major goals of a seascape framework is to link local community and biogeochemical structure and interactions with global processes. There are currently over 20 satellite derived primary productivity models that differ in their regional performance (Carr et al., 2006). Using the carbon-based productivity model as an example, and satellite-derived SST, chl-a, and PAR as drivers, mean root-mean-square-error was reduced by ~20% by parsing into eight seascapes, whether Longhurst or PRSOM-based. The difference was that PRSOM-based seascapes do not rely on a large seasonal parameterization; thus, changes in space and time were driven by changes in mechanistic dependence on hydrographic parameters. This is evident also in the discrete comparison of PRSOM-based and Longhurst-based partitioning. PRSOM-based partitioning was more efficient in explaining seasonal and spatial variability of chl-a, nutrients and NPP than Longhurst-based provinces.

Seascapes represented regions of distinct biophysical forcing of pCO_2 as revealed by multiple linear regression analysis. How the biological pump is driven by trophic interactions, high PP, ballasting or aggregation of cells or how the interaction of these factors change in space and time is not well understood. However, through objective

seascape analysis we were able to describe a transition zone that is divided into several regions within which biological and physical factors interact differently to modulate pCO_2 and, potentially, air-sea CO_2 flux. Considering processes within these distinct seascapes may help elucidate differential controls of the complex ecological phenomena such as the biological pump. For example, abutting the transition zone to the south, the oligotrophic boundary seascape may respond with diazotrophy-fueled blooms from February to November to draw down surface pCO_2. In the spring and summer, NPP was higher in the transition seascape than anywhere in space and time in the North Pacific. In this zone, the chlorophyll effect on pCO_2 is greater than the temperature effect, suggesting that biological processes are driving pCO_2 patterns and possibly air-sea exchange. In the northernmost seascapes, the drawdown effects of pCO_2 by both SST and chl-a seemed to be small relative to mixing.

Previously it was suspected that summer phytoplankton activity in the transition zone kept pace with summer warming, effectively priming the winter solubility pump (Takahashi et al., 2002, 2009) and making the region an annual sink for atmospheric CO_2. This study refines that notion. Whether coarsely or finely defined in the hierarchy, biological effects on pCO_2 in the transition zone were stronger than temperature effects. Several investigators have recognized the challenges of predicting pCO_2 based on its highly variable dependence on different biophysical parameters in space and time. Park et al. (2010) used empirical subannual relationships between climatological pCO_2 and sea surface temperature, along with interannual changes in SST and wind speed to predict changes in surface pCO_2. Permitting the subseasonal regressions to be fit on any three or more sequential months allowed for different phases and shapes of the annual cycle and

optimized the pCO_2: SST relationship for a given coordinate. In the North Atlantic, using a similar domain size to ours, Friedrich and Oschlies (2009a) trained a SOM-based predictive model with ARGO data by explicitly including latitude, longitude, and time in the training set. Hales et al. (2012) found that regional prediction of pCO2 within static coastal seascapes was markedly improved by including time-dependence in a semi-mechanistic model. In our analysis, the objective, hierarchical classification of state space in space and time allowed for seasonality to emerge and for geolocation of boundaries to shift through time. As suggested by Hales et al. (2012), the implicit inclusion of time in the classification of state space allowed us to diminish the effect of time in the predictive models. While satellite-based estimates may suffer from large gaps (Friedrich and Oschlies, 2009), we found that classification of coherent biophysical regions- i.e. seascapes, using only temperature, light and chl-a result in reduced hydrographical variability within a given seascape and increased model prediction capacity. Thus, seascapes may provide a means by which to test different hypotheses regarding the relative importance of different biophysical forcing and to conduct comparisons of oceanic ecosystem functioning (Murawski et al., 2010).

Conclusion: Remotely sensed ecological indicators may detect spatiotemporal modifications to the structure and function of pelagic ecosystems (Platt and Sathyendranath, 2008) and thus can inform the development of new ecological theory or modeling frameworks. This work demonstrated that the seascape concept describes variability in ecosystem level traits and functioning. Imposing objectively derived boundaries can help optimize the modeling of evolutionary pressures on plankton (e.g.

Bragg et al., 2010) and thus provide insight into the feedbacks between local to mesoscale ecology and global biogeochemical cycles. Furthermore, objectively defined, dynamic seascapes represent an important first step toward developing a quantitative framework for pelagic seascape ecology and thus a means for applying the ecosystem concept to the open ocean (Cole, 2005). With increased technological capacity to autonomously and remotely sense the aquatic environment, we now have the capacity for synoptic observations at several spatiotemporal scales, and examining the continuous variability within seascapes is a natural next step. Our results demonstrate the utility of considering spatial and temporal context together. This is a key result for the continued development of seascape ecology theory, which will contribute to the understanding the dynamics of marine systems, especially where gradients are diffuse and where seasonal, interannual, or climate-driven shifts in boundaries are suspected.

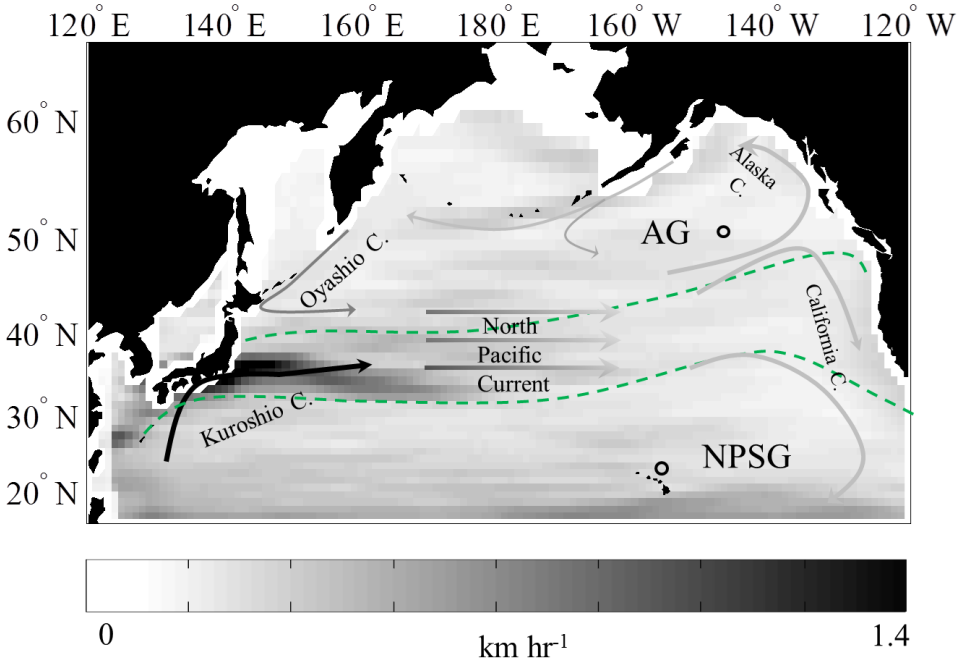

Figure 2.1. The North Pacific Basin domain with approximate locations of major currents. Arrows and their color denote general direction and strength to coincide with underlying mean annual modeled current speeds (2003-2007). Gyre-scale subdomains and associated ocean time series are shown with boxes and open circles, respectively (Station Papa: 50 °N, 145 °W; Station ALOHA: 22.75 °N, 158 °W). The seasonal range of the transition zone chlorophyll front (TZCF, Polovina and others, 2001) is demarcated in green.

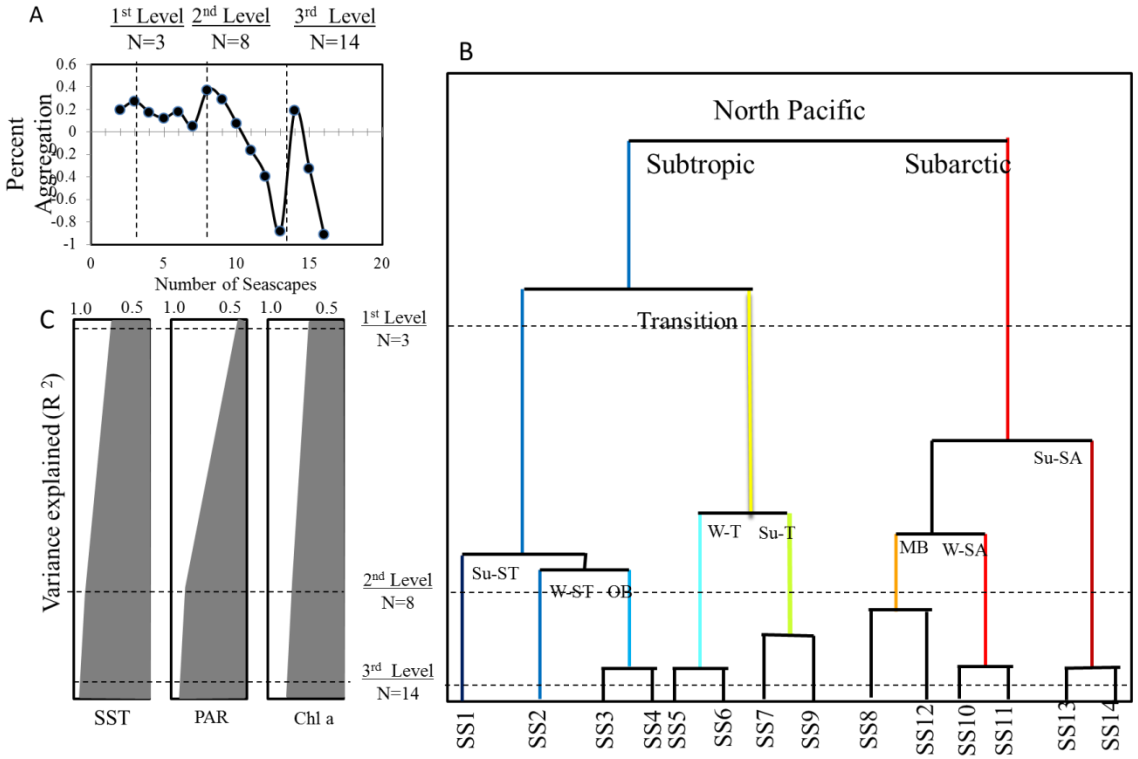

Figure 2.2. Hierarchical structure of North Pacific Seascapes as defined by classification of satellite-derived SST, PAR, and chl-a. A. Percent aggregation defines emergent hierarchical levels at N=3, 8, and 14 Seascapes. B. Relative Euclidean distances of seascapes at three hierarchical levels. Color-coding corresponds to Figures 2.1 and 2. 2 (3rd level not colored). C. Percent of variance of SST, PAR, and chl-a explained through analysis of variance of seascapes at different hierarchical levels. Seascape identifiers and their abbreviations used in text and Table 2.1 are as follows: 1) Summer subtropical (Su-ST); 2) Winter subtropical (W-ST); 3) Oligotrophic boundary (OB); 4) Winter Transition (W-Tr); 5) Summer Transition (Su-Tr); 6) Mesotrophic boundary (MB); 7) Winter in subarctic (W-SA) 8) Summer subarctic (Su-SA).

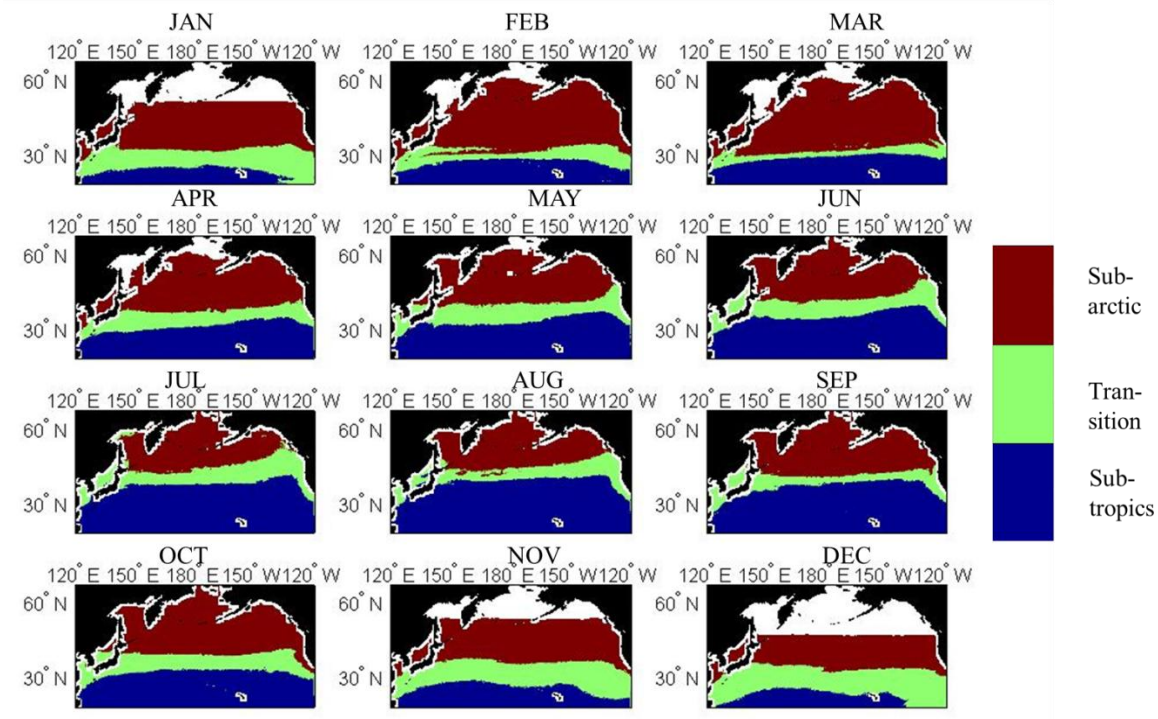

Figure 2.3. Seasonal migration of seascapes in the North Pacific basin: Level 1. Eight seascapes were classified using a combination of PRSOM and HAC; color codes reflect relative relative concentrations of chl-a with red denoting higher concentrations and blue denoting lower concentrations.

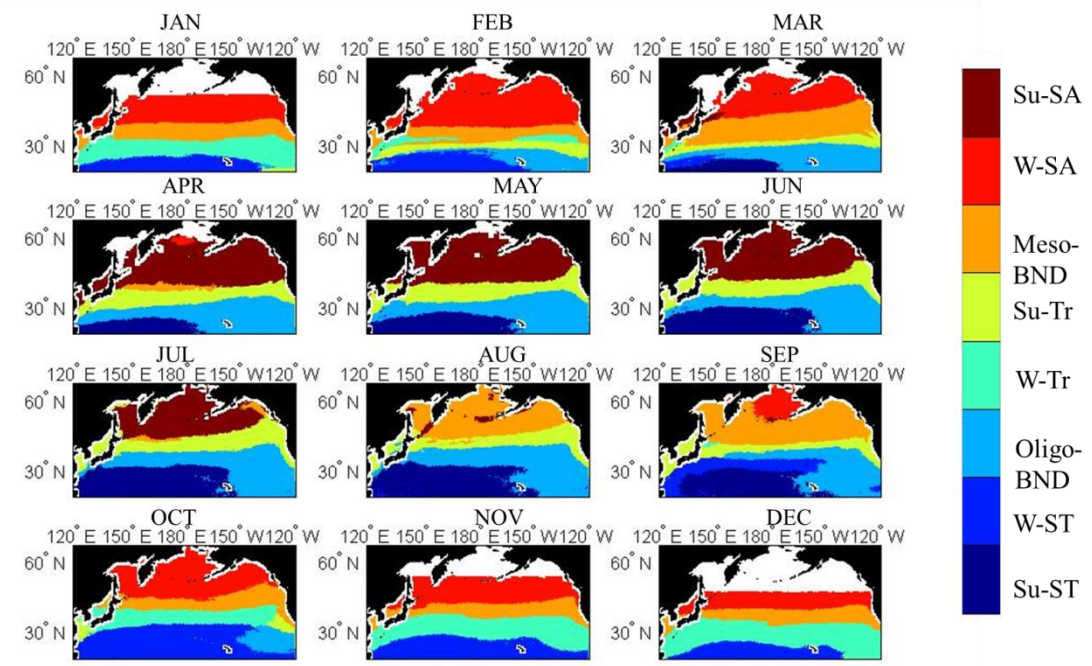

Figure 2.4. Seasonal migration of seascapes in the North Pacific basin: Level 2. Eight seascapes were classified using a combination of PRSOM and HAC; color codes reflect different seascapes ranked by their relative concentrations of chl-a. White areas denote regions excluded because of cloud cover, ice, or high chl-a mask. Seascape identifiers and their abbreviations are as in Figure 2.

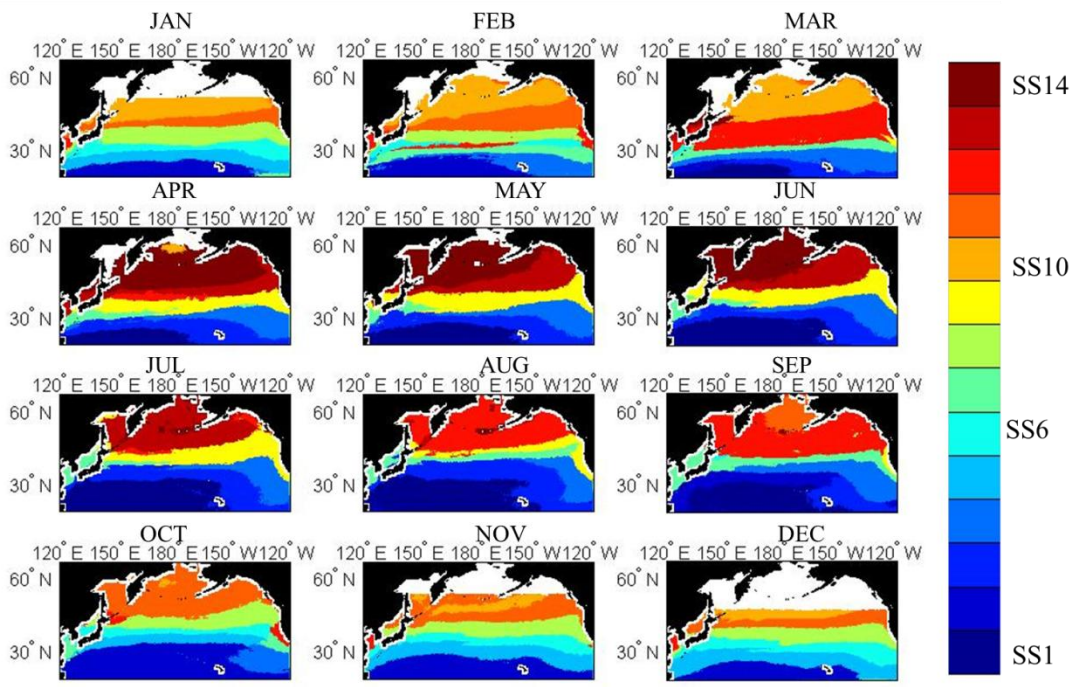

Figure 2.5. Seasonal migration of seascapes in the North Pacific basin: Level 3. Fourteen seascapes were classified using a combination of PRSOM and HAC; color codes reflect different seascapes ranked by their relative concentrations of chl-a.

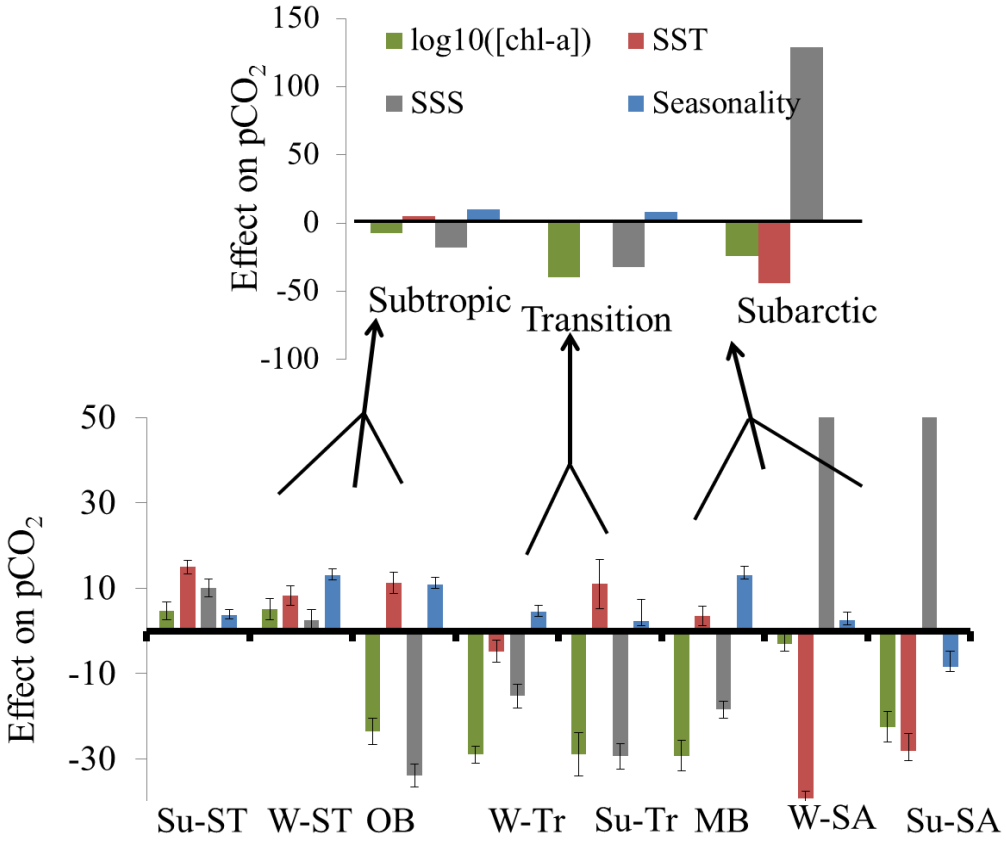

Figure 2.6. Effect sizes on pCO2 of SST, salinity, season, and [chl a]. Effect sizes were calculated using multiple linear regression analysis within seascapes. Only the first two levels are presented, see Table 2.10 for complete details.

Table 2.1. Summary Statistics of mean (standard error) satellite-derived SST, PAR, and chl-a within seascapes at three different hierarchical levels. % effective pixels depicts reduction in sample size following month-wise spatial decorrelation analysis. R^2 is proportion of variance explained by ANOVA of individual variables after decorrelation resampling (see methods for details). Seascapes that share letters are not statistically distinct from one another (Tukey-Kramer Honest Square Distance multiple comparisons analysis).

	% effective pixel	SST	PAR	Log_{10} (Chl-a)
Level 1: 3 seascapes				
Subtropics	0.18	24.3 (0.02)	46.4 (0.04)	-1.21 (0.001)
Transition	0.27	17.6 (0.02)	37.1 (0.05)	-0.71 (0.001)
Subarctic	0.47	8.3 (0.01)	25.0 (0.03)	-0.36 (0.001)
R^2		0.74	0.55	0.74
Level 2: 8 seascapes				
Summer Subtropics, Su-ST	0.24	27.6 (0.02)	52.3 (0.04)	-1.31 (0.001)
Winter Subtropics, W-ST	0.19	26.5 (0.02)	39.8 (0.04)	-1.27 (0.001)
Oligotrophic Boundary, OB	0.38	21.6 (0.02)	46.2 (0.03)	-1.13 (0.001)
Winter Transition, W-TR	0.28	22.3 (0.03)	26.8 (0.05)	-0.99 (0.002)
Summer Transition, Su-TR	0.44	16.0 (0.02)	40.7 (0.03)	-0.60 (0.001)
Mesotrophic Boundary, MB	0.15	12.8 (0.01)	25.5 (0.02)	-0.42 (0.001)
Winter Subarctic, W-SA	0.31	5.67 (0.01)	14.1 (0.03)	-0.40 (0.001)
Summer Subarctic, Su-SA	0.21	5.81 (0.01)	35.6 (0.03)	-0.26 (0.001)
R^2		0.89	0.86	0.80
Level 3: 14 Seascapes				
1	0.35	27.6 (0.02)	52.3 (0.03)	-1.31 (0.001)
2	0.43	26.5 (0.02)	39.8 (0.04)	-1.27 (0.001)
3	0.38	23.7 (0.02)	50.0 (0.04)	-1.16 (0.001)
4	0.19	20.3 (0.02)	44.1 (0.03)	-1.12 (0.001)
5	0.12	23.1 (0.02)	27.7 (0.05)	-1.06 (0.002)
6	0.15	19.4 (0.05)	23.6 (0.10)	-0.76 (0.004)a
7	0.24	20.2 (0.03)	36.7 (0.06)	-0.76 (0.002)a
8	0.05	14.8 (0.02)	17.1 (0.04)	-0.56 (0.001)
9	0.25	14.5 (0.02)	42.0 (0.03)	-0.55 (0.001)
10	0.15	3.43 (0.02)	13.8 (0.03)	-0.49 (0.001)
11	0.21	8.01 (0.02)	14.4 (0.03)	-0.31 (0.001)
12	0.40	12.1 (0.01)	28.3 (0.02)	-0.37 (0.001) b
13	0.14	8.29 (0.02)	37.2 (0.03)	-0.37(0.001) b
14	0.51	3.71(0.01)	34.2 (0.03)	-0.17(0.001)
R^2		0.94	0.90	0.83

Table 2.2. Partitioning of variance between and within seascapes. F-statistics from nested univariate and multivariate analysis of variance are reported separately. Adjusted R^2 includes penalties for increased parameterization. Chlorophyll concentrations were log-transformed prior to analysis. All F-ratios are significant ($p<0.05$) unless otherwise noted (NS).

	N parameters	Satellite Variable			
Level 1		SST	PAR	Chl-a	Multivariate
Seascape	2	305000	335900	369000	447000
Season within seascapes	3	7800	197000	21200	63500
Whole model	5	13000	301400	163000	254000
R^2_{adj} (whole model)		0.77	0.89	0.81	
Level 2		SST	PAR	Chl-a	Multivariate
Seascape	7	85300	96700	54000	133000
Season within seascapes	8	3200	28800	3700	11000
Whole model	15	118700	185000	59600	196000
R^2_{adj} (whole model)		0.9	0.94	0.82	
Level 3		SST	PAR	Chl-a	Multivariate
Seascape	13	75000	54000	33100	86800
Season within seascapes	14	985	10700	2200	4700
Whole model	27	116500	121400	41600	146600
R^2_{adj} (whole model)		0.94	0.94	0.85	

Table 2.3. Partitioning of variance among nested levels of seascapes. F-ratios from nested univariate and multivariate analysis of variance are reported separately. Adjusted R^2 includes penalties for increased parameterization. Chlorophyll concentrations were log-transformed prior to analysis. All F-ratios are significant ($p<0.05$) unless otherwise noted (NS).

	N parameters	Satellite Variable			
		SST	PAR	Chl-a	Multivariate
Level 1	2	1157000	482900	388800	1077000
Level 2 [Level 1]	5	77600	122300	8000	99000
Level 3 [Level 2, Level1]	6	25600	14300	6700	14000
R^2_{adj} (whole model)		0.94	0.90	0.83	

Table 2.4. Nested analysis of variance: effect of hierarchical seascape level on nutrients and pCO_2. F-statistics for each explanatory variable are shown and are significant ($p<0.05$) unless otherwise noted. R^2 denotes variance explained of fully nested model.

	Salinity	NnN	SiO_2	PO_4	NnN/ SiO_2	NnN/ PO_4	pCO_2	NPP
Level 1	1303	1074	772	1768	145	448	20	90
Level 2 [Level 1]	153	66	102	164	39	19	11	312
Level 3 [Level 2, Level1]	64	34	40	124	56	17	29	74
R^2	0.55	0.55	0.42	0.62	0.28	0.38	0.26	0.38

Table 2.5. Nested analysis of variance: relative role of within seascape variability on nutrients and NPP. F-statistics for each explanatory variable are shown and are significant ($p<0.05$) unless otherwise noted. R^2 denotes variance explained of fully nested model.

	Salinity	NnN	SiO_2	PO_4	NnN/ SiO_2	NnN/ PO_4	NPP
Level 2	168	174	74	166	53	102	17.6
Season[Level 2]	20	29	25	21	14	14	79.1
Space[Level 2]	18	5	15	13	5	^{NS} 1.8	4.9
Season*Space[Level2]	21	2.3	8	10	13	2.1	7.7
R^2	0.59	0.58	0.46	0.61	0.26	0.39	0.43

Table 2.6. Mean concentrations and ratios (+/- SE) of nutrients in surface waters of seascapes. Nutrient data collected from World Ocean Database archive. pCO2 data were collected from the Lamont-Doherty Earth Observatory. NPP data are from the carbon-based satellite productivity algorithm (CbPM, Westberry et al., 2008). See text for further methodological detail.

Seascape	N	NnN (µM)	SiO_2 (µM)	PO_4 (µM)	NnN/ SiO_2	NnN/ PO_4	pCO_2 (µatm)	NPP (mg C m^{-2} d^{-1})
Su-ST	385	0.26 (0.02)	2.51 (0.13)	0.08 (0.01)	0.13 (0.01)	4.04 (0.29)	361 (1)	416 (3)
W-ST	187	0.37 (0.09)	3.75 (0.31)	0.14 (0.01)	0.13 (0.03)	3.35 (0.52)	351 (1)	413 (4)
OB	700	0.25 0.02)	3.3 (0.09)	0.18 (0.01)	0.1 (0.01)	2.4 (0.17)	356 (1)	408 (3)
W-TR	282	0.61 (0.06)	2.89 (0.13)	0.15 (0.01)	0.23 (0.02)	5.25 (0.33)	331 (1)	359 (10)
Su-TR	953	1.67 (0.08)	5.1 (0.13)	0.36 (0.01)	0.3 (0.01)	4.53 (0.16)	342 (1)	600 (10)
MB	726	4.67 (0.17)	8.84 (0.25)	0.61 (0.01)	0.47 (0.01)	6.65 (0.18)	340 (1)	517 (8)
W-SA	233	6.31 (0.33)	11.8 (0.55)	0.85 (0.02)	0.57 (0.02)	6.96 (0.25)	342 (2)	266 (13)
Su-SA	519	7.53 (0.21)	14.0 (0.34)	0.9 (0.02)	0.59 (0.02)	7.8 (0.17)	333 (1)	660 (12)

Table2.7 Nested analysis of variance: relative role of within seascape variability on pCO_2 at three hierarchical levels determined from classification. F-statistics for each explanatory variable are shown and are significant ($p<0.05$) unless otherwise noted. R^2 denotes variance explained of fully nested model.

	pCO_2(Level1)	pCO_2 (Level 2)	pCO_2 (Level 3)
SS	24	15	14
Season[SS]	16	10	8
Space[SS]	7	5	3
Season*Space[SS]	25	9	2(NS)
R^2	0.13	0.27	0.41

Table 2.8. Comparison of variance explained between PRSOM and Longhurst classifications within and across months. Shown are F-statistics resulting from analyses of variance of surface [chl], NPP and a representative nutrient (Nitrate + Nitrite). All F-statistics are statistically significant ($p<0.05$) unless otherwise marked (NS). Bold= largest F-statistic and thus largest ratio of between group (explained) to within group (unexplained) variance.

	SeaWiFs [chl-a]			NPP (CbPM)			WOD- [Phosphate] (0-30 m)		
MO	N	PRSOM8	LONG-HURST	N	PRSOM8	LONG-HURST	N	PRSOM8	LONG-HURST
1	10.7	**11.5**	2.4	150	**38.9**	27	139	**65.1**	56.5
2	12.7	**27.9**	4.5	153	12.5	**19**	150	**46.6**	21.9
3	21	**20.6**	4	172	16.1	**32.8**	166	33.8	**41.7**
4	16	**19.9**	5.5	335	4.7	**10.1**	302	**41.2**	38.7
5	20.2	**16.7**	8.9	475	**42.1**	18.6	458	**99.8**	82
6	18.1	**18.9**	12.2	489	**71.2**	34.2	444	181	**191**
7	20.4	**39.9**	18.2	514	**61**	41	493	**297**	142
8	18.2	**43.5**	18.6	568	**97.9**	59.4	538	**304**	187
9	22.1	**25.7**	18.7	296	**43.6**	38.7	245	56	**71.8**
10	19.9	**44.6**	27.5	273	**6.8**	5.6	242	**94.1**	82
11	10.2	**10.8**	6	197	**37.8**	28.3	168	35.9	**36.9**
12	7.3	**9.8**	2.8	94	**10.5**	^{NS} 2.1	92	**42.1**	17.1
Weighted (N) mean		**26.2**	12.2		**47.6**	30.9		**167**	119
Mean		**24.2**	10.8		**36.9**	28.6		**108**	80.7

Table 2.9. Reduction in RMSE from Basin Scale to seascape or province scale of NPP predictive models. PRSOM= seasonally evolving seascape partition (this study); LONG= Longhurst provinces (Longhurst, 2006). Model A: NPP =*f* (SST, PAR, chl-a); MODEL B: NPP= *f* (SST, PAR, chl-a, season, space). SEAS= Scaled effect size of Season for Model B. SPACE= Scaled effect size of Space for Model B. % Reduction is based on RMSE of Basin scale Model A=0.151, MODEL B=0.150. Both chl-a and NPP were $\log_{10}$-transformed prior to analyses.

MODEL	Region	N	RMSE A	RMSE B	SEAS	SPACE
PRSOM	Su-ST	343	0.064	0.063	0	0.04
PRSOM	W-ST	165	0.067	0.065	0.05	0.04
PRSOM	OB	706	0.086	0.080	0.09	0.03
PRSOM	W-TR	214	0.192	0.190	0.12	0.11
PRSOM	Su-TR	915	0.087	0.086	0.03	0.07
PRSOM	MB	692	0.169	0.168	0	0.07
PRSOM	W-SA	225	0.208	0.190	0.26	0.19
PRSOM	SU-SA	507	0.120	0.113	0.13	0.06
AVERAGE			0.124	0.119	0.09	0.08
Weighted AVERAGE			**0.117**	**0.113**	**0.07**	**0.07**
% Reduction			**22.8**	**24.9**		
LONG	BERS	408	0.136	0.131	0.16	0.09
LONG	CCAL	834	0.107	0.104	0.11	0.06
LONG	KURO	654	0.165	0.161	0.19	0.08
LONG	NPPF	100	0.118	0.111	0.3	0.04
LONG	NPSW	591	0.141	0.138	0	0.09
LONG	NPTG	404	0.034	0.033	0.06	0.01
LONG	PSAE	290	0.105	0.093	0.42	0.05
LONG	PSAW	180	0.148	0.146	0.22	0.07
AVERAGE			0.119	0.115	0.18	0.06
Weighted AVERAGE			**0.121**	**0.117**	**0.14**	**0.07**
% Reduction			**19.9**	**22.0**		
PRSOM-LONG/ 0.5 (PRSOM+LONG)			-3.8	-4.1	-117.7	0

Table 2.10. Variable forcing of pCO2 by salinity, SST, [chl a] and Season within seascapes at different hierarchical levels. Effect sizes (+/-SE) for each explanatory variable are shown. Effects are significant ($p<0.05$) unless otherwise noted. R^2 denotes variance explained of full model. Pixels that were present in two or more seascapes were excluded. [chl-a] values were $\log_{10}$ -transformed prior to analysis.

		N	mean(pCO2)	Salinity	SST	[chl a]	Season	R^2
1st level	Subtropics	749	353 (0.49)	-17.8 (1.7)	4.8 (1.4)	-7.6 (2.0)	10.1 (0.9)	0.26
	Transition	219	336 (0.8)	-32.6 (2.8)	*2.7 (3.0) NS*	-40 (2.4)	8.3 (2.0)	0.62
	Subarctic	703	346	129 (4.6)	-43.8 (1.7)	-24 (3.1)	*2.4 (1.8) NS*	0.67
2nd level	Su-ST	244	358 (0.6)	9.9(2.1)	15(1.5)	4.6 (2.1)	3.8 (1.2)	0.34
	W-ST	197	349 (0.7)	2.5 (2.5) NS	8.3(2.2)	5.2(2.5)	13 (8.7)	0.35
	OB	308	353 (0.8)	-33.9 (2.7)	11.3 (2.43)	-23.5 (3.0)	10.9 (1.6)	0.41
	W-TR	145	336 (0.9)	-15.2 (2.8)	-4.8 (2.6)	-29 (1.9)	4.5 (1.5)	0.64
	Su-TR	74	335 (1.54)	-29.4 (5.0)	10.9 (5.7)	-28.9 (3.0)	2.3 (5.0) NS	0.65
	MB	181	333 (0.8)	-18 (2.0)	3.4 (2.3) NS	-29 (3.6)	13.1 (2.1)	0.54
	W-SA	300	356 (0.9)	148 (7.0)	-39.3 (1.7)	-3.1 (3.5) NS	2.5 (1.3) NS	0.78
	Su-SA	222	342 (1.3)	125 (5.2)	-28.0 (4.0)	-22.5 (3.7)	-8.5 (3.8)	0.78
3rd level	SS1	244	358 (0.6)	9.9(2.1)	15(1.5)	4.6 (2.1)	3.8 (1.2)	0.34
	SS2	197	349 (0.7)	*2.5 (2.5) NS*	8.3(2.2)	5.2(2.5)	13 (8.7)	0.35
	SS3	107	352(1.35)	-12.3(4.5)	10.7(3.5)	-17.5 (5.2)	12.7 (2.8)	0.22
	SS4	102	359 (1.1)	-29 (3.3)	27 (3.3)	7.9 (3.2)	16.5 (2.3)	0.65
	SS5	41	338 (1.4)	*4.0(3.6) NS*	*2.5 (4.3) NS*	-11.4 (4.0)	6.4 (2.6)	0.44
	SS6	23	340 (1.4)	-10.6 (2.8)	8.8 (3.9)	-26.4 (2.5)	*3.0 (2.5) NS*	0.88
	SS7	9	343 (2.1)	*-4.4 (8) NS*	163 (43)	-180 (47)	84 (28)	0.84
	SS8	67	328 (0.9)	-14 (1.7)	*-2.5 (2.6) NS*	-15.2 (2.6)	9.0 (2.4)	0.68
	SS9	36	336 (2.2)	-23.2 (4.5)	*8.1 (6.1) NS*	-16.2 (4.2)	3.4 (3.5)	0.56
	SS10	114	377 (1.5)	18.2 (4.9)	-28.8 (3.8)	*-1.3 (7.9) NS*	*1.9 (2.4) NS*	0.51
	SS11	67	341 (1.7)	77.9 (8.7)	*0.1 (5.9) NS*	-13.7 (3.1)	*5.1 (5.1) NS*	0.73
	SS12	96	336 (1.1)	135 (6.7)	-17.8 (3.9)	*-4.4 (3.2) NS*	*2.9 (4.4) NS*	0.84
	SS13	107	337 (1)	-16.6 (3.6)	*3.9 (2.9) NS*	-25 (4.5)	6.0 (2.2)	0.38
	SS14	108	349 (1.8)	134 (7.6)	*-34.2(5.8) NS*	-18 (5.1)	-17 (5.3)	0.82

CHAPTER 3: Satellite-derived seascapes describe unique assemblages and assemblage-environment interactions in the NE Pacific

3.1 ABSTRACT

Pelagic ecosystems comprise approximately 70% of the earth's surface. Metabolism in these regions is dominated by microscopic phyto- and bacterio-plankton. Patchiness of microplankton distributions in space and time combined with dynamic circulation of the seawater medium, however, limits the extrapolation of mechanism observed or inferred from in *situ* measurements to a larger spatiotemporal context. We classified seasonally dynamic satellite-derived seascapes in the North Pacific and collected flow cytometry data from two long-term time series and several opportunistic cruises that spanned several thousand kilometers of the NE Pacific. Analysis of spatiotemporal patterns in the flow cytometry data verified that the seascapes were regions of distinct microbial function. Multiple-response permutation analysis revealed differences in community structure across discrete seascapes, in terms of both absolute and relative abundances. Principal component analysis of the assemblage supported seascape divisions and revealed assemblage-driven structure along environmental gradients with strong associations with chlorophyll a and sea surface temperature and, to a lesser extent, with mixed layer depth and mean photosynthetically active radiation in the mixed layer. Differences of assemblage structure between seascapes and strength of environmental forcing were large in the subarctic and transition zones, but less pronounced in the subtropics, indicating satellite-detected changes in bulk properties that may be associated with local physiology or interannual shifts in seascape boundaries.

3.2 INTRODUCTION

Marine microbes are responsible for approximately half of the global primary production (Field et al., 1998; Behrenfeld et al., 2001) and contribute significantly to the transfer of carbon between the atmosphere and the deep ocean (Emerson and others 1997; Monahan and Denman, 2004). Predicted shifts in sea surface temperature (Behrenfeld and others 2006; Polovina and others 2009, 2011) and carbon chemistry (Feely and others 2008; Dore and others 2010) will likely impact both the structure and function of marine microbial communities (Liu et al, 2010). Quantifying the integrated response of marine ecosystems to climate change, however, is complicated by attributing shifts to physiology or biodiversity (Falkowski and others 2000). Furthermore, the movement and mixing of microbial "media" on multiple scales makes the delineation of systems difficult, thus cross-comparative analyses between systems or between mechanistic models and *in situ* data have been limited. In summary, predicting pelagic ecosystem responses and feedbacks to environmental perturbation is hampered by the lack of an objective framework to scale observations of microbial processes to ocean basins and to define how temporal and spatial scaling of microbial habitats in the open ocean may change regionally.

Just as terrestrial ecosystems are parsed into landscapes, the global ocean can be viewed as a mosaic of distinct seascapes composed of unique combinations of physical, biological and chemical elements (Chapter 2). Like landscapes, seascapes are conceptualized and analyzed as mosaics of discrete patches (Forman 1995; Turner and

others 2001). The dynamics of a system can be studied as the composite dynamics of individual patches and their interactions at adjacent hierarchical levels (Wu and Loucks, 1995; Chapter 2), thus comprising spatiotemporal scales ranging from habitat to province. A key difference between landscapes and seascapes is that the spatial hierarchy common to the conceptualization of landscapes must now be applied to the advective environment, leading to hierarchies in both space and time simultaneously (Chapter 2). From a microbial perspective, seascapes can range from the size and persistence of sinking particles to entire oceanic basins (Karl and Letelier, 2009), depending on the pattern or process of interest. However, the regularity and hierarchical nature of the patches in mixed ocean water means that plankton are distributed in a dynamic, but definite hierarchical seascape topography, where groups of patches coalesce between intermittent turbulent eddies (Mitchell et al., 2008).

With the increased availability and automation of flow cytometers (Thyssen et al., 2008; Sosik et al, 2009), phytoplankton ecologists are beginning to compile global autotrophic and heterotrophic cell abundance maps that highlight multi-scale statistical patterns. Flow cytometry lends itself well to seascape evaluation despite its taxonomic coarseness; it can provide sufficient sample sizes of cell abundances to document patterns at scales relevant to ecology, evolution, and oceanography (Li, 2009). The cell is the primary unit of natural selection for microbes (Levin et al., 2001). Cell abundance is an important ecological indicator for all marine microbes, regardless of trophic level and phylogenetic position (Li et al, 2006). Furthermore, functional grouping based on cell counts, unlike those based on pigment structure, provides a measure of phytoplankton abundance independent from that which can be synoptically assessed via satellite.

Understanding the spatiotemporal patterns of microbial abundances and the environmental factors that drive these patterns remains critical in microbial oceanography and biogeography. Both extrinsic (e.g. environmental) and intrinsic (organismal) processes are sources of heterogeneity and create complex space-time patterns in marine environments. The central tenet of the Bass-Becking hypothesis (reviewed in Fenchel and Finlay, 2004) is that variations in microbial community structure are attributed to environmental heterogeneity; rapid shifts in response to local environmental changes (e.g. during a bloom) are achieved by rapid growth capacity of previously rare groups. In oceanography, extrinsic forcing has tended to dominate especially in relation to turbulent mixing (Margalef, 1967; Cullen et al, 1991). However, intrinsic factors such as grazing, competition and viral lysis and syntrophic structure can also affect the behavior and structure of microbial communities (Sherr and Sherr, 1988; Bouvier and del Giorgio, 2007; Malfatti and Azam, 2009). Furthermore, endogenously driven oscillations of phytoplankton may facilitate the coexistence of several taxa on limited resources (Huisman and Weising, 1999), not only maintaining phytoplankton diversity but also resulting in increased primary production and export of carbon (Huisman et al., 2006). Thus, it remains necessary not only to quantify what environmental factors are important in driving microbial communities, but the importance each factor at each scale.

Here we assessed the seascape approach described in Chapter 2 at the microbial level using a cytometric data set based on multiple field efforts in the NE Pacific including two long-term time series. The goals of these analyses were to determine to what extent satellite-derived seascapes can be used to describe different microbial abundances and community relationships in surface pelagic waters, and to what degree we can scale local

environment-assemblage interactions to the large-scale. In order to validate the seascape concept at the microbial level, first we determined whether seascapes describe different microbial communities, and relatedly, whether boundaries between seascapes describe the intrinsic gradients or discontinuities in assemblage structure. Second, we investigated the environmental forcing of microbial communities using satellite and modeled data to determine the degree to which microbial structure can be predicted by easily obtained metrics. Finally, to determine the utility of the seascape concept to marine ecosystem models, we evaluated the drivers of the ratio of cytometrically-derived autotrophic to heterotrophic carbon to determine how predictive capacity of models are improved using sub-seascape forcing.

3.3 METHODS

3.3.1. Study Area

The North Pacific is a seasonally dynamic basin in which the oligotrophic and subarctic gyres are separated by the broad North Pacific current (NPC). In the eastern basin, the NPC broadens and bifurcates off the coast of the Washington State and British Columbia coast to form the Alaska and California Currents and the subarctic and subtropical gyres. The ecological dynamics of these gyres have been characterized mostly through the efforts at two long-term time series. In the subtropics, the Hawaiian Ocean Time Series (Winn et al, 1990; Karl et al., 2010) has been making near-monthly observations at Station ALOHA (A Long-Term Oligotrophic Habitat Assessment, Station ALOHA; 22.75ºN, 158ºW) since 1988. In the subarctic, Station Papa (OSP, 50ºN, 145ºW) has been

sampled intermittently from the 1940s; however, OSP and Line P that extends from the Strait of Juan de Fuca, have been observed more extensively since the early 1990s as part of Joint Global Ocean Fluxes Study (JGOFS; Freeland, 2007).

3.3.2 Classification

Because of the strong, complex, coupling of plankton to physical forcing at the level of cells (Jassby and Platt,1976), local communities (Steele, 1992; Belgrano and others 2004) and metacommunity (e.g. Liebold, 2006) and mesoscales, we chose a classifier that was robust to nonlinear interactions and maintained underlying biophysical distributions. Detailed description of the classification methodology can be found in Chapter 2 and Saraceno et al. (2006). In brief, we used a probabilistic version of Kohonen's self-organizing map (PRSOM, Anouar et al., 1998) combined with a hierarchical ascending classification (HAC, Jain and Dubes, 1988) to achieve a non-linear, topology-preserving data reduction of seasonal climatologies of satellite derived chl-a, sea surface temperature (SST), and photosynthetically active radiation (PAR). This method classified coherent regions in space and time simultaneously (Chapter 2). As with most self-organizing mapping methods, the PRSOM uses a deformable neuronal net to maintain data similarities and topological order between clusters. The PRSOM, however, introduces a probabilistic formalism; clusters are produced by approximating the probability density function with a mixture of normal distributions and optimizing based on a maximum likelihood function (Anouar and others, 1998). Three levels of hierarchy were objectively

determined. Here we focus on the level at which most biogeochemical variability was explained, resulting in eight seascapes (Chapter 2).

3.3.3 Verification of microbial communities

Differences in microbial community structure within, between, and among seascapes were determined with data collected from the Hawaiian Ocean Time-series (HOT) program (Station ALOHA; 22.75ºN, 158ºW), the Canadian Institute for Ocean Sciences (Line P and Station Papa; 50ºN, 145ºW), as well as cruises associated with the University of Hawaii and the University of Washington. Cell counts of microbial taxa were available for 6 cruises that occurred along Line P during June 2007 to February of 2009, monthly cruises to Station ALOHA from 1998 to 2010 and 5 additional cruises during 2003, 2005, and 2008 that spanned several thousand km in the NE Pacific. In total, nearly 450 stations were included in the analysis (N=447), spanning 40 degrees in latitude (15-54.5 N), over 35 degrees of longitude (198-234 W) and 13 years (1998-2010). Surface data were collected either on station with niskin bottles at 5 and 25 m, or from the ship's flow through system (5 m, Line P only). Paired comparisons revealed no differences in community structure as a function of sampling method (Kavanaugh, unpubl. data). There were four total taxa categories at Station ALOHA (*Prochlorococcus*, PRO; *Synechococcus*, SYN; nanoeukaryotic phytoplankton, EUK; and heterotrophic bacteria, HET) and six for all others after 2007 (small micro-eukaryotic phytoplankton, nanoeukaryotic phytoplankton, *Prochlorococcus, Synechococcus*, High nucleic acid heterotrophic bacteria, and low nucleic acid heterotrophic bacteria). For the cross-basin

analyses, we combined the categories for the high and low nucleic acid groups into a single heterotrophic count and the micro and nano category into a single eukaryotic category. In late 2005, cell enumeration at Station ALOHA switched from Hoechst staining (Campbell et al., 1994) to the use of a Cytopeia Influx flow cytometer to better quantify high-light adapted *Prochlorococcus* (e.g. Viviani et al., 2012). For all other samples, cells were classified and enumerated using a FACS-Caliber flow cytometer (Sherr et al., 2005, 2006). *Prochlorococcus* counts at Station ALOHA from 2001-Sept 2005 were interpolated using simple linear regression based on the seasonal evolution of absolute counts of other taxa at Station ALOHA: Log ($Pro_{N\text{-}cell}/Total_{N\text{-}cell}$) = 0.42 - 0.0164*Log ($SYN_{N\text{-}cell}$) - 0.019*Log ($EUK_{N\text{-}cell}$) - 0.004*Season ($R^2_{1, 68}$ =0.86, $p<0.001$). . Carbon content in each class was calculated using the following conversions: heterotrophic bacteria, 12 fg C $cell^{-1}$ (Sherr et al, 2006); *Prochlorococcus*, 50 fg C $cell^{-1}$ (Campbell and Vaulot, 1994; Partensky et al, 1999); *Synechococcus*, 250 fg C $cell^{-1}$ (Partensky et al, 1999); and small eukaryotic phytoplankton, 1500 fg C $cell^{-1}$ (Zubkhov et al, 2000).

3.3.4 Environmental variables

Archived 18 km resolution monthly satellite data (SeaWiFS chl-a, PAR; AVHRR SST) or modeled mixed layer depth (MLD) were downloaded from the Ocean Productivity Page and matched with *in situ* data using a 3-dimensional (x, y, t) nearest neighbor match.

The change in light through the water column was calculated per pixel using the Beers-Lambert equation:

$$E_z = E_0 e^{-K_d z;}$$

where E_0 was assumed to be surface-incident PAR and downward attenuation of light (K_d) was calculated as the sum of attenuation by surface chlorophyll (K_{chl}) and seawater ($K_{SW= 0.04}$). K_{chl} was calculated using the Morel (1988) model for chlorophyll-specific attenuation. We assume that K_{chl} is the dominant biogenic optical constituent and that relative contributions by detrital and dissolved constituents are minimal and covary with K_{chl} in space. Mean PAR within the mixed layer was determined by sum (PAR_z, z=0 to z=MLD), and dividing by MLD. We recognize that actual conditions experienced by a cell are affected by the short time- and space-scale interactions between turbulence and abundance and character of abundance and composition of chlorophyll-containing cells (Ross et al., 2011). However, here we are concerned with effects of shoaling of the mixed layer at the longer scales of our grid resolution (0.25 degree x 1 month).

3.3.5 Statistical Analysis

Analysis of variance was used to determine whether seascapes described differences in individual taxonomic groups or environmental variables. For the assemblage as a whole, a multiple response permutation procedure (MRPP) was conducted to determine the statistical significance of within-seascape dispersion compared to between-seascape dispersion using Euclidean distances (Mielke & Berry, 2001). This procedure yields three

statistics: the test statistic (T) which describes the separation of seascapes, where T becomes more negative with stronger separation; an A-statistic (-1 : A : 1), describing the effect-size of the grouping or within seascape homogeneity; and a p-value, which evaluates the likelihood that observed differences between seascapes are due to chance (McCune & Grace,2002). We assess the assemblage structure measured in terms of both absolute and relative abundance (to total cell count) of taxonomic groups. Counts were log-transformed and ratios were arc-sine square-root transformed prior to analyses.

To determine whether seascape boundaries captured major or minor gradients in taxonomic structure we conducted ordination analysis on absolute and relative abundance of cells. Ordination has been used in many forms of ecology to describe the strongest pattern of species composition, most generally along single or multiple gradients. In ecology, gradient analyses can be divided into two groups: direct and indirect. Direct gradient analysis is used to determine how the assemblage is organized along a specific gradient of interest (Beals, 1969; Oksanen 1997). Sociological (sensu Beals, 1984) or indirect analysis looks for gradients via covariation and association among taxonomical units. Hybrids of the two exist (e.g. canonical correspondence analysis), and ordinate sample units in constrained species space that is determined by correlations with environmental variables. Disadvantages of most direct and hybrid forms are that they assume that the most important factors leading to community structure are environmental, that we have appropriately predetermined these factors, measured them, and measured them at appropriate scales (Beals, 1984).

In order to account for potential local and global non-linearity between taxonomic abundances, we examined continuous structure of microbial assemblages using both classic (principal components analysis, PCA) and non-classic multidimensional scaling analysis (NMS) on standardized matrices (z-scores). Unlike PCA, NMS does not assume local or global linear relationships between taxa and ordinates variance along principal gradients using ranked order instead of correlation. Thus, it is considered a more robust assessment of shifts in ecological communities where nonlinear interactions are common. However, NMS is non-parametric, thus the advantage of PCA lies in its potential use in predictive models. Initial analyses demonstrated that variance explained and correlations between taxa or environmental variables and the principal coordinates were strikingly similar between ordination methods. We therefore report results only for PCA. Scores along main axes were then calculated and used to represent the direction and magnitude of shifts in multivariate community structure associated with different environmental variables.

In order to determine the relative importance of environmental forcing as well as the relative importance of measured environmental variables on the microbial community within and across seascapes, partial least squares (PLS: Wold, 1985) regression was conducted. PLS is a useful tool to determine the relative effect of multiple explanatory variables on a multivariate data set when the colinearity of the explanatory variables of concern, it is unknown whether the major explanatory variables have been measured and when the number of explanatory and response variables is high relative to the sample size (Carrascal et al., 2009). PLS was conducted on relative abundances of microbial taxa and the ratio of autotrophic to heterotrophic carbon within and across seascapes to determine

the predictive capacity of easily obtained satellite or modeled environmental drivers. Centered and scaled coefficients are reported, whether coefficients are important for projecting latent variables onto X, Y space (Wold, 1985) as well as cumulative variance explained by final model explanatory and response variables (multivariate). PLS produces stable results with regard to both the identification of relevant explanatory variables as well as the magnitude of their effect sizes (Carrascal et al., 2009); variables with low effect sizes and importance <0.8 (Wold, 1985) are generally though to bear little on responses.

3.4 RESULTS

3.4.1. Seascapes

Divisions, seasonal evolution, and biogeochemical patterns among seascapes were previously described in Chapter 2. Briefly, at the basin scale the subtropical, transition, and subarctic divisions emerged as distinct systems with eight, then fourteen, seascapes emerging in a hierarchical fashion from the initial three seascapes. At the second level of hierarchy, three seascapes each arose from the subtropics and subarctic whereas two resulted from division of the transition zone (Figure 3.1). Seascapes were nominally identified based on dominant season, geographic region and/or trophic status based on mean chl-a concentration, specifically: 1) Summer subtropical (Su-ST); 2) Winter subtropical (W-ST); 3) Oligotrophic boundary (OB); 4) Winter transition (W-TR); 5) Summer transition (Su-TR); 6) Mesotrophic boundary (MB); 7) Winter subarctic (W-SA); 8) Summer subarctic (Su-SA). In situ measurement density was minimal in the Su-ST and W-TR (N=15 each), maximized in the OB by contributions of Station ALOHA (N=118) and ~60 in each of the remaining five seascapes (Table 3.1, Figure 3.1d).

3.4.2. Differences across seascapes of environmental variables

As expected, seascapes explained most of the variance in SST, chl-a and PAR (R^2 ANOVA =0.94, 0.90 and 0.83 respectively). Seascapes also explained most of the variance in mixed layer depth and mixed layer PAR (R^2 ANOVA =0.53, 0.77 respectively). Given that the PRSOM-HAC combination chose based on gradients in *climatological* SST, chl-a and PAR, this is not a surprise; however it does suggest that at

the basin scale, year to year differences in environmental variability are less pronounced than seasonal differences.

3.4.3. Differences across seascapes of microbial abundances and assemblage

Microbial abundances and assemblage structure were different across seascapes. Seascape averages explained nearly 75 % of the variability in abundances in eukaryotes, 69% of *Synechococcus*, >60 % of the variability in heterotrophic bacteria and > 90% of the variation in *Prochlorococcus* abundance across the study area (Table 3.1, Figure3. 2). *Prochlorococcus* abundances peaked in the subtropical seascapes, were negligible in the transition and absent in the subarctic seascapes. While there were no differences in absolute *Prochlorococcus* abundances between subtropical seascapes, the relative abundances were higher in the winter seascapes (W-ST and W-TRAN, Figure 3.3) driven primarily by lower heterotrophic bacteria counts. Heterotrophic bacteria peaked in abundance in Meso-BND seascape, followed by the Su-TRAN seascape. Eukaryotic phytoplankton exhibited similar peaks in abundance with distinct maxima in the Meso-BND, followed by the Su-TRAN and the Su-SA. Eukaryotic algae exhibited the smallest relative abundances in the W-ST and Oligo-BND seascapes; however, flow-cytometric methods may miss larger diatoms involved in symbiotic diazotrophic relationships. *Synechococcus* peaked in abundance in the Su-TRAN, with a secondary peak found in the Su-SA.

Total flow cytometrically derived particulate organic carbon (POC) was highest in the Su-TRAN and MB seascapes with estimated POC of 60-70 $\mu g\ l^{-1}$ compared to ~ 25

µg l^{-1} in the subtropical seascapes and ~40 µg l^{-1} in the subarctic (Figure 3.4). While eukaryotic algae and *Synechococcus* were large contributors to POC in the transition, the dominant contributor was heterotrophic bacteria. Thus, both the Su-TRAN and MB had relatively low Ac: Hc ratios, ~1 and 0.7, respectively.

Multivariate cytometric community structure was strongly different between seascapes as revealed by the MRPP analyses (Table 3.2), in terms of both absolute ($A=0.79$, $p<0.0001$) and relative abundances ($A=0.59$, $p<0.0001$). Pairwise comparisons indicated that subarctic seascapes and the Su-TRAN seascape were distinct from all other seascapes (Tables 3.3 and 3.4). In the subtropics, the Su-ST was distinct from both the Oligo-BND and W-TRAN seascapes, but not different from the W-ST. In addition, the W-ST was also not distinct in terms of microbial assemblages from the Oligo-BND, but was different from the W-TRAN.

At broad scales, community dissimilarity in the NE Pacific was driven by the presence or absence of *Prochlorococcus,* shifts in abundances of eukaryotic phytoplankton and gradients in SST and chl-a (Figure 3.5 a). These variables were strongly correlated with the first PC axis that explained over 75% of the variation in community structure (Table 3.5). A secondary gradient (PC2= 20.1%) was associated by the opposing shifts in abundances of heterotrophic bacteria and *Synechococcus*. These divisions were correlated with changes in mixed layer depth, mixed layer depth light, and subseasonal, local temperature effects. Excluding *Prochlorococcus* from the analyses resulted in similar spatial patterns but moderate shifts in the variance attributed to each axis with decreases

in the relative importance of PC1 (from 75 to 68%, data not shown: DNS) and increases in the relative importance of PC2 (from 20 to 25%, DNS).

Ordination patterns were only weakly different when communities were characterized in terms of relative abundances (Figure 3.5 b, Table 3.6). The first PC explained slightly more variance than the non-relativized data (81.7% v. 75.4%), but total variance explained was not different (95.7% v. 95.5%). Exceptions to this occurred with the second PC, where in general environmental effects were dampened compared to the absolute set, and the effect of the relative abundance of *Synechococcus* became more pronounced, demarcating differences between the Su-SA W-SA and MB subarctic seascapes.

3.4.4. Difference in environmental forcing of seascapes

At the basin scale, three variables were necessary to describe ~75 % of the community structure, with chl-a and SST being somewhat equally important and then followed by PAR (Tables 3.7 and 3.9). However, within each seascape, the dominant forcing varied regarding their magnitude and what attribute of the community structure they most affected. For example, chl-a was an important correlate to community structure across the basin but its relevance as a predictor is opposite (Su-ST) or lower subtropics (W-ST, Table 8). Conversely, SST is relatively less important in the subarctic seascapes, and is absent as an effect in the W-TRAN (Tables 3.8 and 3.10). Finally, while MLD and MLDPAR were not important explanatory variables at the basin scale, for individual taxa or seascapes they were relatively important (Tables 3.8 and 3.9). For example, the local

positive effects of MLDPAR on *Synechococcus* in the Su-ST, W-SA and Su-SA led to a relatively strong effect of MLDPAR basin wide on *Synechococcus*. Across all taxa, however, MLD and MLDPAR were important for driving patterns primarily only in the Su-TRAN and W-SA.

While the environmental variability constrained by the partial least squares (PLS) regression analysis was on average >90%, the percentage variation in taxa explained by the model was highly variable. Environmental variability explained substantial variability in both absolute and relative cytometric structure for both TRAN seascapes, the Su-ST and the W-SA, however little variability in cytometric structure (absolute or relative) was revealed by environmental forcing in the MB. Nevertheless, as suggested from the general patterns above, within-seascape tuning of PLS resulted in dramatically improved predictive capacity for absolute abundances (Figure 3.6), relative abundances (Figure 3.7), and most particularly for predicting the ratio of autotrophic to heterotrophic carbon (Ac:Hc, Figure 3.8).

Basin scale predictive capacity of Ac: Hc was dramatically improved by incorporating local environmental forcing within seascapes, with variance explained by the model increasing from 17 to 45 % (Figure 3.8 b, Table 3.11). Adding interannual variability to within-seascape forcing increased the variance of Ac: Hc explained to 61% (Figure 3.8 c). Adding interannual variability increased variance explained within each seascape, from an average of 11% to 64%. Across seascapes, predictive skill from environmental variables was highest in the TRAN and ST seascapes, and moderate in the subarctic seascapes, although the relative importance of environmental drivers was

different (Table 3.12). The addition of interannual variability also improved within-seascape predictive capacity, primarily within the subarctic summer, the two boundary seascapes (OB and MB) and secondarily within the W-ST.

3.5 DISCUSSION

Here we have described a quantitative seascape framework for the NE Pacific that is derived from easily obtained satellite metrics and is relevant to the scale of microbial assemblages. Satellite-derived seascapes describe differences in microbial structure and appear to follow natural discontinuities of underlying intrinsic gradients as revealed by principal component analysis. Seascapes also describe variation in extrinsic (environmental) drivers of community structure. While chl-a, SST, and PAR capture basin-scale patterns well, addition of mixed layer dynamics and local tuning of parameters resulted in substantial gains in predictive model skill. Thus, the framework presented may be useful for scaling and validating ocean ecosystem models and developing macroecological theory for pelagic microbial systems.

Open ocean time-series programs have advanced mechanistic understanding of pelagic microbial ecology and documented shifts in the subtropical gyre (Karl et al., 1995, 2001; Corno et al., 2008) and subarctic North Pacific (Hare et al., 2000; Harrison, 2002). Up to now, *in situ* validation efforts of would-be seascapes have been primarily hydrographical (Oliver and Irwin, 2008) or biogeochemical (Chapter 2). Biogeographical comparisons across contemporary satellite-derived regions have been limited to exploring single taxa (i.e. Gomez-Pereira et al., 2010); alternately, the different biophysical relationships that these regions represent should give us insight as to changes in entire microbial assemblages (Margalef 1978, Cullen et al., 2002). In our study, we found that seascapes represented seasonal shifts in microbial assemblages, thus providing a means of spatially extrapolating the seasonal patterns found at single stations (Fuhrman et al.,

2006; Giovannoni and Vergin, 2012). Now embedded in a seascape framework, the rich history from open-ocean time series can form a bridge between the spatiotemporal scales of microbial assemblages in surface waters to that of the global satellite monitoring system.

Variability in NE Pacific microbial communities is nonrandom at the population level, with satellite-derived seascapes representing differences in abundances and structure of microbial communities. This result agrees with genetic analyses of bulk water or sediments that have documented spatiotemporal shifts in individual taxonomic groups (Bibby et al., 2009, Cermeno et al., 2010) as well as shifts in the co-occurrences of bacterioplankton and *Prochlorococcus* (Eiler et al., 2011). However, here we document shifts in community structure at the level of the mixed population. While we recognize that the functional grouping of flow cytometry may be coarse compared to genetic analyses of bulk water, the sampling of flow cytometry (<3 ml) is more relevant to that of microbial cell ecology than a typical genetic analysis (> 10,000 ml). Thus, our results represent a robust verification of satellite-derived seascapes at the microbial scale. Furthermore, because of the robustness of our method to small sample sets, particularly the PLS regression, we now have a framework by which sparsely sampled indicators can be tested against intrinsic and extrinsic forcing within and across seascapes.

At broad scales, the three variables SST, chl-a and PAR define 75% of the variance in community structure and greater than 70 % of the variance for most individual functional groups. This result confirms those of studies that consider the predictive power of chl-a or chl-a and SST for predicting ecologically meaningful regions

(Platt and Sathyendranath,1999) and/or size structure of cells (Uitz et al., 2006; Barnes et al, 2011). However, the predictive capacity of these parameters tends to diminish at local to mesoscales where non-linearities or delays (Hill et al., 2012) in biological responses to physical forcing or ecological interactions such as competition, grazing, or viral lysis may contribute to patterns of abundance. Importantly, we cannot disentangle the effects of intrinsic factors from those of environmental parameters not measured, or patchiness of satellite-based parameters at spatial scales < 0.25 degree. Nevertheless, we assert that the seascapes provide an objective framework by which to test hypotheses regarding the nature of organization of pelagic planktonic communities, both in the field and with modeled scenarios.

The strength of within-seascape environmental forcing and the role of different particular factors in driving community structure were different across seascapes. In particular, the distribution of *Prochlorococcus* tends to have profound regional and local forcing. Differences between relative abundances in subtropical seascapes were driven by small shifts in relative abundances of *Prochlorococcus* and heterotrophic bacteria from winter to summer. While there were pronounced differences in Su-ST and W-ST, they were not as strong between Oligo-BND and Su-ST. In general, seascape differences were less distinct in the subtropics. Three potential reasons could contribute to this. Subtropical assemblages may be affected by mesoscale (sub-monthly) events not captured by monthly satellite averages, chl-a shifts characterized by satellites may reflect photoacclimation in the subtropics, and assemblages may be affected by not just seasonal but also interannual variability of the boundaries of subtropical seascapes. Model prediction was substantially improved by adding year-to-year variability, although this in

itself does not preclude the other possibilities. Thus, the relative importance of seascape variability compared to other sources of spatiotemporal variability in the subtropics remains to be determined.

In experimental settings, plankton patches have found to exhibit regular topography at scales of 10 centimeters to meters (Mitchell et al., 2008). Here we show hierarchical structure of microbial assemblages that link the scale of shipboard sampling (1 m – 10 m) to seascapes to basin-scale environmental variability via satellite-derived properties. The hierarchical patch structure may link large-scale processes and microscale interactions, acting as fundamental components of marine ecosystems that influence grazing efficiency, taxonomic diversity, and the initiation of aggregation and subsequent carbon flux (Mitchell et al., 2008). The ratio of heterotrophs to autotrophs may be indicative of the trophic status of the water column (Gasol et al., 1997) and thus a biomass-based metabolic indicator of the functioning of the biological pump. In our study, the relative abundance of heterotrophs was different between seascapes and was associated with the assemblage-driven gradients within seascapes. On a macroscale, the relative abundance of autotrophs to heterotrophs was associated with temperature gradients in the subtropics and but correlated with chl-a in the subarctic.

Locally, however, several factors likely interact to drive the relative abundance of autotrophs to heterotrophs. Furthermore, our observations are limited by the unknown variability of carbon per cell in our sample set, the role of allocthonous dissolved organic matter, and the relative activity of cells, especially heterotrophic bacteria. The latter likely contributed to somewhat low Ac: Hc values especially in the Su-TR and MB

seascapes where total FCM-derived organic carbon was greater than 50 µg C l^{-1}. We also cannot infer mechanism from our observations. For example, increases in SST may lead to increased bacterial remineralization or increased grazing efficiency on small phytoplankton (Chen et al., 2012), both of which would result in decreased Ac: Hc in the subtropics. Nevertheless, we assert that our objectively derived seascapes that are validated for patterns associated biogeochemical and microbial assemblages may provide both an objective extent by which to parameterize models as well as spatiotemporal boundaries of inference for future mechanistic experiments.

Seascapes may provide an objective means to determine whether local environmental perturbations (habitat effects) or the large-scale, long-term legacy of historical differentiation in habitats (provincial effects) describe extant differences in microbial community structure and thus merge microbial oceanography with macroecology (Brown, 1984, 1995, Martiney et al., 2006, Li 2009*).* In our study, *Prochlorococcus* was strongly correlated with shifts in light, temperature, and chl-a across seascapes at the basin scale. While the distribution of *Prochlorococcus* was weakly structured in reference to environmental variables within any given seascape, local tuning did improve within seascape predictive power. This suggests that large-scale modeling of *Prochlorococcus* may need to incorporate both habitat and provincial effects on microbial abundances and their subsequent structure. The interaction between habitat and history may be scale-dependent and may vary among populations or systems. Determining whether the seascape concept presented here describes an empirical hierarchy or one of co-evolution of multiple populations, as suggested for landscapes

(Lidecker 2008), requires further testing at multiple scales with modeled and *in situ* data where available.

Objective seascape studies may allow us to constrain uncertainty when predicting phytoplankton functional diversity (e.g. Alvain et al., 2006) with only a handful of satellite variables and the addition of space, time and history. In our seascape-based analyses of assemblages in the subarctic and subtropical gyres, we were able to account for ~ 60% to almost 90% of the variability of single taxa as well as document the shifts and drivers of microbial community structure within and across seascapes. Imposing objectively derived boundaries can help optimize the modeling of selective pressures on phytoplankton (Bragg et al., 2010) and thus provide insight into the feedbacks between local ecology and global biogeochemical cycles. The seascapes may thus provide an objective basis to quantify spatiotemporal patterns of phytoplankton diversity (Barton et al., 2010; Follows et al., 2007) and phenology (Ji and others, 2010), and address fundamental questions such as how ecosystem size, connectivity, and stability (Cermeno et al., 2010) may affect phytoplankton richness. In our study, environmental forcing explained different amounts of variability for different seascapes suggesting that there is spatial heterogeneity in the strength of local drivers of microbial community structure. We cannot disentangle the effects of sub-pixel and unmeasured environmental variation from assemblage-driven forces. Nevertheless, the seascape provides an objective extent by which future studies, both in situ and modeled, can test these hypotheses.

Conclusion: On land, the field of global change biology uses the lens of landscape ecology to extrapolate mechanism and mean responses derived from community ecology

and ecophysiology to the global scale; conversely, the same lens provides larger spatiotemporal context and thus informs our understanding of how regional processes affect local variability. Here we present an objective classification of distinct seascapes that have been spatiotemporally validated at the microbial level in both oligotrophic and HNLC regions- the suite of which cover over 90% of the global ocean (Moore et al., 2004; Karl et al., 2010). Satellite-derived seascapes in these regions have different environmental forcing and represent shifts in phytoplankton and bacterioplankton abundances, community structure and carbon allocation. For the first time, we bring together the rich history of ocean time series with the synoptic coverage of satellite-derived seascapes in a spatiotemporally explicit manner akin to the context of landscape ecology. The resultant objectively defined, dynamic seascapes represent an important first step toward developing a quantitative framework for pelagic seascape ecology and a means for testing ecological concepts in the open ocean.

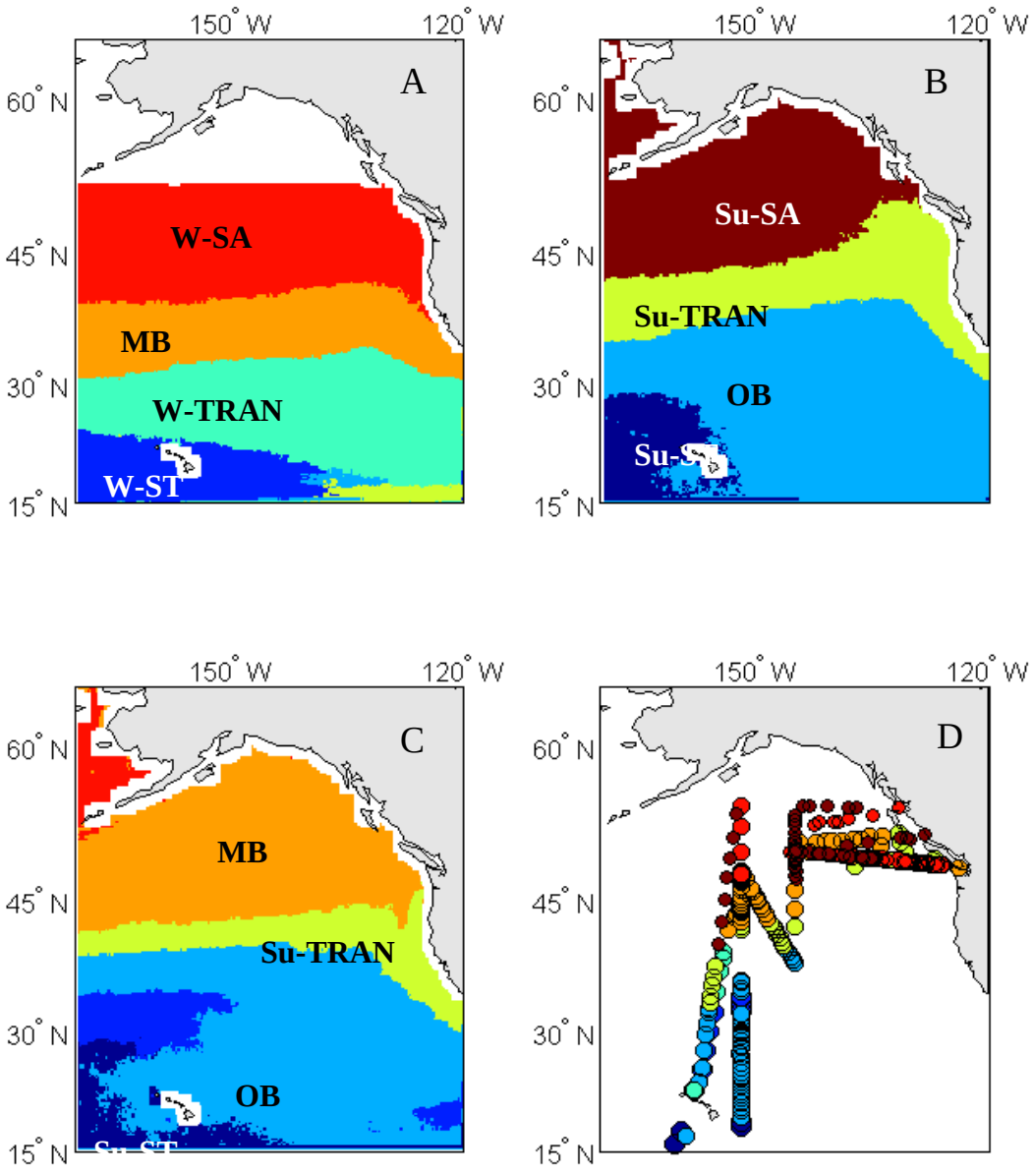

Figure 3.1. Seasonal progression of and sampling locations within seascapes in the North Pacific: A) January; B) May; C) October; D) Flow cytometry sample locations. Sample locations are color coded by seascape; size differences of circles are to allow visualization of samples taken at the same coordinates over multiple time periods. Eight seascapes are represented in the seasonal cycle: 1) Summer subtropical (Su-ST); 2) Winter subtropical (W-ST); 3) Oligotrophic boundary (OB); 4) Winter transition (W-TR); 5) Summer transition (Su-TR); 6) Mesotrophic boundary (MB); 7) Winter subarctic (W-SA); 8) Summer subarctic (Su-SA)

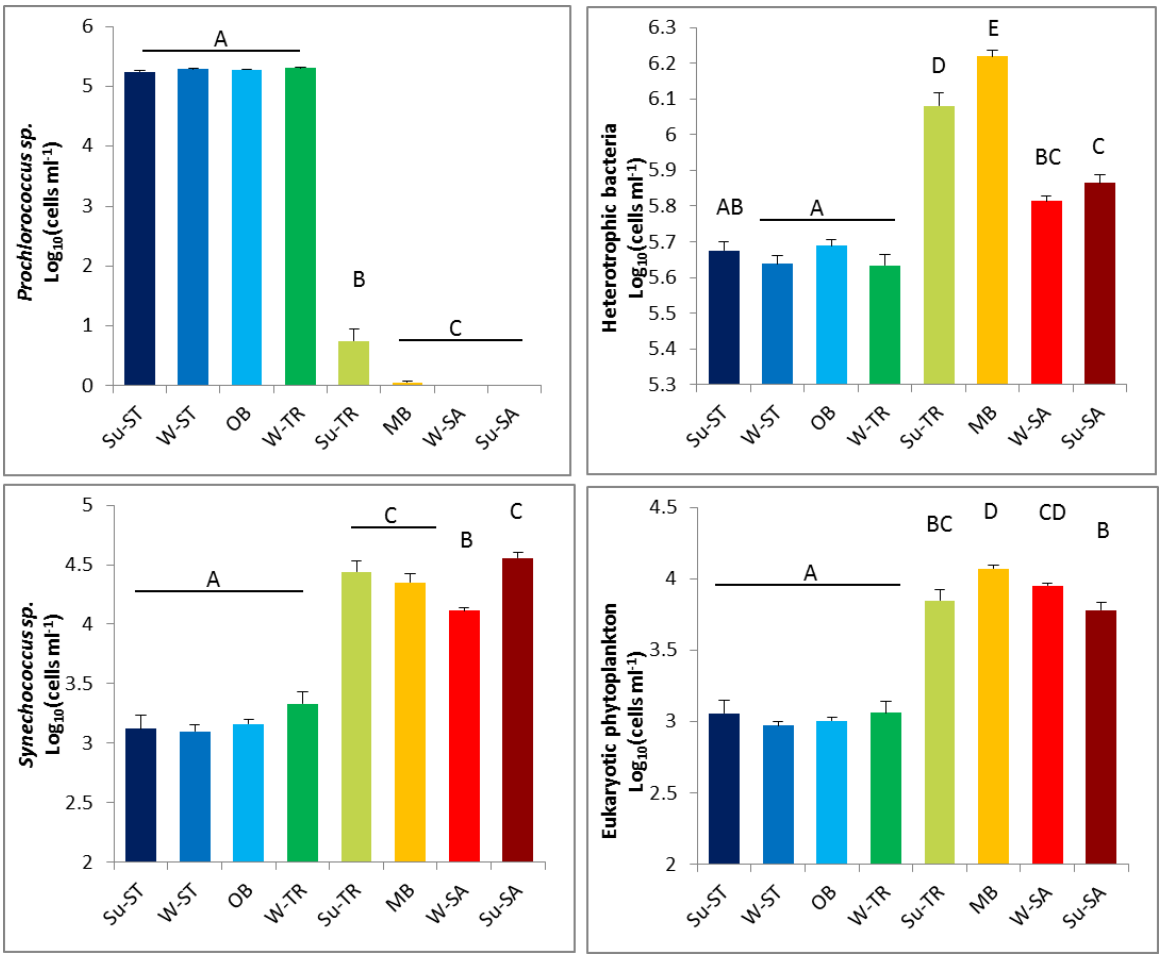

Figure 3.2. Differences of cell abundances across seascapes for *Prochlorococcus*, Heterotrophic bacteria, *Synechococcus*, and Eukaryotic phytoplankton. Letters that are unique denote pairs that are statistically different after adjusting for multiple comparisons (Tukey-Kramer HSD, $p<0.05$). Color codes correspond to seascapes as in Figure 3.1.

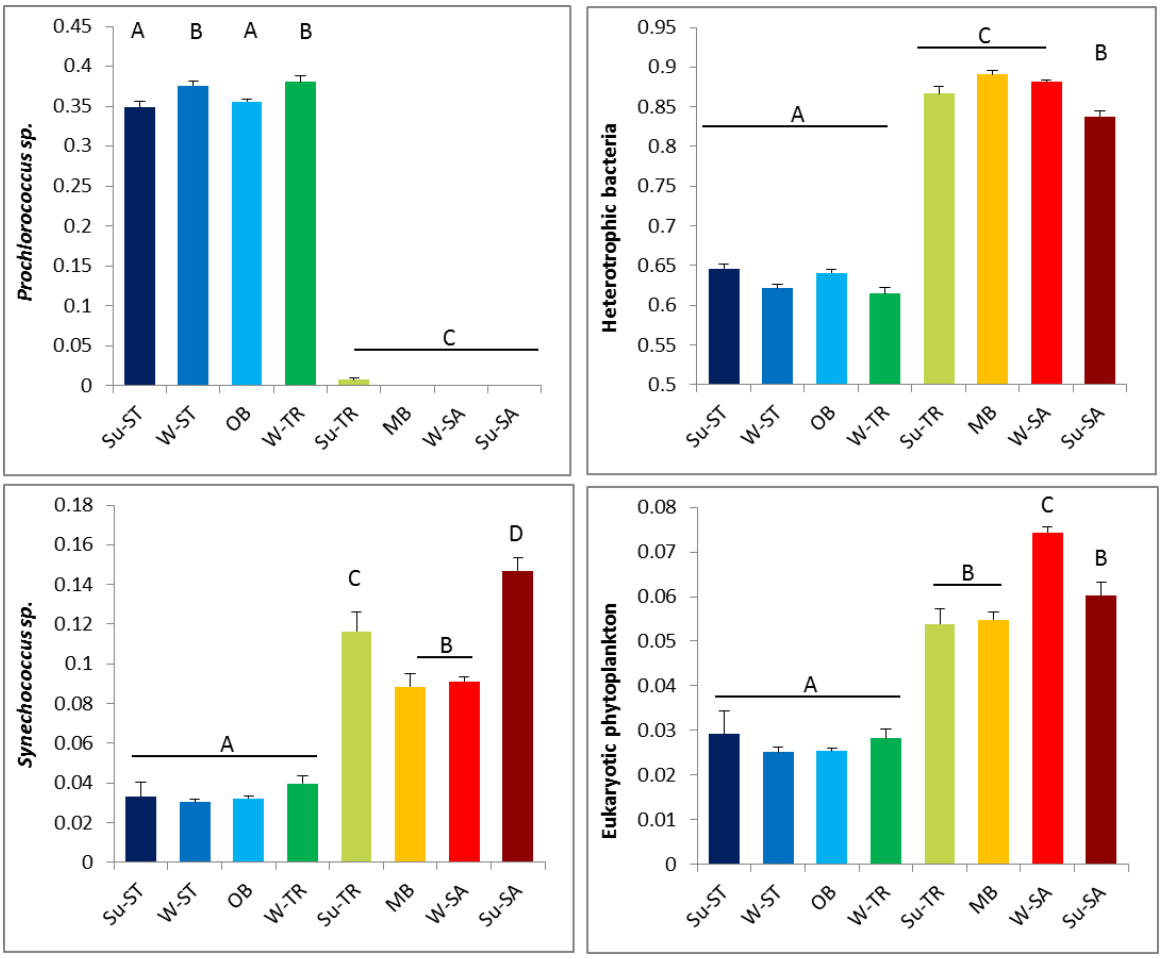

Figure 3.3. Differences of relative abundances across seascapes for *Prochlorococcus*, Heterotrophic bacteria, *Synechococcus*, and Eukaryotic phytoplankton. Proportions have been arcsin-squareroot transformed prior to analysis. Letters that are unique denote pairs that are statistically different after adjusting for multiple comparisons (Tukey-Kramer HSD, $p<0.05$). Color codes correspond to seascapes as in Figure 3.1.

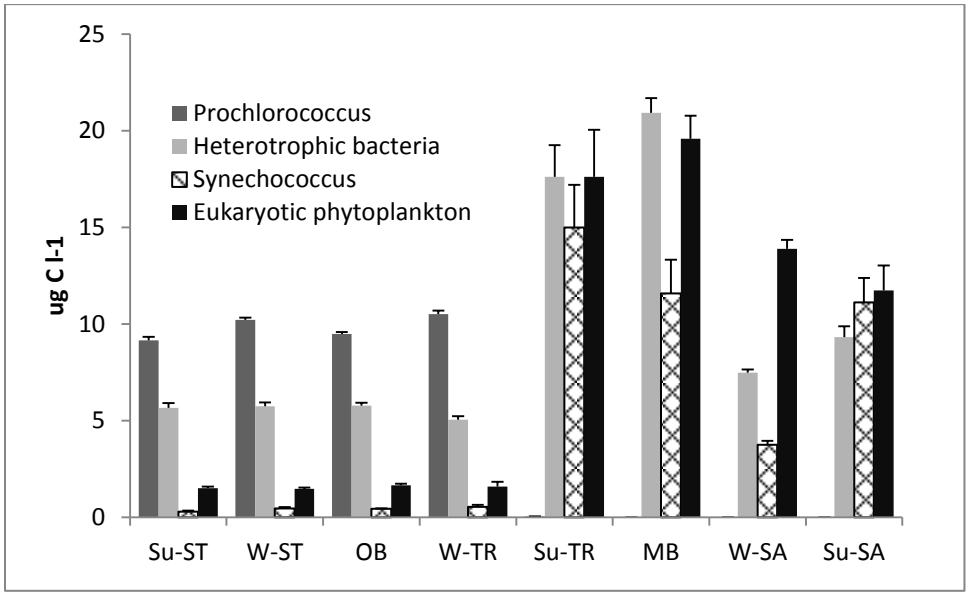

Figure 3.4. Mean (+/- SE) contributions of different functional groups to particulate organic carbon across NE Pacific Seascapes.

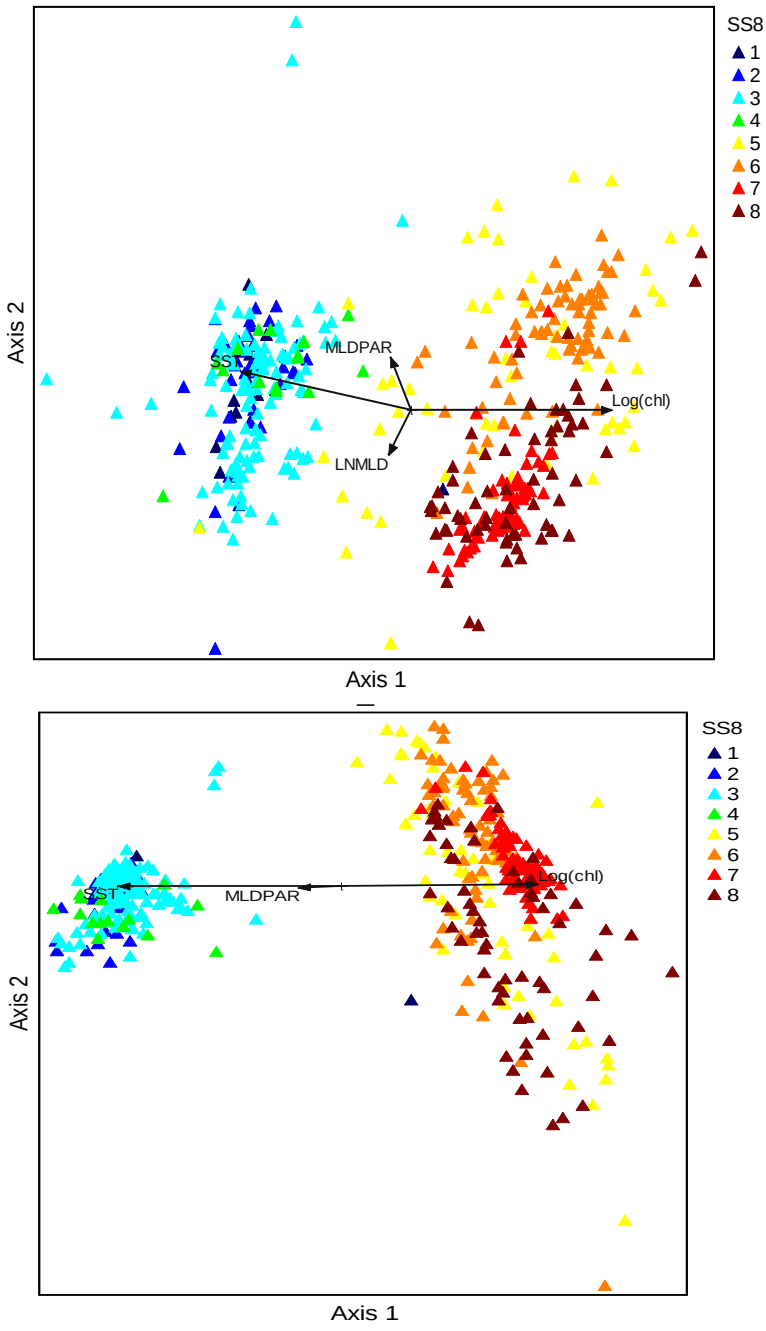

Figure 3.5. Principle component analysis of a) absolute and b) relativized cytometric abundances. Environmental variables are overlain as vectors. Color codes correspond to seascapes as in Figure 3.1.

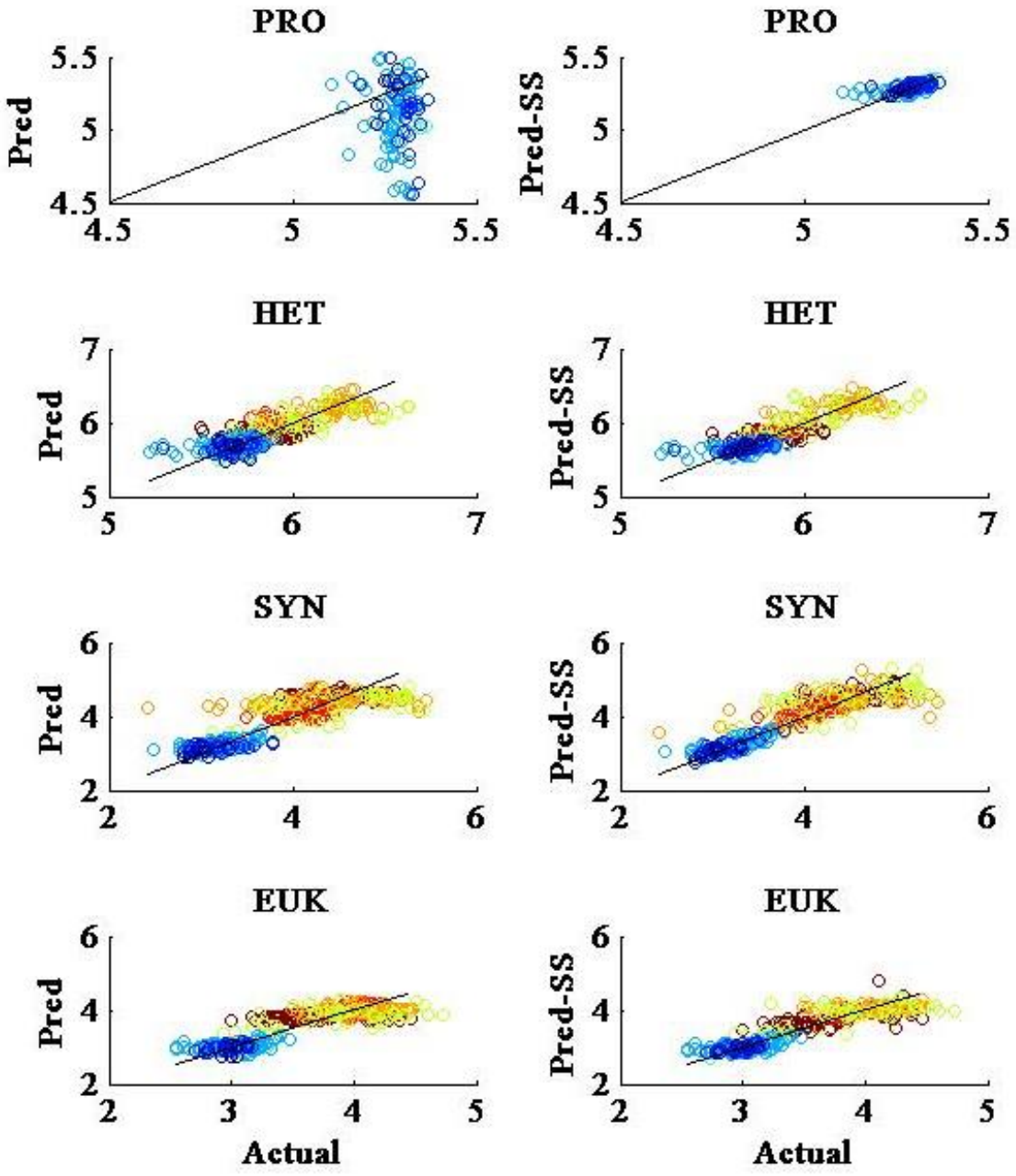

Figure 3.6. Partial Least Squares regression results: Actual vs. predicted (PRED) log-transformed cell abundances of Prochlorococcus (PRO), Heterotrophic bacteria (HET), Synechococcus (SYN), and nano-eukaryotic phytoplankton (EUK). Predicted values are from partial least squares regression of chl-a, SST, PAR, MLD, and MLDPAR at basin and seascape (SS) scales. Line denotes 1:1. Color codes correspond to seascapes as in Figure 3.1.

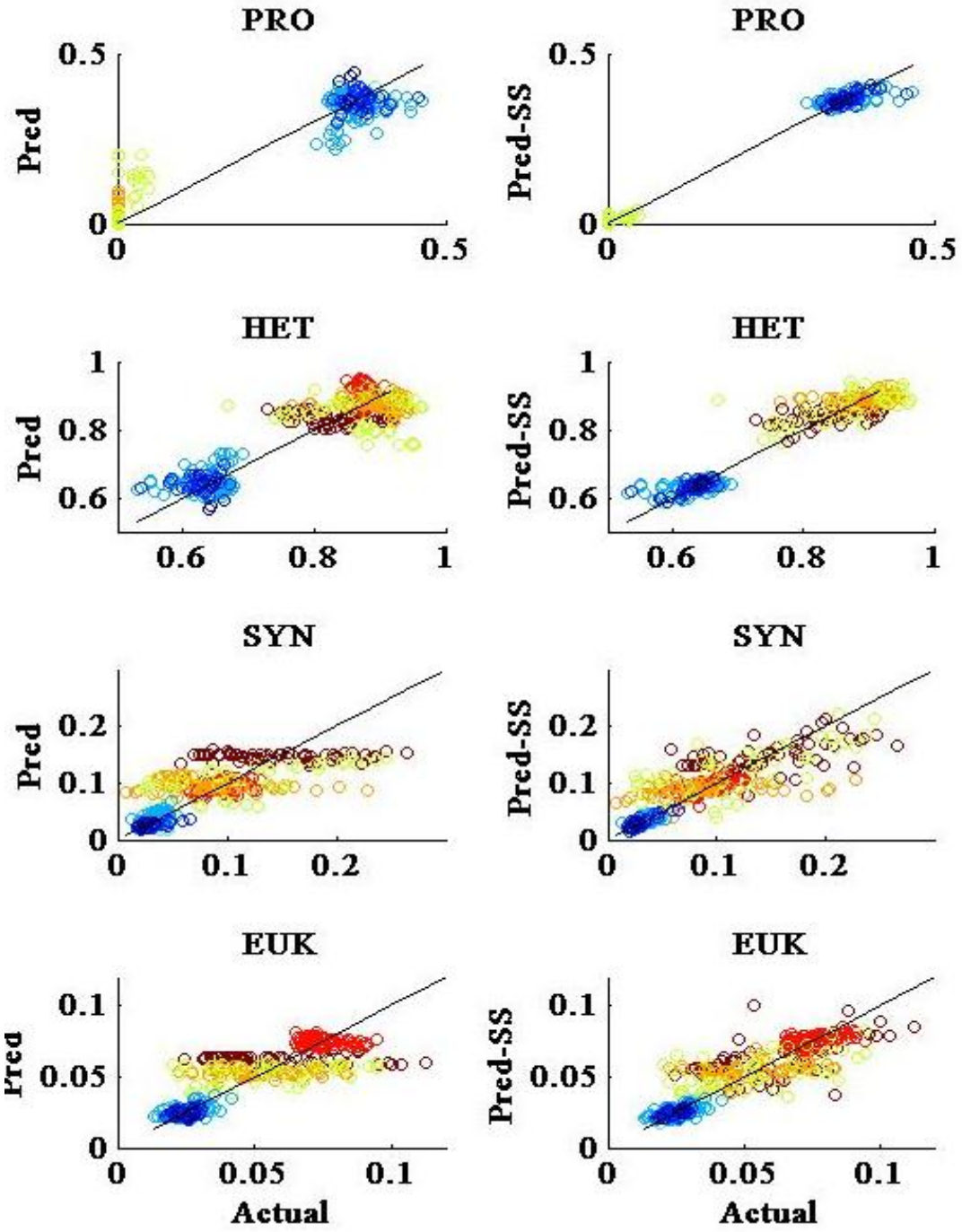

Figure 3.7. Partial Least Squares Regression results: Actual vs. predicted (PRED) of cell proportions of Prochlorococcus (PRO), Heterotrophic bacteria (HET), Synechococcus (SYN), and nano-eukaryotic phytoplankton (EUK). Predicted values are from partial least squares regression of chl a, SST, PAR, MLD, and MLDPAR at basin and seascape (SS) scales. Line denotes 1:1. Color codes correspond to seascapes as in Figure 3.1.

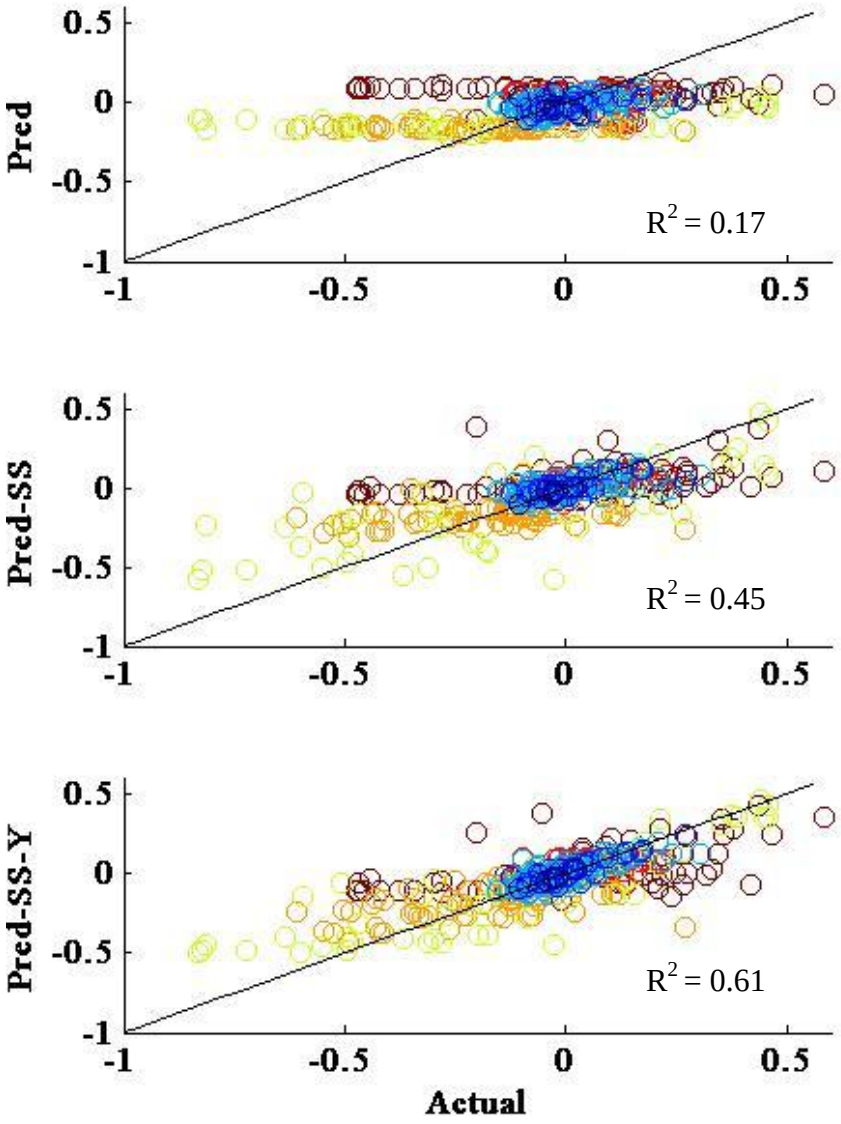

Figure 3.8. Partial Least Squares Regression results: Actual vs. predicted (PRED) log-transformed Autotrophic to Heterotrophic carbon ratios. Predicted values are from partial least squares regression of chl a, SST, PAR, MLD, and MLDPAR at basin and seascape (SS) scales and with the parameterization of interannual variability (Y). Line denotes 1:1. Color codes correspond to seascapes as in Figure 3.1.

Table 3.1. Mean (+/- SE) environmental variables and cytometric cell counts for the Eastern North Pacific. Variance explained (R2) is as a result of univariate analyses of variance. Values are significant ($p<0.05$) unless marked (NS). Eight seascapes are represented: 1) Summer subtropical (Su-ST); 2) Winter subtropical (W-ST); 3) Oligotrophic boundary (OB); 4) Winter transition (W-TR); 5) Summer transition (Su-TR); 6) Mesotrophic boundary (MB); 7) Winter subarctic (W-SA); 8) Summer subarctic (Su-SA)

	N	Chl-a (ug $l^{-1)}$	SST (C.)	PAR (Em^2 d^{-1})	MLD (m)	MLD-PAR (Em^2 d^{-1})	PRO cells (10^5 ml^{-1})	HET cells (10^5 ml^{-1})	SYN cells (10^5 ml^{-1})	EUK cells (10^5 ml^{-1})
Su-ST	15	0.06 (0.01)	25.1 (0.2)	56.2 (0.7)	43.7 (5.1)	22.2 (1.7)	1.78 (0.06)	4.84 (0.29)	3.2 (2.1)	2.1 (1.2)
W-ST	38	0.08 (0.002)	24.9 (0.2)	37.4 (0.8)	55.5 (3.4)	12.2 (0.8)	1.97 (0.04)	4.56 (0.21)	1.6 (0.2)	1.0 (0.05)
Oligo-BND	118	0.07 (0.002)	23.8 (0.2)	48.8 (0.6)	44.8 (1.8)	18.5 (0.5)	1.89 (0.02)	4.86 (0.13)	2.1 (0.3)	1.1 (0.05)
W-TRAN	15	0.1 (0.01)	22.9 (0.6)	29.4 (0.7)	63.4 (5.4)	7.9 (0.5)	2.02 (0.06)	4.43 0.28)	3.0 (0.7)	1.4 (0.3)
Su-TRAN	53	0.3 (0.03)	13.2 (0.5)	38 (0.7)	22.1 (1.1)	19.0 (0.4)	0.01 (0.01)	14.6 (1.3)	66.1(9.8)	12.0 (1.5)
Meso-BND	74	0.51 (0.03)	13.5 (0.2)	28.3 (0.3)	21.5 (0.3)	13.5 (0.3)	0.0 (0.0)	17.4 (0.60)	51.0 (8.3)	13.4 (0.8)
W-SA	71	0.31 (0.01)	5.74 (0.1)	12.6 (0.2)	67.5 (3.6)	3.26 (0.2)	0.0 (0.0)	6.82 (0.31)	14.5 (8.1)	9.4 (0.4)
Su-SA	63	0.33 (0.04)	7.2 (0.1)	37.4 (0.4)	52.9 (1.9)	10 (0.4)	0.0 (0.0)	8.09 (0.54)	55.1 (10)	9.2 (1.1)
Variance explained (R^2)	8	0.83	0.94	0.9	0.53	0.77	0.96	0.63	0.64	0.73

Table 3.2. Multivariate differences in microbial community structure. Chance-corrected within group agreements for community structure considering absolute or relative (normalized) abundances for two nested levels. A = 1 - (observed delta/expected delta). A_{max} = 1 when all items are identical within groups (delta=0). A = 0 when heterogeneity within groups equals expectation by chance. A < 0 with more heterogeneity within groups than expected by chance.

	N Seascapes	T	A	p
Absolute abundance	8	-115	0.79	<0.00001
Relative abundance (%)	8	-119	0.59	<0.00001

Table 3.3. Pairwise comparison between Seascapes: Differences of community structure based on absolute abundances. Differences based on Euclidean distances within and between groups of observations of log-transformed abundances. See Table 1 for seascape codes.

Seascape	Seascape	T	A	p
Su-ST	W-ST	-0.33	0.00	0.28
Su-ST	OB	-1.77	0.01	0.06
Su-ST	W-TRAN	-3.50	0.07	0.01
Su-ST	Su-TRAN	-32.10	0.45	0.00
Su-ST	MB	-59.25	0.66	0.00
Su-ST	W-SA	-58.68	0.84	0.00
Su-ST	Su-SA	-52.74	0.75	0.00
W-ST	OB	-0.73	0.00	0.18
W-ST	W-TRAN	-3.05	0.03	0.02
W-ST	Su-TRAN	-53.62	0.60	0.00
W-ST	MB	-77.40	0.79	0.00
W-ST	W-SA	-75.90	0.89	0.00
W-ST	Su-SA	-70.16	0.83	0.00
OB	W-TRAN	-1.31	0.00	0.10
OB	Su-TRAN	-107.90	0.65	0.00
OB	MB	-133.85	0.80	0.00
OB	W-SA	-132.25	0.86	0.00
OB	Su-SA	-126.52	0.83	0.00
W-TRAN	Su-TRAN	-32.89	0.45	0.00
W-TRAN	MB	-60.20	0.66	0.00
W-TRAN	W-SA	-59.55	0.83	0.00
W-TRAN	Su-SA	-53.62	0.75	0.00
Su-TRAN	MB	-13.47	0.07	0.00
Su-TRAN	W-SA	-25.61	0.15	0.00
Su-TRAN	Su-SA	-13.31	0.08	0.00
MB	W-SA	-13.45	0.05	0.00
MB	Su-SA	-20.21	0.08	0.00
W_SA	Su-SA	-45.89	0.21	0.00

Table 3.4. Pairwise comparison between Seascapes: Differences of community structure based on relative cytometric abundances. Differences based on Euclidean distances within and between groups of observations of arcsine square-root transformed proportions.

Seascape	Seascape	T	A	p
Su-ST	W-ST	-1.55	0.01	0.08
Su-ST	OB	-0.41	0.00	0.26
Su-ST	W-TRAN	-5.35	0.08	0.00
Su-ST	Su-TRAN	-31.52	0.29	0.00
Su-ST	MB	-46.99	0.33	0.00
Su-ST	W-SA	-53.66	0.54	0.00
Su-ST	Su-SA	-38.37	0.31	0.00
W-ST	OB	-3.12	0.01	0.01
W-ST	W-TRAN	-3.21	0.03	0.01
W-ST	Su-TRAN	-57.85	0.46	0.00
W-ST	MB	-73.76	0.52	0.00
W-ST	W-SA	-74.73	0.70	0.00
W-ST	Su-SA	-65.14	0.49	0.00
OB	W-TRAN	-5.68	0.02	0.00
OB	Su-TRAN	-111.25	0.48	0.00
OB	MB	-128.53	0.56	0.00
OB	W-SA	-129.58	0.69	0.00
OB	Su-SA	-120.14	0.53	0.00
W-TRAN	Su-TRAN	-35.32	0.32	0.00
W-TRAN	MB	-50.79	0.36	0.00
W-TRAN	W-SA	-56.79	0.58	0.00
W-TRAN	Su-SA	-42.22	0.34	0.00
Su-TRAN	MB	-7.34	0.03	0.00
Su-TRAN	W-SA	-35.67	0.16	0.00
Su-TRAN	Su-SA	-4.42	0.02	0.00
MB	W-SA	-35.39	0.13	0.00
MB	Su-SA	-22.22	0.10	0.00
W_SA	Su-SA	-41.50	0.18	0.00

Table 3.5. Pearson's correlations of environmental variables with the first two Principal Components from PCA ordination of absolute (A) and relative (R) cytometric taxonomic abundances.

	Chl-a	SST	MLDPAR	MLD
A Axis 1 (80.7)	0.91	-0.80	-0.23	-0.38
A Axis 2 (14)	-0.04	0.43	0.52	-0.50
R Axis 1 (74.5)	0.86	-0.92	-0.41	-0.19
R Axis 2 (20.1)	-0.09	0.03	0.10	0.14

Table 3.6. Pearson's correlations of taxa with the first two Principal Components from PCA ordination of absolute (A) and relative (R) cytometric taxonomic abundances

	Eukaryotic phytoplankton	Prochlorococcus	Synechococcus	Heterotrophic Bacteria
A Axis 1 (80.7)	0.92	-0.9	0.88	0.79
A Axis 2 (14)	-0.07	0.25	-0.18	0.62
R Axis 1 (74.5)	0.86	-0.98	0.83	0.72
R Axis 2 (20.1)	-0.06	-0.47	0.66	-0.46

Table 3.7. Partial least squares predictive capacity of absolute cytometric abundance and resultant model complexity across and within NE Pacific Seascapes. Resultant model statistics reported: MRM-PRESS= minimum root mean predicted residual sum of squares; N_f= number of latent factors; N_{VIF} = number of variables with importance factor >0.8; % VAR ENV= total variance of environmental variables explained by N_f; % VAR TAXA= total cytometric variance explained by N_f. Bolded values highlight VIF>0.8 (see text).

	Basin	Su-ST	W-ST	OB	W-TRAN	Su-TRAN	MB	W-SA	Su-SA
MRM-PRESS	0.46	1.35	0.89	0.87	0.9	0.81	0.96	0.7	0.94
N_f	5	4	3	4	2	5	2	5	3
N_{VIF}	3	4	4	2	4	3	4	4	5
% VAR ENV	100	99.9	90.1	99.9	75.3	100	73.4	100	92.6
% VAR TAXA	79.8	46.5	36.9	31.8	60.6	49.8	18.1	59.3	26.6
Variable Importance Factor									
Chl-a	**1.3**	**1.36**	0.74	0.39	**1.18**	**1.18**	**1.45**	0.77	**1.31**
SST	**1.18**	**0.9**	**1.33**	**1.48**	0.03	**1.3**	**0.57**	**1.18**	**0.87**
PAR	**0.9**	**0.97**	**0.9**	**1.32**	**1.25**	**0.91**	**1**	**0.99**	**0.84**
MLD	0.76	0.77	**1.01**	0.73	**1.08**	0.77	**0.87**	**1.8**	**0.97**
MLDPAR	0.66	**0.86**	**0.91**	0.64	**0.94**	0.7	**0.9**	**1.01**	**0.91**

Table 3.8. Predictive coefficients for environmental variables on taxonomic group abundances across (BASIN) and within NE Pacific Seascapes. Coefficients are derived from partial least squares multivariate regression analysis on scaled and centered values (Z-scores centered on mean) . Bolded values indicate effect sizes greater than 0.2 standard deviations. R2 values represent predictive skill for individual taxa for the entire basin or a particular seascape and do not depict nested effects.

	TAXA GROUP	Chl-a	SST	PAR	MLD	MLDPAR	R^2
BASIN	PRO	**-0.33**	**0.67**	0.13	0.06	-0.15	0.93
	HET	**0.84**	**0.26**	0.07	**-0.39**	-0.08	0.73
	SYN	**0.54**	**-0.60**	**-0.47**	**0.51**	**1.00**	0.74
	EUK	**0.41**	**-0.37**	-0.01	**-0.29**	-0.17	0.76
Su-ST	PRO	**-0.83**	**0.44**	0.12	**-0.24**	**0.39**	0.56
	HET	**-0.82**	**0.45**	0.04	**-0.24**	**0.37**	0.71
	SYN	**-0.24**	**0.20**	**0.69**	-0.11	**0.24**	0.52
	EUK	**0.26**	**0.48**	0.19	-0.05	0.10	0.17
W-ST	PRO	0.17	**-0.23**	**-0.21**	-0.20	0.05	0.13
	HET	0.10	0.10	-0.06	-0.29	0.18	0.18
	SYN	0.04	**-0.75**	**-0.21**	-0.10	-0.04	0.74
	EUK	**0.32**	**-0.33**	**-0.38**	**-0.31**	0.05	0.4
OB	PRO	0.07	**0.26**	**-0.49**	-0.18	0.00	0.2
	HET	0.12	**0.28**	**-0.29**	**-0.24**	0.13	0.16
	SYN	0.06	**-0.57**	-0.25	-0.12	-0.04	0.57
	EUK	-0.07	**-0.42**	-0.18	-0.12	0.02	0.3
W-TRAN	PRO	**0.25**	0.01	**-0.50**	**-0.42**	0.06	0.55
	HET	0.15	0.01	**-0.48**	**-0.53**	0.17	0.26
	SYN	**0.39**	0.00	**-0.40**	-0.04	**-0.21**	0.7
	EUK	**0.33**	0.00	-0.37	-0.08	-0.16	0.5
Su-TRAN	PRO	-0.03	**0.81**	**0.51**	-0.11	**-0.52**	0.45
	HET	**-0.32**	0.05	**2.02**	**-2.91**	**-2.08**	0.45
	SYN	**-0.48**	**-0.77**	**0.83**	**-1.17**	**-0.99**	0.51
	EUK	**-0.30**	-0.41	1.23	**-1.55**	**-1.31**	0.43
MB	PRO	0.00	-0.03	-0.07	0.07	-0.07	0.03
	HET	**0.59**	0.17	0.17	-0.07	-0.06	0.32
	SYN	**0.63**	**0.21**	**0.23**	-0.12	-0.02	0.33
	EUK	-0.01	-0.04	-0.08	0.07	-0.06	0.02
W-SA	PRO	0.00	0.00	0.00	0.00	0.00	na
	HET	**0.20**	**0.33**	**-0.62**	**1.97**	**2.85**	0.64
	SYN	**0.39**	0.60	**-1.31**	**5.30**	**6.22**	0.59
	EUK	**-0.65**	**0.70**	**2.41**	**-6.03**	**-7.70**	0.53
Su-SA	PRO	0.00	0.00	0.00	0.00	0.00	na
	HET	**0.55**	**0.22**	-0.02	0.07	-0.17	0.29
	SYN	-0.07	-0.06	-0.08	**-0.30**	**0.25**	0.18
	EUK	**0.58**	**0.38**	0.14	0.19	**-0.24**	0.3

Table 3.9. Partial least squares predictive capacity of relative cytometric abundance and resultant model complexity across and within NE Pacific Seascapes. Resultant model statistics reported: MRM-PRESS= minimum root mean predicted residual sum of squares; N_f= number of latent factors; N_{VIF} = number of variables with importance factor >0.8; % VAR ENV= total variance of environmental variables explained by N_f; % VAR TAXA= total cytometric variance explained by N_f. Bolded values highlight VIF>0.8 (see text).

	Basin	Su-ST	W-ST	OB	W-TRAN	Su-TRAN	MB	W-SA	Su-SA
MRM-PRESS	1.03	1.12	0.82	0.85	0.84	0.78	1	0.84	0.97
% VAR ENV	100	100	90.8	99.9	85.8	99.9	73.6	100	73.2
% VAR TAXA	75.2	73.3	47.1	35.1	84	51	11	40.9	21.7
Nf	5	5	3	4	3	4	2	5	2
NVI	3	4	4	4	4	4	5	4	5
Variable Importance Factor									
Chl-a	**1.2**	**1.12**	0.73	0.51	**1.08**	**0.84**	**1.13**	0.7	**1.14**
SST	**1.3**	0.7	**1.27**	**1.49**	**0.96**	**1.41**	**1.03**	**1.17**	**0.95**
PAR	**0.99**	**0.81**	**0.87**	**0.99**	**1.24**	**1.03**	**1.09**	**0.85**	**0.87**
MLD	0.57	**1.16**	**0.99**	**0.82**	**0.88**	**0.97**	**0.83**	**1.1**	**1**
MLDPAR	0.73	**1.12**	**1.05**	**0.93**	0.78	0.57	**0.88**	**1.1**	**1.01**

Table 3.10. Predictive coefficients for environmental variables on taxonomic group proportions across (BASIN) and within NE Pacific Seascapes. Coefficients are derived from partial least squares multivariate regression analysis on scaled and centered values (Z-scores centered on mean). Bolded values indicate effect sizes greater than 0.2 standard deviations. R2 values represent predictive skill for individual taxa for the entire basin or a particular seascape and do not depict nested effects.

	TAXA GROUP	Chl-a	SST	PAR	MLD	MLDPAR	R^2
BASIN	PRO	**-0.25**	**0.73**	0.14	0.14	**-0.16**	0.93
	HET	**0.21**	**-0.51**	0.00	**-0.48**	**-0.31**	0.83
	SYN	**0.24**	**-0.92**	**-0.56**	**0.85**	**1.49**	0.6
	EUK	**-0.03**	**-0.67**	0.11	**-0.26**	**-0.40**	0.63
Su-ST	PRO	**0.39**	**0.38**	**0.93**	**-11.12**	**-11.43**	0.82
	HET	**-0.38**	**-0.38**	**-0.95**	**10.99**	**11.28**	0.83
	SYN	0.10	**-0.32**	**0.29**	**4.75**	**4.82**	0.54
	EUK	0.04	**1.23**	**1.28**	**-14.58**	**-14.36**	0.63
W-ST	PRO	-0.07	**-0.22**	-0.08	**0.26**	**-0.21**	0.35
	HET	0.06	0.25	0.08	**-0.25**	**0.21**	0.37
	SYN	0.04	**-0.72**	**-0.15**	0.00	-0.08	0.73
	EUK	**0.25**	**-0.34**	**-0.20**	-0.06	-0.06	0.36
OB	PRO	-0.14	**-0.26**	0.17	**0.25**	-0.19	0.21
	HET	0.13	**0.29**	-0.16	**-0.25**	0.19	0.21
	SYN	0.02	**-0.67**	-0.11	-0.01	-0.10	0.59
	EUK	-0.11	**-0.59**	-0.02	-0.01	-0.04	0.36
W-TRAN	PRO	**0.68**	**0.24**	**1.04**	**0.55**	-0.13	0.91
	HET	**-0.73**	**-0.27**	**-1.00**	**-0.55**	0.15	0.9
	SYN	**0.59**	**0.23**	-0.03	0.19	**-0.27**	0.71
	EUK	**0.78**	**0.56**	0.10	0.08	-0.18	0.75
Su-TRAN	PRO	0.17	**0.90**	**0.30**	**0.29**	**-0.20**	0.46
	HET	**0.41**	**0.93**	0.05	-0.14	0.03	0.59
	SYN	**-0.44**	**-0.98**	-0.09	0.11	-0.02	0.58
	EUK	-0.16	**-0.51**	0.10	0.18	-0.06	0.37
MB	PRO	-0.05	-0.08	-0.10	0.07	-0.06	0.04
	HET	**-0.24**	**-0.18**	-0.04	0.01	0.06	0.08
	SYN	**0.36**	**0.29**	0.10	-0.05	-0.04	0.15
	EUK	**-0.32**	**-0.30**	-0.17	0.11	-0.03	0.14
W-SA	PRO	0.00	0.00	0.00	0.00	0.00	0
	HET	**-0.16**	**-0.67**	**0.34**	**-2.91**	**-2.86**	0.43
	SYN	**0.53**	**0.58**	**-1.69**	**6.76**	**7.73**	0.47
	EUK	**-1.03**	**0.59**	**3.72**	**-9.76**	**-12.72**	0.29
Su-SA	PRO	0.00	0.00	0.00	0.00	0.00	0
	HET	**0.28**	0.00	0.05	**0.26**	**-0.25**	0.21
	SYN	**-0.39**	-0.05	**-0.11**	**-0.31**	**0.29**	0.27
	EUK	**0.42**	**0.20**	**0.23**	**0.18**	-0.15	0.14

Table 3.11. Partial least squares predictive capacity of absolute cytometric abundance and resultant model complexity across and within NE Pacific Seascapes showing year to year variability. Resultant model statistics reported: MRM-PRESS= minimum root mean predicted residual sum of squares; N_f= number of latent factors; N_{VIF} = number of variables with importance factor >0.8; % VAR ENV= total variance of environmental variables explained by N_f; % VAR TAXA= total cytometric variance explained by N_f; Proportion Y= Proportion of year pairs measured in which had high (>0.8) importance factors. Bolded values highlight VIF>0.8 (see text).

	Basin	Su-ST	W-ST	OB	W-TRAN	Su-TRAN	MB	W-SA	Su-SA
MRM-PRESS	0.86	0.75	0.86	0.75	1.05	0.58	0.95	0.85	0.97
% VAR ENV	99	83	56.5	57.6	38	100	93	87.6	97.4
% VAR TAXA	30	99	52.6	57.8	60.5	76	28.7	37	34.4
N_f	15	4	2	3	1	6	4	2	5
N_{VIF}	14	10	14	13	8	6	9	6	6
CHL A	**1.07**	**1.63**	0.75	**0.93**	**1.66**	**0.98**	**1.48**	**1.17**	**1.44**
SST	**1.27**	0.79	**1.60**	**1.28**	0.08	**2.26**	0.43	**1.58**	**1.51**
PAR	**1.16**	**0.83**	**1.18**	**0.91**	0.34	**1.76**	**1.86**	**1.53**	**1.15**
MLD	**1.71**	**0.81**	**1.32**	**1.07**	**1.36**	**1.67**	**1.25**	**1.36**	**1.50**
MLDPAR	**1.22**	0.78	**1.45**	**1.37**	**1.49**	**1.04**	**1.28**	**1.33**	**1.33**
Y[1999-1998]	**0.81**		0.57	0.62					
Y[2000-1999]	0.78		**0.88**	0.78	0.68				
Y[2001-2000]	0.79		**1.01**	**1.09**	0.68				
Y[2002-2001]	**0.82**	**1.09**	**0.94**	**0.94**	0.75				
Y[2003-2002]	**0.85**	**1.09**	**1.00**	**1.04**	0.79				
Y[2004-2003]	**0.83**	**1.09**	**0.95**	**1.09**	**1.14**	0.67	1.13		0.80
Y[2005-2004]	**0.82**	**1.37**	**0.90**	**1.16**	**1.52**	0.67	1.13		0.80
Y[2006-2005]	**0.85**	**1.44**	**0.85**	**1.11**	**1.20**	0.67	1.13		0.80
Y[2007-2006]	**0.87**	**1.30**	**0.88**	**1.04**	0.57	0.67	1.13		0.80
Y[2008-2007]	**0.93**	**1.30**	**0.82**	**0.96**	**1.13**	**1.47**	**1.69**		**2.18**
Y[2009-2008]	**0.98**	0.66	**0.81**	0.70	**1.13**			**2.67**	
Y[2010-2009]	0.76	0.66	0.37	0.45					
Proportion Y	*0.75*	*0.78*	*0.85*	*0.67*	*0.50*	*0.2*	*0.2*	*1*	*0.2*

Table 3.12. Predictive coefficients for environmental variables on the ratio of Autotrophic to Heterotrophic Carbon (aC:hC) across (BASIN) and within NE Pacific Seascapes. Coefficients are derived from partial least squares multivariate regression analysis on scaled and centered values (Z-scores centered on mean) . Bolded values indicate effect sizes greater than 0.2 standard deviations. aC:hC, Chl-a, MLD and PAR were log-transformed prior to analysis. R^2 denote % of variance explained of actual data by modeled data across seascapes (R^2: BASIN), nested within seascapes (R^2: Seascape), and nested within Seascapes with the addition of interannual variability (R^2: Seacape Y).

	BASIN	Su-ST	W-ST	OB	W-TRAN	Su-TRAN	MB	W-SA	Su-SA
Chl-a	-0.11	**0.54**	0.07	**-0.25**	**0.32**	**-0.27**	0.19	-0.01	**-0.37**
SST	**-0.72**	-0.01	**-0.23**	**-0.29**	0.13	**-1.04**	0.00	0.17	-0.03
PAR	**-0.48**	0.12	-0.15	-0.14	-0.03	-0.09	**0.69**	0.14	-0.18
MLD	**1.07**	0.14	0.15	0.13	0.14	0.03	0.05	0.09	**-0.33**
PAR	**1.44**	-0.15	-0.17	-0.18	-0.19	0.05	**0.29**	-0.04	**0.21**
Y[1999-1998]	-0.03	0.00	-0.03	-0.02	0.00	0.00	0.00	0.00	0.00
Y[2000-1999]	0.01	0.00	0.03	0.05	**0.29**	0.00	0.00	0.00	0.00
Y[2001-2000]	0.08	0.00	-0.09	0.18	**0.29**	0.00	0.00	0.00	0.00
Y[2002-2001]	-0.03	-0.08	-0.04	-0.06	-0.06	0.00	0.00	0.00	0.00
Y[2003-2002]	-0.18	-0.08	-0.04	-0.14	-0.06	0.00	0.00	0.00	0.00
Y[2004-2003]	0.18	-0.08	-0.02	-0.12	-0.10	-0.08	0.19	0.00	-0.10
Y[2005-2004]	-0.11	**-0.25**	-0.02	-0.17	-0.18	-0.08	0.19	0.00	-0.10
Y[2006-2005]	-0.04	**-0.30**	-0.02	-0.15	-0.13	-0.08	0.19	0.00	-0.10
Y[2007-2006]	**-0.40**	-0.07	-0.03	-0.11	0.03	-0.08	0.19	0.00	-0.10
Y[2008-2007]	**0.44**	-0.07	-0.02	-0.07	-0.10	**0.57**	**0.42**	0.00	**0.59**
Y[2009-2008]	0.17	-0.01	0.10	0.16	-0.10	0.00	0.00	**0.47**	0.00
Y[2010-2009]	-0.05	-0.01	0.01	0.08	0.00	0.00	0.00	0.00	0.00
R^2: BASIN	0.17	0.05	0.27	0.14	0	0.33	0	0	0.06
R^2: Seascape	0.45	0.87	0.45	0.32	0.92	0.51	0.1	0.34	0.15
R^2: Seascape,Y	0.61	0.98	0.81	0.62	0.98	0.74	0.28	0.36	0.35
% increase with Y	0.36	0.13	0.80	0.94	0.07	0.45	1.80	0.06	1.33

CHAPTER 4: ALOHA from the EDGE: Seascapes provide spatiotemporal context of Eulerian Time-Series on seasonal and interannual time scales

4.1 ABSTRACT

Global analyses of satellite-and modeled data suggest decreased phytoplankton abundance and primary productivity and increased areal extents of oligotrophic systems in response to increased sea surface temperature (SST). However, concomitant changes have not been evident *in situ* suggesting either physiological or structural reorganization not observed from space or uncharacterized spatiotemporal variability. To address this spatiotemporal variability hypothesis, we characterized interannually evolving seascapes in the North Pacific using a probabilistic self-organizing mapping (PrSOM) algorithm coupled with a traditional hierarchical agglomerative clustering (HAC) algorithm. Seascapes were classified from a 14-year time series of satellite-derived, SST chl–a, and photosynthetically active radiation (PAR).

Three distinct seascapes were evident that affect the seasonal and interannual variability observed at Station ALOHA: a transition seascape and two oligotrophic seascapes. On interannual scales, *in situ* phytoplankton abundance (as measured by chl-a), net primary productivity (NPP), and the relative abundances of eukaryotic phytoplankton and *Synechococcus sp*. increased during periods of encroachment by the transition seascape. Conversely, the relative abundance of *Prochlorococcus* increased and chl-a and NPP decreased when the highly oligotrophic seascape encroached on the station. Expansion of the subtropics oscillated, reaching a peak near 2006 and receding until 2009. The dynamic range (~6 million km^2) of subtropical expansion is derived almost entirely by a

reduction in the extent of the transition zone, resulting in a transfer of ~1.2 Pg-C of total primary production between the highly exportive transition ecosystem to the highly recycled subtropical ecosystem. The multivariate seascape approach described here provides a way to connect satellite and *in situ* data and results allowing objective comparisons of systems' responses to climatic forcing.

4.2. INTRODUCTION

Covering over 20 million square kilometers, the North Pacific Subtropical Gyre (NPSG) is the largest surface circulation feature on the planet (Sverdrup et al, 1946; Karl et al., 2010). The permanently stratified surface layer in this system is associated with generally low vertical fluxes of inorganic nutrients into the well-lit surface region resulting in generally low primary production (PP) and export of carbon to the deep ocean. However, because of their size, open ocean regions are responsible for over half of oceanic primary production and for a significant portion of export production (Emerson et al, 1997). There is considerable debate, however, as to how these processes are changing with longer term shifts in environmental forcing such as changes ocean chemistry (Dore et al, 2010) and temperature (Karl et al., 2001; Corno et al., 2007; Saba et al., 2010). Accurate estimation of global ocean production and export, therefore, will require not only reliable estimation of NPSG ecosystem processes (Karl, 2010) but also the context in which these processes are occurring, including an accurate characterization of both spatial and temporal heterogeneity.

Because of their immense size and age, oligotrophic gyres were previously considered climax systems and thus relatively stable in space and time; however, they are now recognized to display substantial spatial, seasonal, and interannual variability (Karl, 2010). While dominated by small phytoplankton and regenerated productivity (Letelier et al., 1996; Li et al., 2012) relatively short-lived perturbations in the NPSG such as deep vertical mixing events followed by water column stratification (DiTullio and Laws, 1991), the passage of cyclonic eddies (Letelier et al., 2000; Wilson and Adamec, 2001), Rossby waves (Sakamoto et al, 2004) and the breaking of internal waves contribute not

only to momentary increases in net primary productivity (NPP) but also to the decoupling of autotrophic and heterotrophic processes and subsequent export of particulate carbon. On longer time scales, *in situ* primary production and phytoplankton biomass (as determined by chl-a) in the North Pacific Subtropical Gyre (NPSG, measured during various programs such as VERTEX or the Hawaiian Ocean Time Series, HOT) have increased over the past three decades (Karl et al., 2001; Corno et al., 2007). These increases have been linked to a shift in the phase of the Pacific Decadal Oscillation (PDO, Karl et al., 2001) or el Nino Southern Oscillation (ENSO)/PDO interactions (Corno et al., 2007) and resulting changes in stratification.

Although the HOT time series program at Station ALOHA (22.75 °N, 158 °W: A Low Oligotrophic Habitat Assessment) is considered the benchmark station of the NPSG (Karl, 2010), the patterns of increased biomass and primary productivity found *in situ* are not matched by the synoptic patterns observed through analyses of derived satellite products. Behrenfeld et al. (2006) showed that global ocean net primary production and phytoplankton biomass (as defined by chl-a) decreased from 1999–2006 in response to increased water column stratification. Hypothesized as an increase in the multivariate ENSO index, this trend was largely driven by changes in the subtropical gyres. Both Polovina et al. (2008) and Irwin and Oliver (2009) have noted ENSO or PDO-associated increases in the areal extent of the most oligotrophic water in subtropical gyres. Finally, a recent analysis of SeaWiFs data suggests gradual, yet significant, decreases in surface chl-a over the past 13 years (1997-2010) in subjectively defined polygons that encompassed the oligotrophic regions of the North Pacific as well as other basins (Signorini and McClain, 2011). While one analysis of long-term *in situ* data support the

trends found in these large scale studies (Boyce et al., 2010), the majority of *in situ* time series do not (Chavez et al., 2011). These findings suggest that more complete regional context needs to be considered when examining the role of interannual variability.

In modeled scenarios, climate induced SST changes and subsequent expansion of oligotrophy result in decreased NPP and fisheries yields in the currently productive subarctic Pacific (Polovina et al., 2011). However, how changes in extent of the subtropical gyres affect the transition region between the subtropics and subarctic has not been assessed. This region is known to have high NPP (Ch2, and other citations) and export production (Chapter 5, Howard et al., 2010; Juranek et al., 2012, Lockwood et al., in press). Furthermore, the transition region is a large sink for atmospheric carbon (Takahashi et al., 2009), as well as a foraging area for many commercially important and endangered or threatened species including squid, tuna, and loggerhead turtles (Polovina et al., 2001). Thus understanding the spatial temporal heterogeneity of oligotrophic system boundaries and the resultant effects, both on observed properties within these systems as well as potential effects on adjacent systems remains an important research endeavor.

To address this and other issues, we have used multivariate satellite data to derive seasonally evolving seascapes in the North Pacific (Chapter 2). These seascapes demarcate heterogeneous regions in the subtropical North Pacific based on climatological and seasonal interactions of chl-a, SST, and PAR as measured by satellite data. Three subtropical seascapes were described in previous chapters that have measurable differences in nitrate to phosphate and nitrate to silicate ratios (Chapter 2) and slightly different community structure (Chapter 3). Here we use the dynamically defined

seascapes to further our understanding of the ocean dynamics at Station ALOHA. Station ALOHA is typically in the subtropical seascapes, however, in the winter, more temperate transition water can encroach on Station ALOHA with concomitant increases in phytoplankton abundances and shifts in their relative abundances. We hypothesized that the large intra-seascape variability associated with year-to-year effects (after accounting for shifts in concurrent environmental drivers) were due to shifts in seascape boundaries (Chapter 3). These same shifts in boundaries may contribute to mismatches when extrapolating results at Station ALOHA to regional scales. To address this issue, we studied the seasonal and interannual expansion and contraction of objectively derived NE Pacific seascapes. The location of Station ALOHA within these seascapes is highlighted, with trends of *in situ* and satellite-derived conditions parsed by seascape. Specifically, we address the following questions:

1. What are the interannual trends of expansion across subtropical seascapes?
2. How does seascape expansion affect the interannual patterns of phytoplankton abundance and primary productivity observed at Station ALOHA?
3. What are potential effects of subtropical expansion on the extent and functioning of the adjacent transitional seascapes?

4.3. METHODS

4.3.1. Background

In a previous study using similar methodology (Chapter 2) we found that the seasonal cycle of the North Pacific could be described by eight seascapes that were classified using satellite-derived SST, chl-a and PAR and a probabilistic self-organizing mapping algorithm, PRSOM (Anouar et al, 1998; Saraceno et al., 2006). These seascapes described significant differences in both satellite and *in situ* data, including nutrients and microbial assemblages. Here we apply the PRSOM in two steps: first to the climatological seasonal mean of the 10-year data set and then to individual years.

4.3.2. Classification

We used archived monthly averages and 8-day composites of the latest processing of satellite data provided by the Ocean Productivity Group (*www.science.oregonstate.edu/ocean.productivity*), as used in their primary productivity algorithms. These data have been cloud-filled which results in reduced variability at seascape boundaries associated with patchy cloud cover (Kavanaugh unpubl. data) and minimizes associated errors in calculating interannual changes in seascape extent. We downloaded Level 3 18-km binned 8-day composites and monthly averages of SeaWiFS (reprocessing version, 2010; R2010) and MODIS-Aqua (R2012) chl-a, PAR, and Advanced Very High Radiometer and MODIS-Aqua SST; the 18 km data were subsequently binned into ¼ degree for this study. The SeaWiFs (SW) data record extends from 1998-2010 albeit with episodic gaps during 2008-2010 due to sensor failure. Where

missing, SW chl-a and PAR were modeled using linear regression from the comparable MODIS (R2012) product. Linear regression was conducted at each pixel using the 8-day composite of each sensor for each month over the years 2003-2010. Predicted chl-a did not vary more than 25% from actual chl-a (usually less than 10%) and predicted PAR varied less than 10% from actual PAR The predicted 8-day composite was then used to only fill gaps in the real SeaWiFs 8-day composites; monthly averages were computed from the combined product. For SST, AVHRR data were used up until 2009 and MODIS SST was used for 2010. The interactive effects of sensor and cloud mask between the AVHRR and MODIS data did not lend itself to simple regression at local scales; however, the meso- to gyre-scale patterns between data sets agreed well. Chl-a values >8 mg m^{-3} were masked to minimize the effect of coastal regions and maximize variability in the open ocean, the chl-a data was $\log_{10}$-transformed, and all data sets were normalized (to a scale of -1 to1) prior to classification (Chapter 2).

Monthly climatological grids were vectorized and concatenated to allow classification of space and time simultaneously. The PRSOM reduced the 3-variable (SST, PAR, chl-a) spatiotemporal data set onto a 15×15 neuronal map resulting in 225 classes, each with its own 3-D weight based on the maximum likelihood estimation (3-D MLEs). The neural net size (15x15) was chosen to maximize sensitivity to mesoscale processes while preventing underpopulated nodes (defined as less than 500 pixels). The 3-D MLEs were then further reduced using a hierarchical agglomerative clustering (HAC) with Ward linkages (Ward, 1963). This linkage method uses combinatorial, euclidian distances that conserve the original data space with sequential linkages (McCune et al., 2002). Euclidian distances here are equivalent to within-group and total

sum of squares. As described in Chapter 2, stepwise agglomerations that resulted in local, rapid increases in an objective function (McCune and Grace, 2002) were used to determine meaningful hierarchical levels.

To assess interannual variability, the multivariate annual cycle was classified using PRSOM for each year. Rather than completing the HAC cycle for individual years, the resultant neuronal weights were assigned to the class of the most similar climatological weight. Similarity was assigned using a nearest neighbor algorithm which minimized the euclidian distance between the annual and climatological MLEs, here denoted *w*:

$$Class_{ann} = Class_{clim}\ (\min\ [(w_{annCHL}-w_{climCHL})^{2} + (w_{annPAR}-w_{climPAR)}^{2} + (w_{annSST}-w_{climSST})^{2}]^{0.5})$$

The annual classes were then mapped from the neuronal grid back to geographical and temporal space. To maintain the annual cycle, seascapes that represented seasonal extremes (summer or winter) were merged. As our focus was on the subtropics and transition, we also merged the three subarctic seascapes into a single seascape. This allowed us to compare the dynamics of four regional classes—subtropics, oligotrophic boundary, transition, and subarctic on an interannual scale.

4.3.3 Seascape Area

Total seascape area was assigned based on the sum of all 0.25-degree pixels in a given seascape. Surface area of each pixel was calculated by correcting for the spheroid-effect on distance between lines of longitude.

Core regions were identified within each seasonally and interannually migrating seascape where the likelihood of a particular seascape identity was greater than 0.6 (i.e. more than half of the time). This allowed us to objectively separate shifts associated with the migration of seascapes from that of changes within the mean state of the seascape.

4.3.4 Additional satellite and modeled data

In addition to SST, chl-a and PAR, net primary productivity (NPP) data and modeled mixed layer depth (MLD) data were downloaded. NPP was modeled using the updated carbon-based productivity model (Westberry et al., 2008). MLD data are a result of a several models (http://www.science.oregonstate.edu/ocean.productivity/mld.html).

The change in light through the water column was calculated per pixel using the Beers-Lambert equation:

$$E_z = E_0 e^{-K_d z};$$

where E_0 was assumed to be PAR and downward attenuation of light (K_d) was calculated as the sum of attenuation by surface chlorophyll (K_{chl}) and seawater ($K_{SW} = 0.04$). K_{chl} was calculated using the Morel (1988) model for chlorophyll-specific attenuation. We assume that K_{chl} is the dominant biogenic optical constituent and that relative contributions by detrital and dissolved constituents are minimal and covary with K_{chl}. Mean PAR within the mixed layer was determined by integrating PAR over the MLD and dividing by MLD. While turbulent diffusivities can affect chl-a: carbon (Ross et al., 2011), here we are interested in scales of weeks to months.

4.3.5 In situ data

In situ primary productivity and assemblage structure in the subtropical North Pacific was assessed using archived data from Station ALOHA (http://hahana.soest.hawaii.edu/hot/hot-dogs/interface.html). Surface data were collected on station with niskin bottles at 5 and 25 m. Net primary productivity was determined by 12-hour incubation with 14C bicarbonate (L12, Karl et al., 1996). The relative dominance of *Prochlorococcus* to eukaryotic phytoplankton was determined using flow cytometric counts (FCM). Community composition was also inferred from the relative concentrations of monovinyl and divinyl chl-a (MV- and DV-chl-a, respectively) using high performance liquid chromatography (HPLC, Goericke and Repeta). In late 2005, cell enumeration switched from Hoechst staining to the use of a Cytopeia Influx flow cytometer to better quantify high-light adapted *Prochlorococcus*. Cell count methodology (N-cell) from 2001-Sept 2005 underestimated Prochlorococcus and overestimated heterotrophic bacteria. To correct for this, these counts were interpolated using simple linear regression based on the seasonal evolution of absolute counts of other FCM-derived taxa at Station ALOHA: Log (Pro N-cell/Total N-cell) = 0.42 - 0.0164* Log (*Synechococcus* N-cell) - 0.019*Log (Eukaryotic phytoplankton N-cell) - 0.004 *Season (R^2 1, 68 =0.86, $p<0.001$; Chapter 3).

4.3.6. Climatic indices

To infer the effect of climatic forcing on interannual seascape extent and subsequent seascape identity at Station ALOHA, three different indices were used. The multivariate El-Nino Southern Oscillation Index, or MEI, is computed from a principal coordinate analysis of six variables including sea level pressure, zonal and meridional wind components, cloudiness and sea surface and air temperatures (Wolter and Timlin,1993). These data are graciously available from NOAA (http://www.esrl.noaa.gov/psd/enso/mei/). The North Pacific Gyre Oscillation (NPGO, Di Lorenzo et al., 2008; http://www.o3d.org/npgo/) is the second dominant mode calculated from North Pacific sea surface height anomalies and is associated with accelerated North Pacific, Alaska and California Currents (Chavez et al., 2011). The Pacific Decadal Oscillation (PDO, Zhang et al., 1997; Mantua et al., 1997) is associated with the dominant mode of North Pacific SST anomalies and is available from the University of Washington (http://jisao.washington.edu/pdo/).

4.3.7 Statistics

Here we focus on the temporal trends primarily of the subtropical and transition seascapes. Anomalies for biogeochemical rates, pigments, and cell counts were calculated by subtracting the monthly climatological mean from each seascape and plotting over time. Interannual changes in seascape boundaries were tracked by determining the areal extent as well as the minimum extent (0.05 quantile) maximum (0.95 quantile) latitudinal and longitudinal extent seascape boundaries and subtracting the

climatological monthly mean. Resultant shifts of seascape identity (SSID) at Station ALOHA were assessed by ranking the seascapes from 1 to 3 and subtracting the monthly climatological mean. All *in situ* data were passed through a 2 standard deviation filter after removing the seasonal cycle, thus we omit the effects of local- to meso-scale shifts in abundances or rates (e.g. blooms). Anomalies and smoothed time series were compared to assess the shifts in local conditions at Station ALOHA associated with the seascape anomaly. We then assessed the relative importance of shifting boundaries using multiple linear regression on *in situ* NPP and chl-a with seascape identity (boundary effect), core region anomaly (mean state effect), and interactions as predictors. All values were scaled by subtracting the mean and normalizing by the dynamic range of the data set. Thus, regardless of scale, a predictor's relative effect on the response could be determined. All effect sizes can be interpreted as the percent change in the response that results from a percent change in the predictor.

4.4 RESULTS

4.4.1. Seascape spatiotemporal structure

We use the likelihood of seascape presence to define the geographic fidelity of core regions within seascapes, the fidelity of boundaries within a season and on interannual scales, and the relative position of Station ALOHA within the transition and two oligotrophic seascapes (Figure 4.1). The subtropical seascape (ST) occupies the western oligotrophic gyre and expands to the east and north during summer. The oligotrophic boundary seascape (OB) occupied a large region east of the Hawaiian Islands and southwest of the California Current System but seasonally extended north and west to border the transition zone chlorophyll front (data not shown) and bound the ST . The transition seascape (TRAN) approximated the seasonal migration of the transition zone chlorophyll front. This region is generally bounded between 30-45 °N but in the winter, the southern TRAN boundary can extend well into the subtropics.

The areal extent of seascapes exhibited large intra- and inter-annual variation (Figure 4.2). Increases in the areal extent of the combined subtropical region (ST and OB combined; Figure 4.2a) occurred from 1999 to 2006, however individual seascapes within the subtropics oscillated in areal extent during the same time (Figure 4.2b). The increase in areal extent of the subtropics coincided with both mesoscale and interannual declines in the areal extent of the TRAN (Figure 4.2c) seascape but had no relationship with the subarctic (SA) seascape. From 2007 to 2009, the combined subtropical region receded with concomitant increases in the areal extent of the TRAN seascape.

4.4.2 Changes in mean seascape traits through time

While seascapes expand and contract due to forcing on seasonal or interannual scales, core regions ("core", Figure 4.3) were identified where (pseudo) Lagrangian expansion effects were minimal and Eulerian estimates of temporal variability were assessed. Removing the monthly means from the time series allowed visualization of mesoscale and interannual trends; however, in some cases, changes in the range of the seasonal cycle resulted in a quasi-seasonality to remain in the time series (Figure 4.4).

Chl-a in the ST increased from 2000- 2006, then decreased in the migrating seascape and core region (Figure 4.4). In the OB, chl-a appeared to steadily decrease in both the seascape and the core seascape region. In the TRAN, chl-a increased out of phase with the transition core during 2000 and 2005; however both decreased in chl-a after 2007.

Declines in NPP were apparent in all seascape and core regions toward the end of the time series. NPP actually increased in the ST through ~2005 then steadily decreased. Declines were low and steady in the OB until 2007 and in the transition until mid-2008 after which NPP dramatically declined in both seascapes. The seasonal range of NPP also appeared to shift in the ST and the TRAN but not the OB. Heightened seasonality appeared in the early and late portions of the time series in the ST seascape and during 2003-2005 and 2007-2009 in the TRAN seascape.

Though the seasonal range of SST in the ST appears to change – dampening from 2002-2005, overall there appeared to be no secular change in SST in the ST seascape during our study period. SST patterns in the ST generally followed the inverse of chl-a in

that region, although the absolute magnitude of SST in the seascape was slightly cooler than that of its core region. In both the migrating seascape and the core region, SST increased in the OB through 2004. SST in the TRAN seascape was cooler and more variable than that of its core region, with anomalously cool periods during 1998 and 2005.

MLD appeared to shoal across subtropical seascapes; however, the magnitude of this change in the ST was obscured by changes in seasonality. MLD in the TRAN did not appear to increase or decrease but the seasonal range shifted. Shallow summers (2001-2003) appeared to precede large seasonal variability (2003-2006) which was followed by deeper winter mixing after 2006. Mean light in the mixed layer (MLDPAR) increased by ~18-24% in the ST (15-18 E m^{-2} d^{-1}) and OB (~13-16 E m^{-2} d^{-1}) from 1999-2005. This was due primarily to shoaling MLD, not incident irradiance, as PAR did not change in the subtropics. MLDPAR did oscillate in the TRAN seascape and core, peaking in late 2004. This likely interacted with shallow summer MLD to lead to high MLDPAR in the TRAN during that year.

4.4.3 Seascape identity at Station ALOHA

Seascapes ST, OB, and TRAN were assigned numerical values (1, 2, and 3, respectively) to allow assessment of the mean seascape identity (SSID) at Station ALOHA. Station ALOHA at 22.75 N, 158 W, showed a strong seasonal cycle (Figure 4.5a) with TRAN water dominating conditions during December and January and OB for the rest of the year. Across the time series (Figure 4.5b), the OB-like conditions dominated the identity

at Station ALOHA with the climatological average SSID index of 2.18. During 2000, 2004, and 2006 excursions toward ST-like water was associated with expansion of the ST and contraction of the TRAN. The large excursion toward TRAN-like conditions at Station ALOHA initiating in 2008 was associated with larger scale contraction of the subtropics and expansion of the TRAN seascape.

Station ALOHA SSID changed as the result of latitudinal and longitudinal changes in the location of the ST: OB and TRAN: OB boundaries (Figure 4.5c, d). Large-scale N-S oscillations were evident in the southern extent of the transition region near Station ALOHA with southern migration evident in the latter half of the time series. While the meridional ST boundary movement was minimal compared to the zonal, they both exhibited large-scale maxima (further north and east) during 2002-2005.

4.4.4 Climatic drivers of seascape identity

Changes in areal extent of seascapes and temporal variability of SSID at Station ALOHA were associated with both the Multivariate ENSO Index (MEI) and the North Pacific Gyre Oscillation (NPGO). Positive anomalies of these two climatic indices were associated with increased extent of the subtropics and conversely, decreases in the transition seascapes. Therefore, the likelihood of Station ALOHA being associated with transition-like water decreased with positive anomalies of the NPGO and MEI, resulting in a negative correlation (Figure 4.6). These relationships were slightly stronger when the climate index led the expansion by ~ 18 months. Conversely, when TRAN-like

conditions influenced Station ALOHA, positive MEI and NPGO anomalies followed after 6-18 months respectively.

4.4.5 Changes in traits at Station ALOHA

Comparing the smoothed time series suggests that satellite-derived seascape identity, *in situ* chl-a and *in situ* NPP were coherent until 2002, out of phase until 2006, and coherent again after 2006 (Figure 4.7). Shifts in seascape tendency toward TRAN was correlated with increases in *in situ* NPP ($r=0.29$, $p<0.01$) and a tendency, albeit not statistically significant, toward increased chl-a ($r=0.18$, $p<0.06$).

With the exception of episodic blooms, primary production in the upper 25 m of the water remained typically <8.5 mg C m^{-3} d (median=6.3 mg C m^{-3} d^{-1}). However, interannual oscillations were evident (Figure 4.7a) with a low in mid-2000 preceding a period of relatively high PP from 2001-2003, followed by likely changes in seasonality and another low in late 2006. After 2006, NPP increased through 2008 and declined toward the end of the time series. Throughout the data record, NPP was generally coupled to SSID with positive anomalies of NPP generally associated with interannual excursions toward TRAN seascape.

In situ chl-a in the upper 25 m of the water was also coupled to SSID, albeit less closely than was NPP (Figure 4.7b), with the exceptions of 2003-2005. In particular, during 2004 and 2005, chl-a was relatively high when Station ALOHA was associated with the ST seascape. Median values of surface DV-chl-a and MV-chl-a were similar

(38.5 v. ~43 mg m^{-3}); however, they both exhibit large interannual excursions (Figure 4.7c). DV-chl a was minimal in early 1998 and then again during 2003-2004. Between mid-2005 and early 2006, DV-chl-a increased by approximately 50%, then decreased rapidly through 2007. MV-chl-a values were relatively constant early in the time series (Fig. 6 b); small decreases (~10 %) during 2003 preceded a sharp rise in early 2004 and relatively high concentrations persisting through mid-2006. The combination of DV- and MV chl-a led to oscillations in Total chl-a with minima present during 1998 and 2003 followed by a bimodal increase of ~25% above the median occurring in late 2004 and early 2006 associated with the peaks in MV and DV chl-a respectively.

On interannual scales, phytoplankton community structure, as measured by the proportion of *Prochlorococcus* to total phytoplankton abundance, was strongly correlated with SSID (Figure 4.7 d). *Prochlorococcus* is always present in high abundances at Station ALOHA (generally > 1.4 x 10^8 cells l^{-1} or over 91 % of all phytoplankton cells). However, during periods where TRAN-like states dominated Station ALOHA, *Prochlorococcus* was relatively less abundant while eukaryotic phytoplankton and *Synechococcus* abundances increased.

4.4.6. Effects of expansion at Station ALOHA

Seascape identity was as important as changes in the core seascape for driving variability of in *situ* NPP and chl-a (Table 4.1). Positive anomalies of *in situ* chl-a were associated with tendencies toward TRAN-like seascapes (SSID effect= 0.49 +/-0.2, $p<0.01$) leading to a 0.5 % increase in chl-a for every % increase in TRAN water in the Station ALOHA

SSID. While there were no simple relationships with trends from adjacent seascapes, there was a positive effect of interaction with the OB seascape (SSID*OB effect= 1.26 +/-0.6, $p<0.05$). In other words, if the OB core had relatively high chl-a and the SSID was trending positive, *in situ* chl a was markedly high. Positive anomalies of *in situ* NPP were also associated with TRAN-like waters (effect=0.98 +/- 0.21, $p<0.0001$) and positive shifts in NPP of the OB core (0.83 +/- 0.32, $p<0.01$). There were also significant negative effects resulting in the interaction of trends within the ST seascape and SSID when the boundary shifted (ST*SSID effect=-1.90 +/- 0.78). This was interpreted as context-dependent effects on *in situ* NPP when Station ALOHA was in the ST seascape (negative SSID anomaly). If Station ALOHA was identified by the ST seascape and the ST core was anomalously high, the resultant *in situ* NPP would increase.

4.4.7 Effects of expansion on adjacent seascapes

The effects of expansion of the subtropical seascapes on the TRAN and SA region were complex. Increases in areal extent of the entire subtropics were derived from decreases in the extent of the TRAN seascape (Figure 4.8, Table 4.2: r=-0.83), with little effect on the subarctic. However, the patterns of NPP in the TRAN and SA as a function of expansion depended somewhat on which subtropical seascape was expanding. Slight positive NPP anomalies in the TRAN and SA were associated with expansions of the ST (Table 4.2, r=0.21 and 0.17, respectively) whereas slight negative anomalies were associated with expansions of the OB (r=-0.12 (NS) and -0.31, respectively). These patterns were independent of whether the trend was assessed through the seascape mean or core mean.

Taken together, the maximum range of subtropic expansion (~6 million km^2, Figure 4.8) was associated with an approximate increase in net annual production in the subtropics by ~1.2 Pg C yr^{-1}. However, this expansion was at the expense of the TRAN seascape and resulted in a loss of annual production of ~1.3 Pg C yr^{-1} from the transition with no change in the subarctic.

4.5 DISCUSSION

Where satellite metrics suggest changes in oligotrophic systems in response to increased SST (Behrenfeld and others 2006; Irwin and Oliver 2009), concomitant changes have not been evident at Station ALOHA (Corno et al., 2007) or BATS (Lomas et al., 2010) suggesting either physiological or structural reorganization not observed from space or as yet uncharacterized spatiotemporal variability. Certainly, the former has been discussed in terms of shifts toward abundances of dominant taxa better quantified by the pigment phycoerythrin (e.g. *Trichodesmium*, White et al., 2008), or deviations caused by taxon-specific shifts and related sensitivities using HPLC and fluorescence-based chlorophyll data for tuning of satellite chl-a algorithms (Saba et al., 2010). However, our perception of community structure and processes is affected by the oceanographic context in which we observe it: episodic events (e.g. volcanoes or eddies) or boundary shifts (i.e. edge effects) may affect our understanding of the system. As oligotrophic regions of the ocean oscillate on a seasonal or interannual basis (this study, Irwin and Oliver, 2009), this can lead to dramatic changes at Station ALOHA as conditions are dominated by waters with different trophic status, plankton communities and contextual history. Here we observed changes in seascape boundaries associated with changes in the MEI and NPGO. Shifts in boundary locations resulted in changes in different seascape states at Station ALOHA with decreased *in situ* NPP associated with periods of encroachment by subtropical waters. Increased subtropical seascape extent was also associated with decreased areal extent of the transition seascapes, resulting annual production in the transition.

Subtropical seascape extent and the likelihood of Station ALOHA to occupy more oligotrophic waters were associated with positive NPGO and MEI indexes. While we saw no effects of the PDO, previous evidence suggest that during positive PDO, the Aleutian Low is further south and leads to a southern anomaly in the transition zone chlorophyll front and higher than average primary productivity in the subtropics (Chai et al., 2003). Positive NPGOs are associated with more northward Aleutian Lows (Chavez et al., 2011) along with stronger North Pacific and California currents, higher pressure and deeper thermocline depths at the center of the subtropics (Di Lorenzo et al., 2008; 2009) potentially leading to decreased access to deep nutrients.

The location of Station ALOHA at the edge of several systems (this study) and pivot points of climate forcing (Chavez et al., 2011) may result in different climate effects depending on the direction from which they emanate. Previous studies have documented suggested that during positive ENSO phases, water column stabilization restricts upward mixing of new nitrate and selects for organisms that can fix atmospheric nitrogen (Campbell et al., 1997; Karl et al., 1995; 2001). While not a feedback, we see coupling where positive MEI may lead to decreased NPP at ALOHA by influencing from the south. A negative phase of the NPGO may be associated with weakened gyre, and increased NPP from temperate waters encroaching from the north. When the gyre is weak, the decreased temperature differential may contribute to slackening of trade winds in the eastern basin, and subsequent positive MEI. Positive ENSO phases are then thought to feed into stronger NPGO conditions through atmospheric teleconnection (Di Lorenzo et al., 2009). However, the MEI does not differentiate between the canonical and

non-canonical ENSOs (Wolter and Timlin, 2011), thus the similar, but lagged patterns seen between the MEI and NPGO at Station ALOHA may be connected as suggested by global SST analysis (Chavez et al., 2011).

Investigators interested in the expansion of oligotrophic regions should consider the interactions of phytoplankton with associated physical conditions and how these interactions shift through time. Limited by the satellite record at the time of publication, earlier studies on expansion of oligotrophic systems (Polovina et al., 2008; Irwin and Oliver, 2009) suggested secular increases to ~2006 but also evoked ENSO. Using a longer record, Signorini and McLean (2011) found mostly secular decreases in declines of [chl-a] over large subjectively chosen regions. Our results support general declines in NPP and chl-a, but in a spatially heterogeneous fashion. The seascape approach, in combination with a longer data record, has allowed us to deconvolve more of the spatial and temporal variability in the expansion of oligotrophic systems and verify satellite trends with *in situ* data. Similar to previous studies, we see expansion of all the subtropics up until 2006-though the expansion is associated with oscillations of two distinct oligotrophic seascapes. After 2006, however, we saw declines in the areal extent of the subtropics. Irwin and Oliver (2009) reported general increases through time in the most oligotrophic provinces in their classification, with oscillatory behavior found across all oligotrophic provinces. The ST seascape generally had mean chl-a<0.06 ug L^{-1} suggesting that this region was persistently highly oligotrophic ; water classified in the OB was consistently below 0.2 ug chl-a L^{-1} (mean =0.09). Comparison across multiple methods of water classification, using different criteria and methodologies and longer time series will ultimately be necessary determine the relative strengths of periodic

forcing compared to secular increases predicted by anthropogenic induced SST shifts on changing boundaries of oceanic ecosystems.

In our study, Station ALOHA is rarely located in the most oligotrophic seascape of the North Pacific. However, when it is, *in situ* chl-a and NPP generally decrease relative to when eastern Pacific OB water or TRAN water characterizes the station. Furthermore, we see shifts in community structure associated with interannual seascape identity. *Prochlorococcus*, while always numerically abundant in the subtropics (Campbell and Vaulot, 1993), become less dominant on interannual scales when transition waters encroach on the time series station. Previous studies suggest that anomalously high salinity following the 1998 ENSO and PDO shift (Lukas and Santiago-Mandujano,2008) resulted in reduced stratification, increased mixing and subsequent increases in the pigment-based biomass of small eukaryotic phytoplankton (Bidigare et al., 2009). This may be in part why we see increased monovinyl chl-a and increased relative abundances of small photosynthetic eukaryotic cells during 2004. However, the strong anticorrelation of the relative abundance of *Prochlorococcus* and SSID at Station ALOHA on interannual scales suggests that multiple time and space scales are interacting. *In situ* NPP and chl-a at Station ALOHA were also correlated to interannual shifts in the OB but not to shifts in the ST. The exception occurred during 2004 to 2006 when the interannual trends of the ST and the seascape identity anomaly were out of phase. Because chl-a and NPP were anomalously high in the ST, we saw higher chl-a and NPP in situ at ALOHA than predicted by seascape state when ST waters encroached on the station. Overall, however, the effect of changes in the mean state of the system was minimal compared to interannual shifts in the boundaries of systems.

Subtropical expansion was correlated with changes in areal extent and net annual production in the adjacent transition seascape. Contrary to longer term model results (Polovina et al., 2011), we found no decreases in subarctic area, NPP, or annual production. While area-driven decreases of annual production in the transition were nearly matched by area-driven increases of annual production in the subtropics, the shift towards regenerated productivity and subsequent effects on export production should not be ignored. Both gas exchange and the energy required for foraging are area-dependent. For CO_2 uptake, summer transition zone productivity either "primes the pump" for winter cooling (Takahashi et al., 2009) or can even surpass cooling in terms of its relative CO_2 drawdown effect (Lockwood et al., 2012; Howard et al., 2010) . The transition is also an important foraging region for fish, seabirds, and turtles (Polovina et al., 2001) with concentration of zooplankton associated with frontal convergence (Hyrenback et al., 2002). Whether the documented zonal variability of convergence (Bograd et al, 2004; Ayers and Lozier, 2010) and the subsequent spatial variability in trophic (Polovina et al., 2001) or biogeochemical responses (Chai et al., 2003) are associated with differential expansion of the ST or OB regions remain to be assessed. Nevertheless, we show that subtropical expansion is associated with contraction of the transition seascape and a large area-driven decrease in annual production in the transition, with likely profound subsequent effects on North Pacific ecosystem functioning and global carbon cycling.

Conclusion: Through the lens of pelagic seascape ecology, we have viewed a dynamic mosaic of different systems in the North Pacific that expand and contract on interannual scales. Station ALOHA and other ocean time series programs, with their mechanistic insight, is an ideal location to observe shifts in these systems as their boundaries and

mean states respond to climatic forcing. However, ocean time series are limited in spatiotemporal coverage, satellites are limited to the surface, and models are limited in their complexity. Thus, an integrated ocean observing system that incorporates all three will be necessary (Saba et al., 2010). Our results suggest that the seascape framework, through its capacity to scale context and mechanism, may serve as an important and unifying component of such an observing system.

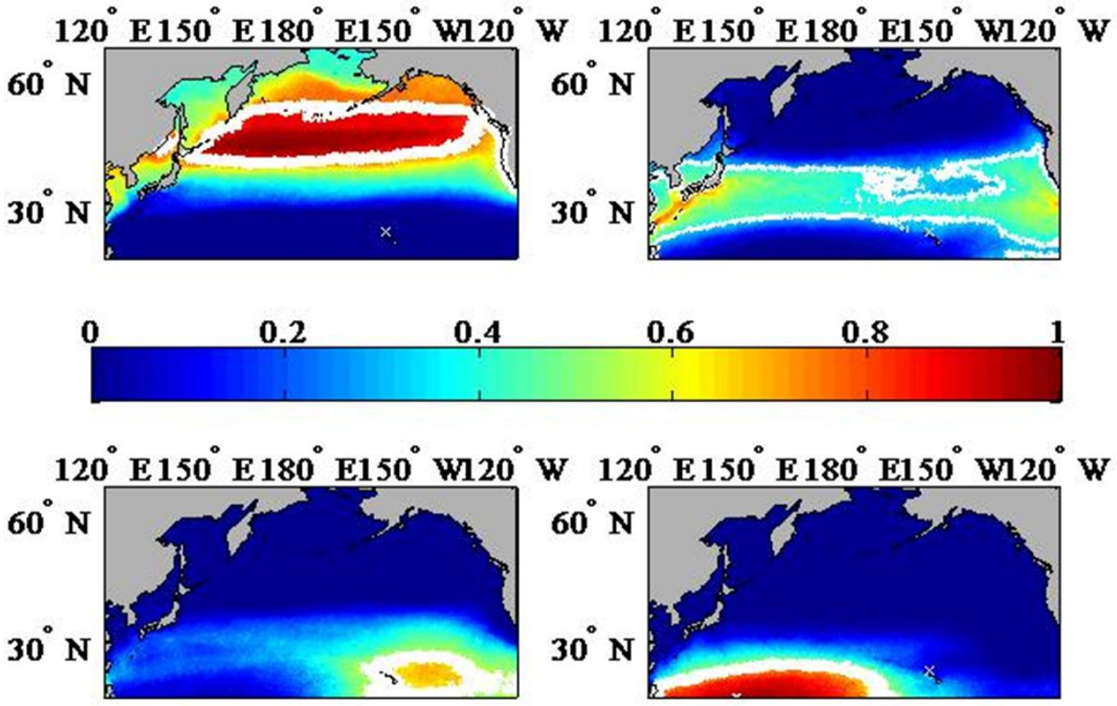

Figure 4.1. Occupation likelihood of North Pacific seascapes from 1998-2010. Color denotes probability of occurrence (N=156) for: A. Subarctic (SA); B. Transition (TRAN); C. Oligotrophic Boundary, (OB) and D. Subtropic (ST) seascapes. White lines delimit core regions with high likelihood of occurrence (see text).

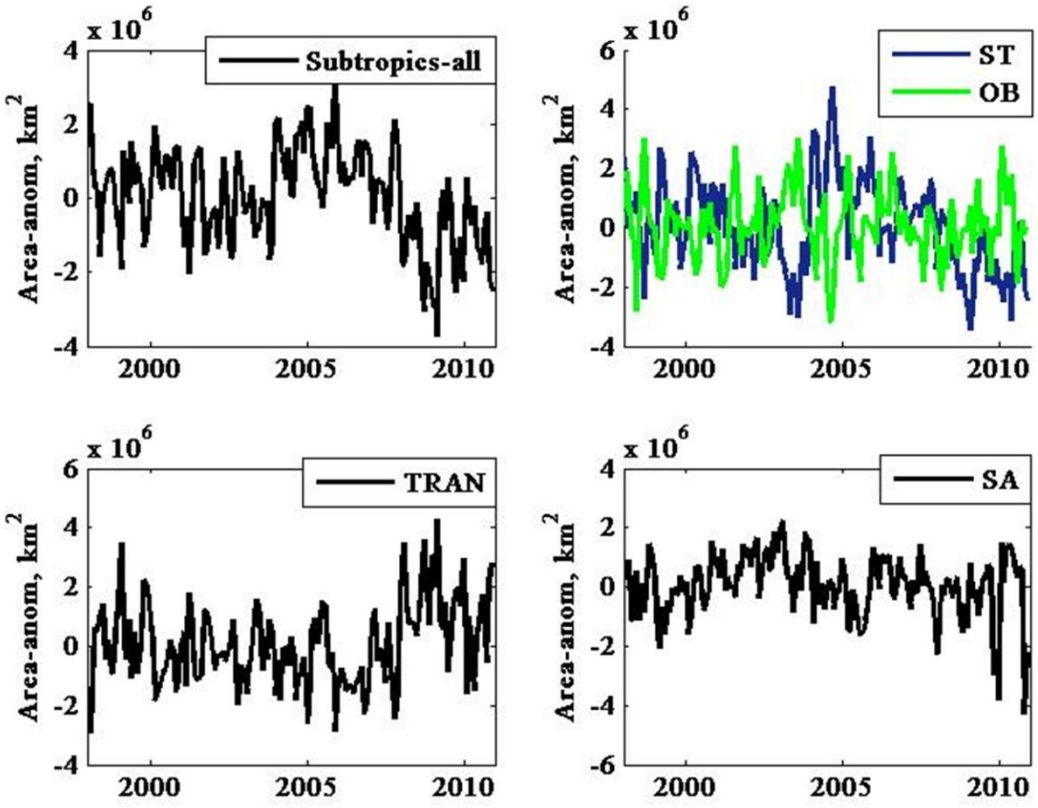

Figure 4. 2. Changes in extent of North Pacific seascapes from 1998-2010. All signals have had the monthly climatological means removed. A. All subtropics showing additive effects of Subtropic (ST) and Oligotrophic Boundary (OB) seascapes; B. Oscillation of area extent of ST (blue) and OB (green) seascapes. C. Transition seascape and D. Subarctic seascape.

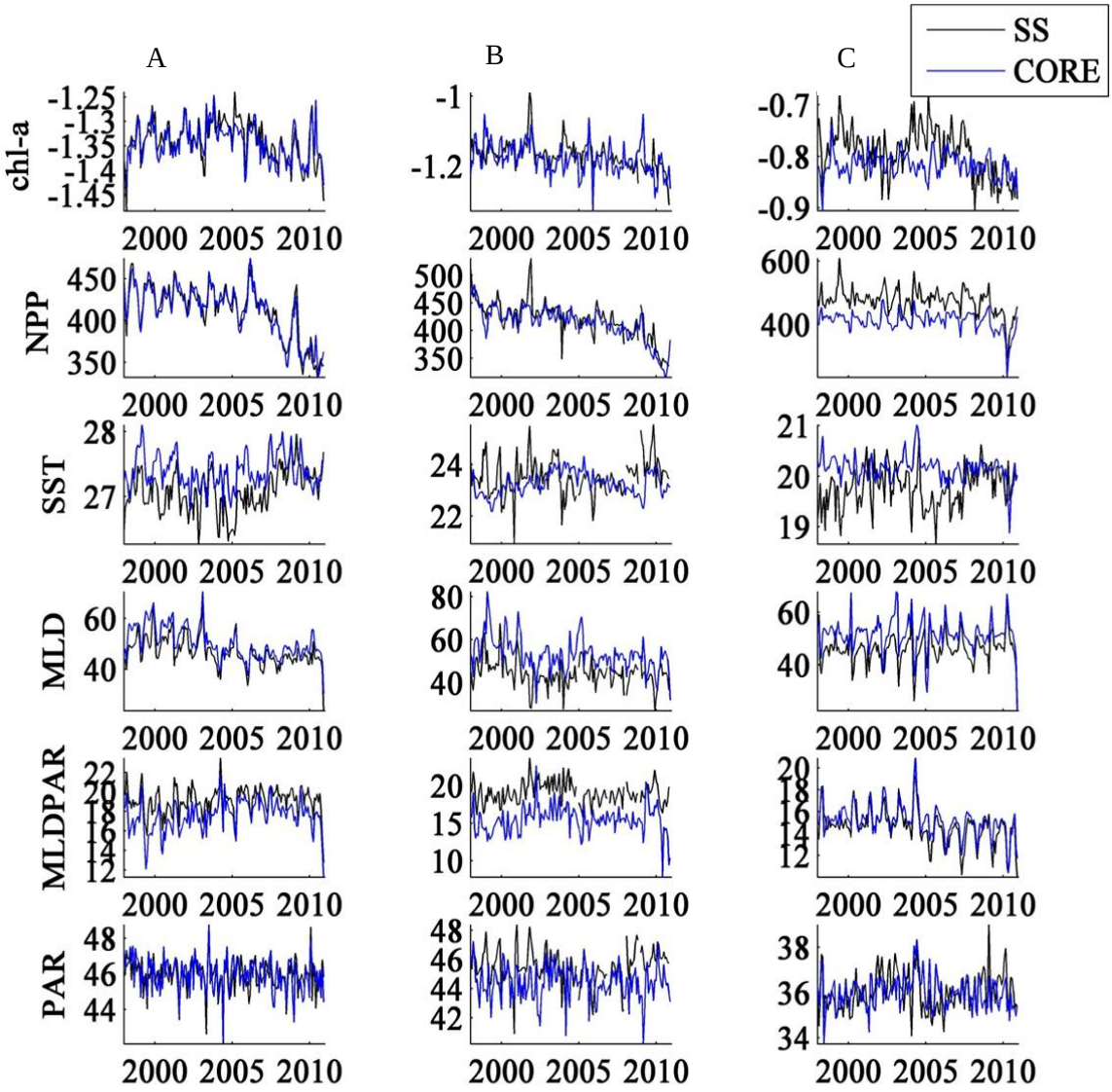

Figure 4.3. Changes in mean states from 1998-2010 in A. Subtropic, B. Oligotrophic Boundary, and C. Transition seascapes. Black line denotes trend in seasonally and interannually migrating seascape; Blue denotes concurrent trend in a seascape core region. All signals have had the monthly climatological mean removed to highlight interannual variability. Chlorophyll-a (chl-a) values are log10-transformed. NPP=net primary production (mg C m^{-2} d^{-1}), SST= sea surface temperature (deg. C), MLD= mixed layer depth (m), MLDPAR= mean photosynthetically active radiation in mixed layer (Einsteins m^{-2} d^{-1}), PAR= surface photosynthetically active radiation (Einsteins m^{-2} d^{-1}).

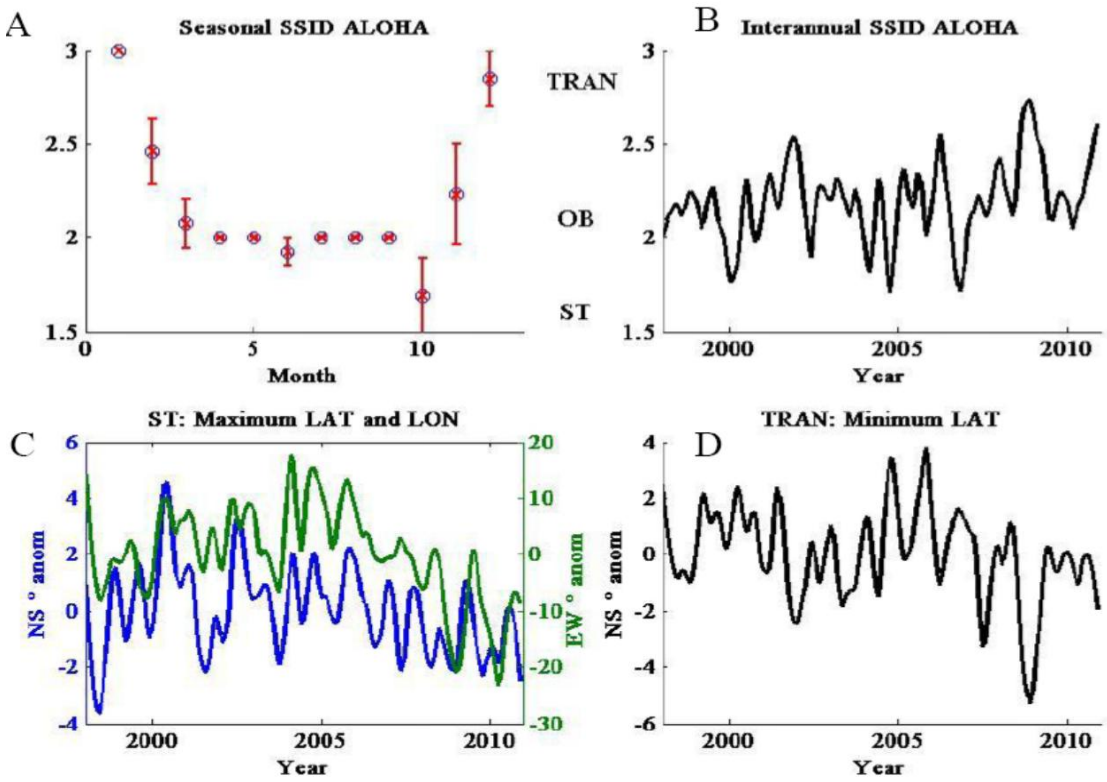

Figure 4.4. Seasonal and interannual seascape Identity at Station ALOHA. Seascape identity was indexed with 1=ST, 2=OB and 3=TRAN. A: Seasonal cycle showing mean (+/- SE) seascape identity index (SSID). B: Smoothed (12-month loess) changes in interannual identity with climatological mean (SSID=2.18) included. C: Smoothed (12-month loess) changes in latitudinal extent of northern (blue) and eastern (green) ST boundary, centered on Station ALOHA. D: Smoothed (12-month loess) changes in latitudinal extent of southern TRAN boundary, centered on Station ALOHA.

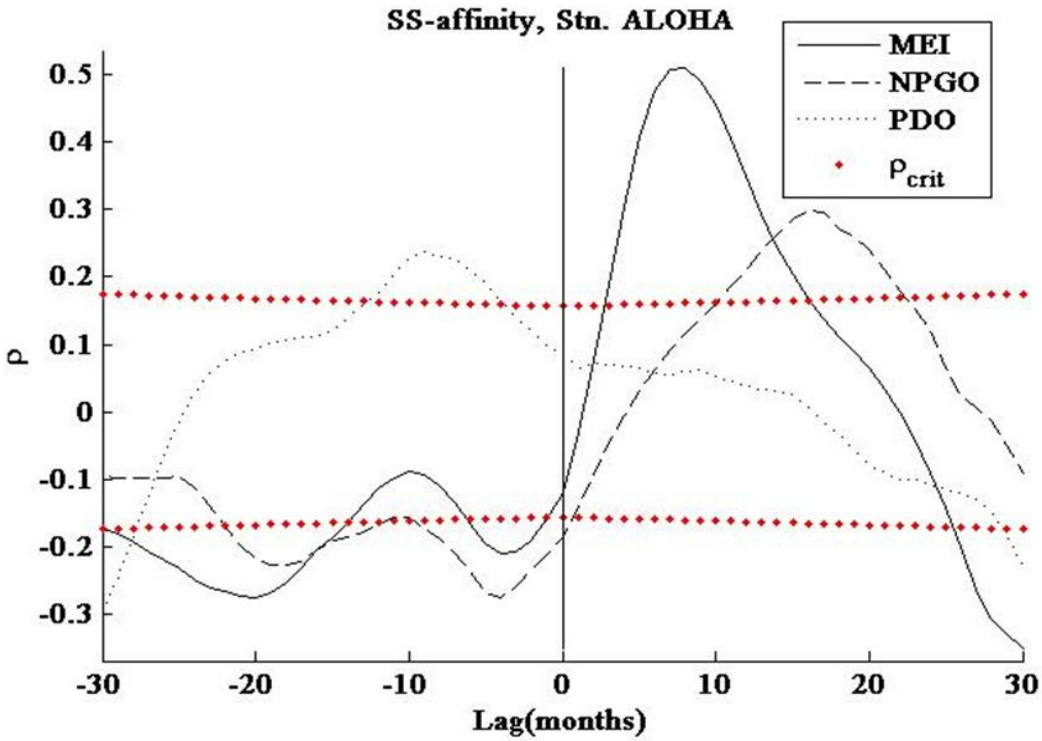

Figure 4.5. Cross correlation of climate indices with seascape identity index (SSID) at Station ALOHA. SSID was smoothed as in Figure 5. ρ-crit= significant correlation at 95% confidence. Negative lags= climate leads SSID; positive lags=SSID leads climate index.

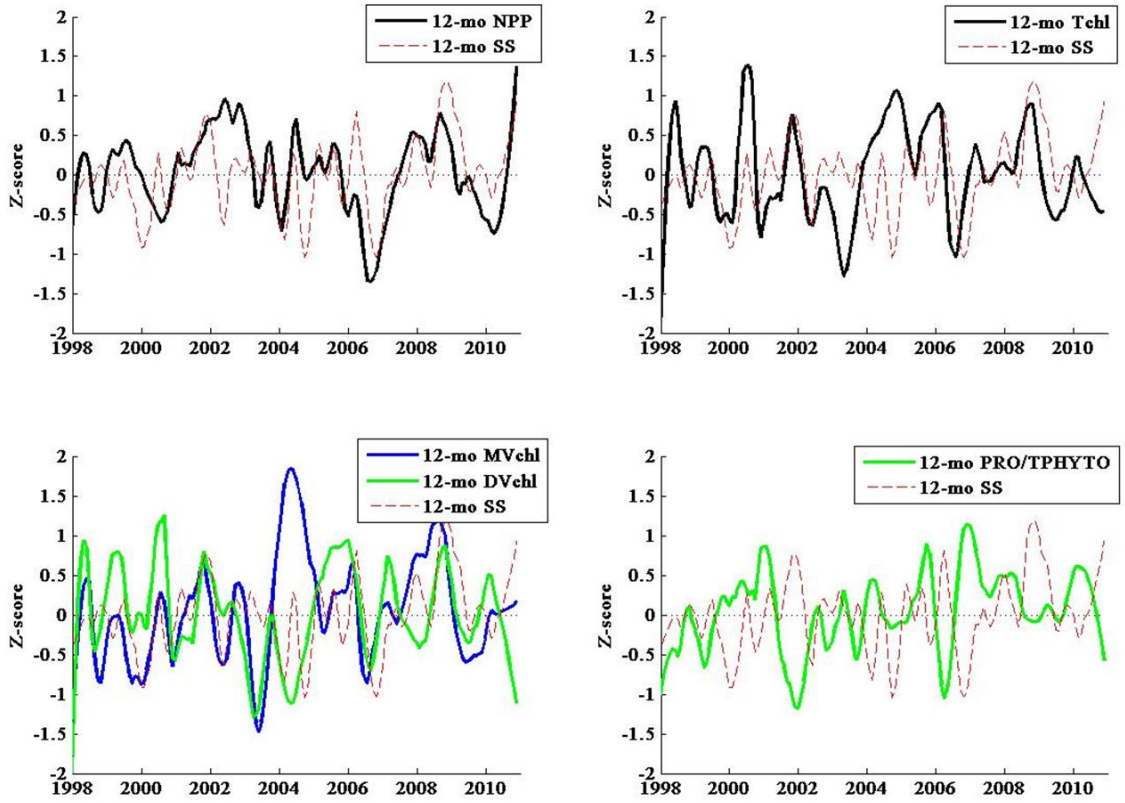

Figure 4.6. Changes in *in situ* properties at Station ALOHA. Values denote z-scores calculated after subtracting monthly climatological means; dashed red line denotes SSID. A: Net primary production. B: Total chlorophyll-a (chl-a). C: Monovinyl (MV) and divinyl (DV) chl-a. D: percent of total cells enumerated via flow cytometry that are identified as *Prochlorococcus* sp.

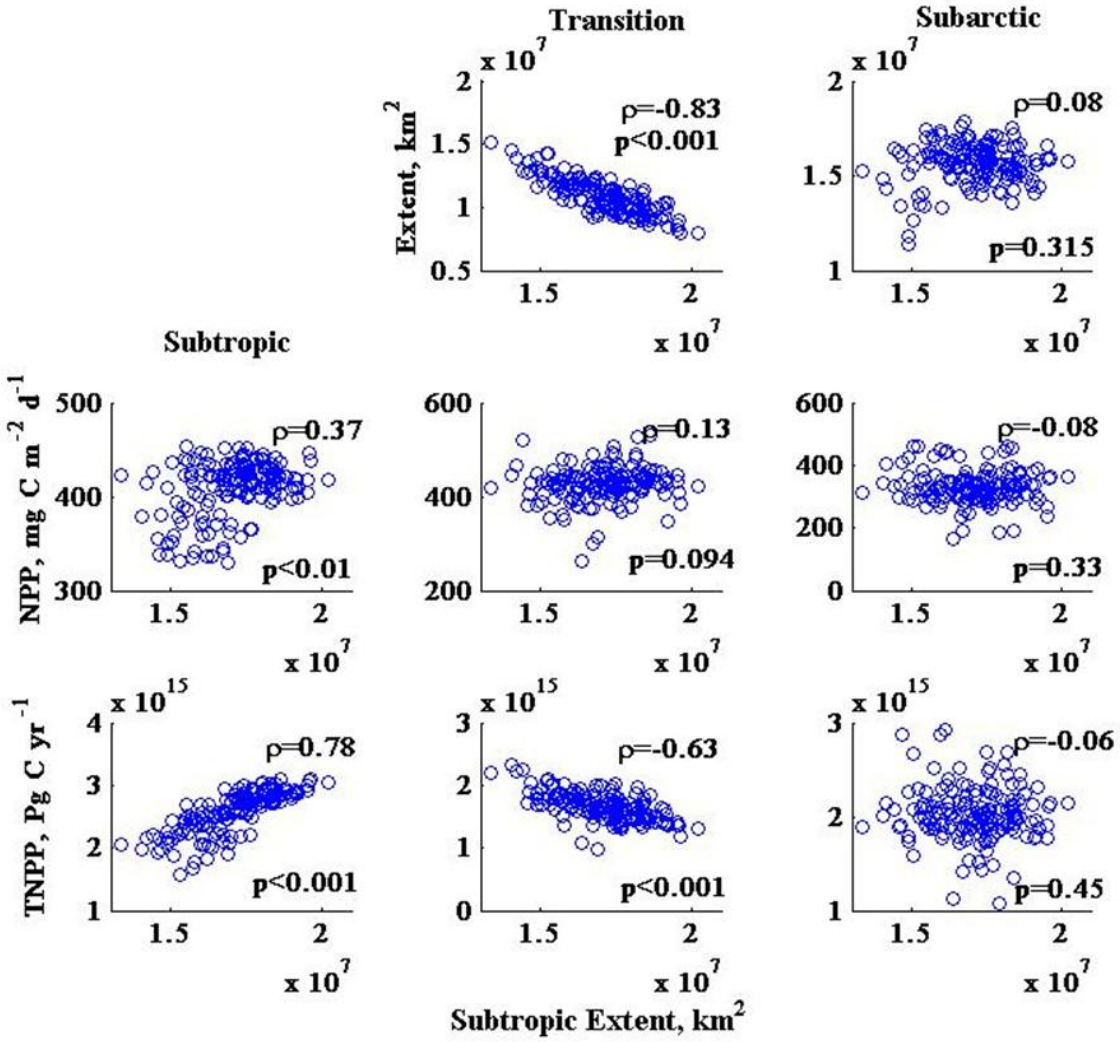

Figure 4.7. Effect of subtropical expanions on areal extent, net primary productivity (NPP) and total annual seascape production. Correlations and significance of each relationship is shown.

Table 4.1. Effect of mean seascape state and shifting identity on *in situ* chl-a and NPP as determined from multiple linear regression analysis.

	Scaled effect	Standard Error	T-statistic	p-value
chl-a				
Intercept	-0.07	0.07	-1.09	0.28
Seascape (SSID)	**0.49**	**0.20**	**2.51**	**0.01**
OBCHL	0.16	0.19	0.83	0.41
STCHL	-0.17	0.16	-1.05	0.29
OB * SSID	**1.26**	**0.62**	**2.03**	**0.04**
ST * SSID	-0.65	0.53	-1.23	0.22
NPP				
Intercept	-0.03	0.07	-0.40	0.69
Seascape (SSID)	**0.98**	**0.21**	**4.66**	**<.0001**
OB	**0.83**	**0.32**	**2.55**	**0.01**
ST	-0.34	0.27	-1.27	0.21
OB * SSID	0.88	1.27	0.69	0.49
ST * SSID	**-1.90**	**0.78**	**-2.44**	**0.02**

Table 4.2. Correlation coefficients of expanding subtropical seascapes with areal extent, NPP, and total primary production of North Pacific Seascapes. Red denotes significant positive correlation, blue denotes significant negative correlation ($p<0.05$); italicized $p<0.01$, bold $p<0.001$. Black= not significant.

Y: Area	X: All Subtropics	X: ST	X: OB
ST	***0.67***		***-0.53***
OB	*0.27*	***-0.53***	
TRAN	***-0.83***	***-0.54***	*-0.26*
SA	0.08	0.01	-0.08
Y: NPP			
ALL subtropics	***0.37***		
ST	***0.36***	*0.27*	0.05
OB	0.18	0.13	0.03
TRAN	0.13	*0.21*	-0.12
SA	0.08	0.17	***-0.31***
Y: Annual net primary production			
ALL subtropics	***0.78***		
ST	***0.69***	***0.93***	***-0.42***
OB	***0.34***	***-0.34***	***0.81***
TRAN	***-0.63***	***-0.33***	***-0.29***
SA	0.06	0.16	*-0.27*

CHAPTER 5: Constraints on primary and community production across N.E. Pacific seascapes

5.1 ABSTRACT

The subarctic subtropical transition zone represents the largest large sink of atmospheric carbon dioxide in the North Pacific and second largest in the world ocean, yet the relative importance of physical and biological processes in this drawdown is debated. In a step toward understanding the spatiotemporal variability of ecophysiological factors that contribute to the efficacy of the biological pump, near-continuous measurements of net primary production (NPP), net community production (NCP) and several ecophysiological variables were collected across subarctic, transition, and subtropical seascapes of the Northeast Pacific during August and September of 2008. Fluorescence diagnostics suggested that the mesotrophic boundary was neither iron nor macronutrient limited. Mesoscale processes and shifts in community structure contributed to high export efficiency in the subtropics. High biomass contributed to high NPP in the subarctic and ultimately to high NCP in the transition seascape. Here the convergence of moderate export efficiency (as quantified by the ratio of NCP to NPP) and high NCP drove biological mediation of air-sea exchange. Spatial succession from nanophytoplankton to microphytoplankton led to strong positive associations of pigment diversity with NCP, which contributed to DIC drawdown from 46 to 42 °N. Furthermore, NPP and NCP were strongly spatially coupled in both the transition ($r_{1, 39}$ =0.70; $p<0.0001$) and subtropics ($r_{1, 45}$= 0.68, $p<0.0001$) suggesting the promise for future empirical modeling efforts. Our

effort provides a first step in understanding the role of spatial variability in the modulation of primary and export production in an ecologically and geochemically important region. The spatially explicit seascape approach provides insight regarding the ecophysiological mechanism underlying the strength of the biological component of air-sea flux.

5.2 INTRODUCTION

The ocean carbon cycle modulates global climate by acting as a sink for atmospheric carbon dioxide (Siegenthaler and Sarmiento, 1993), but climate also affects the magnitude of the ocean's carbon sink by altering the functioning of the biological and solubility pumps (Emerson et al., 1997; Monahan and Denman, 2004). Although we have been able to characterize the location of carbon source and sink regions of the ocean and how they change on a seasonal basis (Takahashi et al. 2002, 2009), our understanding of how the efficiency of biological carbon sequestration will change in the future is still rudimentary. In general, biological systems will respond to perturbations by adjusting bulk processes, such as primary production and respiration rates, and through shifts in ecosystem structure (Falkowski et al. 1998). However, predicting the effects of global change on the ocean is problematic (e.g. Falkowski et al., 2000) because ecosystems respond non-linearly at both the physiological and community level as organisms respond to gradients and patches in the environment. Thus, accurate monitoring of the biological pump in conjunction with high resolution measurements of physiological and taxonomic diversity are necessary to characterize how the oceans will modulate and, in turn, be affected by future climate trends.

The de-coupling between production and remineralization that controls the efficiency of the biological pump represents an interaction between environmental variability and the evolutionary drive to optimize energy use and limited resources (Margalef 1968). Production of organic matter in the surface ocean is governed by the availability of light and nutrients, while export to depth depends on the effectiveness of

remineralization processes and ballasting throughout the water column (Brix et al. 2006). Net primary production (NPP) describes the difference between gross primary production (GPP) and autotrophic respiration in the light and dark. The difference between NPP and local heterotrophic respiration of organic matter is termed net community production (NCP) (Williams, 1998). At steady state and when averaged over sufficient length scales, NCP should be equivalent to export production (Laws et al. 2000), i.e. the flux of organic carbon out of the euphotic zone driven by the biological pump. This export takes place by sinking or advection of particulate and dissolved organic matter or via zooplankton migration. Understanding these processes and their relevant time and space scales will provide insight into ecosystem resilience and the maintenance of the biological pump under the stress of environmental change.

Over longer time and larger space scales, the magnitude of new production is related to the magnitude of GPP. However, the ‘‘efficiency’’ of the biological pump, or the fraction that reaches the deep sea, is controlled by numerous processes including: aggregation of organic particles, microbial remineralization, grazing and fecal pellet production, and interactions between organic aggregates and ballast minerals such as $CaCO_3$ and SiO_2 (as reviewed by De la Rocha and Passow, 2007). These processes, their interactions, and spatiotemporal variability have proven difficult to proxy and thus the efficacy, or effectiveness, of the biological pump and the spatiotemporal relationships between GPP, NPP and NCP are challenging to recreate in a mechanistic fashion. For example, ecosystem or empirical models that attempt to derive these relationships from satellite-derived chl-a and SST (Laws et al, 2000; Dunne et al., 2005) perform reasonably well globally but are limited in their capacity at local to gyre scales.

Phytoplankton communities respond to environmental variability by adjusting their community structure and physiological status (Falkowski et al., 2000), however the time scales of ecological and physiological responses are different and may or may not be spatially coherent. Serret et al. (2002) found that the threshold GPP necessary to support net autotrophy suggested by metaanalysis (Duarte and Regaudie de Gioux 2009) and theoretical studies (Lopes-Urrutia et al., 2006) had poor predictive capacity outside of the subtropics primarily due to a failure to account for different species effects. Iron availability is highly spatially and temporally variable; iron-limitation changes the physiological response of the phytoplankton assemblage to light and temperature (Boyd et al, 2994, Carr et al., 2006, Maldonado et al., 1999), which may affect the strength of the NPP: NCP relationship. Therefore, if we do not account for regional differences in diversity and physiology in an objective and spatially explicit fashion, we reduce our ability to predict how the biological pump will respond to future climate change.

5.2.1 Geochemical context:

The subarctic-subtropical transition zone from the Kuroshio extension into the eastern subarctic gyre is the largest sink region for atmospheric carbon dioxide in the North Pacific (Takahashi et al. 2009). Here, while biological uptake of dissolved inorganic carbon (DIC) tends to counteract the warming effect in the summer; the bulk of the drawdown has been attributed to winter cooling and the resultant increase in solubility of CO_2 in seawater (Takahashi et al., 2002). However, recent calculations of net community production across the eastern transition zone suggest that the effect of biological

drawdown is as, or more, important than the effect of solubility (Howard et al., 2010; Lockwood et al. in press). How the biological pump is primed in this geochemically important region, in terms of its efficiency in both carbon sequestration and mechanisms of subsequent export, is not understood. Furthermore, interannual changes in the extent (Chapter 4, Polovina, 2008; Polovina et al. 2011; Irwin and Oliver, 2009) and biological functioning of the oligotrophic gyres (Behrenfeld et al. 2006, Corno et al., 2007, Lomas et al., 2011) and the transition zone (Chapter 4) may affect the magnitude of air sea exchange. This uncertainty highlights the importance of consistent measurements of both NPP and NCP and a mechanistic understanding of the spatiotemporal variability in the physiological and ecological effects on NPP, NCP and the ratio between them.

Investigation of the spatial patterns within and between different bodies of water should provide insight as to the relative coupling of these processes and indicate whether we can empirically predict patterns of export. Over the course of a three-week cruise spanning the eastern subarctic, transition and subtropical regions, we measured NPP, NCP, and several ecophysiological variables at very high resolution (minutes to hours). Thus, we were able to obtain a data set that allowed evaluation of local (including diurnal variability) and basin-scale drivers of both gross and net community production. Previous studies indicated that microbial community composition, biogeochemical patterns, and biophysical forcing of pCO_2 were different across seasonally dynamic seascapes (Chapters 2 and 3). Here we apply a similar logic to high-resolution spatial data to understand the relative impact of various processes on carbon cycles in the upper ocean, specifically:

1. What is the relative strength of physiological, ecological and environmental factors in influencing NPP and NCP within and across seascapes?

2. How does the spatial relationship of NPP: NCP change as a function of seascape?

3. Finally, to inform future modeling efforts, how do the magnitude, efficiency, and community compositions of the biological pump vary in space?

5.3 METHODS

5.3.1 Regional analysis

Distinct seascapes were determined *a priori* based on the biophysical climatology described in Chapter 2. In brief, seascapes were classified by a combination of a probabilistic self-organizing map and a hierarchical clustering algorithm. This method maintains underlying biophysical distributions that reasonably describe pseudo-Lagrangian water history and results in objectively defined water masses that are statistically distinct both in terms of the satellite variables, in situ communities, and biogeochemical patterns (Chapters 2 and 3). Distinct water masses were identified using monthly climatologies of SST, chl-a, and PAR as measured by the MODIS-Aqua and SeaWiFs sensors.

Here we present divisions in the August/September 2008 ship tracks based on the location of boundaries in August based on the regions as defined in Chapter 2. Four seascapes were sampled over four legs of the cruise. The first approximated Line P from Vancouver Island to Ocean Station Papa (50 °N, 145 °W). The second consisted of a

southward transect along 145 °W to approximately 38 °N. The third consisted of a diagonal across the transition from 38 °N, 145 °W to 48 °N, 152 °W. The final leg consisted of a transect along 152 °W which crossed the transition a third time, traveling due south along 152 °W toward the Hawaiian Islands. Stations were sampled approximately every degree; however, high-resolution sampling from the ship's flow-through system occurred near continuously.

5.3.2 Community Structure and Dominant Size Classes

In order to understand how changes in the assemblage affect NPP and NCP, we measured phytoplankton pigment diversity and derived size classes from high-performance liquid chromatography (HPLC). Photosynthetic or accessory pigments were determined using C8 column (Goireke and Repeta, 1992). Pigment diversity was assessed using the Shannon-Weiner diversity index (H') on HPLC-derived pigment concentrations, specifically:

$$H' = \sum_i^h p_i \ln(p_i)$$

where p_i is the fraction of the i^{th} pigment to total pigment concentration in a sample and H' is the sum across all h pigments in a sample.

Size classes were derived from HPLC pigments using the equations described by Bricaud et al. (2004) and Uitz et al (2004). In brief, the percent contribution of pico-, nano-, and microphytoplankton to total chl-a was determined using weighted sum of

accessory pigments; total biomass by each class was calculated by multiplying by total chl-a.

The relative abundance of diatoms to haptophytes (including coccolithophores) was proxied using the ratio of fucoxanthin (FUCO) and its derivative 19-hexanoylfucoxanthin (19-HEX). We acknowledge the debate regarding the common usage of 19-HEX to indicate oceanic coccolithophores because of its occurrence across multiple coccolith and non-coccolith forming taxa (Jeffrey and Wright, 1997; Van Lenning et al., 2004). However, recent investigations have found good agreement of pigment concentrations with coccolithophore biovolume (Dandonneau et al., 2007).

5.3.3 Fast repetition rate fluorometry

Fast repetition rate fluorometry (FRRf) was used as a diagnostic of nutrient stress (Behrenfeld et al., 2005) as well as a means of spatially extrapolating discrete primary production measurements (Kolber et al., 1998). The FRRf uses rapid flashlets to saturate the photosystems allowing both the determination of the quantum yield of fluorescence (Fv/Fm) and the functional cross-section of PSII (σ_{PSII}, from the slope of the saturation curve). The FRRf was installed on the ship's flow-through system allowing near-continuous measurement of Fv/Fm and $\sigma_{PSII.}$ Diurnal patterns of Fv/Fm were compared across seascapes by binning measurements to the nearest hour and averaging across days within seascapes.

In theory, the FRRf measures the light reactions and approximates gross oxygen evolution (GOE) a measurement of GPP (Kolber et al., 1998). Thus, the FRRf provide a

means of interpolating GPP in space and over relatively short time scales (see Corno et al, 2005; Suggett et al. 2009). However, the ^{14}C rates used for tuning, when scaled to day length, were equivalent to 24 hr. ^{13}C incubations (Kavanaugh, unpubl.) that used standard light and dark bottle incubations (Hama et al., 1983) suggesting that they approximated NPP rather than GPP. Thus, for our study we empirically derive a spatially variable NPP proxy (NPPp) based on the product of the FRRf-derived parameters, chl-a, and mean daily photosynthetically active radiation (PAR). Specifically,

$$NPPp = m\ (Fv/Fm \times \sigma_{PSII} \times [chl\text{-}a] \times PAR \times c1) + c2$$

Where surface chl-a was determined through spatial interpolation of Fm (Corno et al. 2005), c1 is the constant applied in Corno et al. (2005) and m and c2 were regionally tuned from linear regression between the maximum primary productivity determined from 14C incubations ($P_{max:\ Table}$ 5.1). Because fluorescence quenching and number of reaction centers were not measured, we merely apply c1 as a scalar to constrain the error on the intercept of the ^{14}C-FRRf relationship. Photosynthetically active radiation was measured using a Biospherical PAR sensor deployed on a gimbaled mast in a non-shaded region of the ship and diurnal means determined using a daily running average.

Because we were interested in the spatial variability in NPPp, diurnal variations in FRRf-derived properties were removed using a medium loess-smoothing filter (6-26 hr.) prior to spatial turning. Spatial tuning of both the Fm: chl-a relationship and the FRRF: ^{14}C relationship was then conducted using least squares regression in two domains based on the dominant taxa (di-vinyl chl-a vs. mono-vinyl chl-a). For comparison with the ^{14}C measurements, the nearest geo-referenced measurement to the CTD cast or underway water grab was used with error assessed over +/- 15 minutes.

5.3.3 ^{14}C incubations

At just post-dawn, surface water was collected at 5-m depth from the rosette or from the underway system. Photosynthesis vs. irradiance (P vs. E) curves were derived from ^{14}C uptake measurements after 1-h incubations of 10 ml subsamples in temperature-controlled photosynthetrons, modified from the design of Jassby and Platt (1976). The maximal C-assimilation rate (P_{max}) was determined using a non-linear fit of the P vs. E curves (Jassby and Platt, 1976). For this analysis, 17 P_{max} assimilation experiments were successfully parameterized and used to tune the FRRf-derived NPP proxy measurements.

5.3.4 Net Community Production and Export Efficiency

Net community production was calculated via membrane inlet mass spectrometry (MIMS) from the balance of net O_2 production in the water and loss to the atmosphere by gas exchange (Reuer et al. 2007); the ratio with Ar removes much of the physically induced O_2 saturation changes. Briefly, a gear pump continuously draws water from the ship's seawater supply line through a cuvette fitted with a semi-permeable silicone membrane. Gases permeating the membrane are introduced into a triple filter quadrupole mass spectrometer (Hiden Analytical). The measured O_2/Ar ion current ratio is normalized to the O_2/Ar ratio of air-equilibrated seawater standards maintained in a temperature controlled water bath. The MIMS-based O_2/Ar measurements are further calibrated with the high precision discrete samples along the ship's track (Lockwood et al., in press; Howard et al., 2010). The MIMS allows for near continuous assessment of

NCP in the surface water (Tortell and Long, 2009, Lockwood et al., 2012). NCP is a mixed layer property and reported in terms of percentage saturation O_2 or C mmoles m^{-2} d^{-1}.

We calculated a particle export ratio (PE; Dunne et al., 2005) based on the ratio of NPPp to NCP:

$$PE = NCP \text{ (mmoles m-2 d-1)} / NPPp \text{ (mg C } m^{-3} d^{-1}) \text{ x MLD (m).}$$

We recognize the time scale differences between MIMS-derived NCP (8-14 days) and the NPPp (1 day). Thus, our calculated PE would be analogous to export efficiency if the day's NPP was equivalent to the average NPP over the timescale of oxygen exchange and that the light dynamics of the mixed layer depth were sufficiently integrated over the scale of the FRRf interpolation.

5.3.5 Additional measurements

Sea surface temperature, PAR, salinity and pCO_2 were collected as part of the ship's flow-through system. Underway pCO_2 was measured from surface water and air from the ship's bow with an automated infrared detection system described in detail elsewhere (Feely et al., 1998; Pierrot et al., 2009). Nutrients were collected at discrete stations and depths (Lockwood et al., 2012); only surface values (~5 m) are reported here. Sea surface height deviations were downloaded from NOAA Coastwatch (*http://oceanwatch.pifsc.noaa.gov/).*

5.3.6 Statistics: Relative effects of ecophysiological factors on NPP and NCP

Mixed step-wise multiple linear regression ($P_{enter,leave}$=0.25) was used to determine the influence of mean daily PAR, temperature, temperature variability, salinity, chl-a, Fv/Fm, σPSII, pigment diversity, the % of chl-a represented by pico, nano, and microphytoplankton as well as their respective chl-a biomass (% x [chl-a]) on NPP. We then used the same multiple linear regression (MLR) technique determine the influence of the above-mentioned variables and NPP on NCP. For both models, regressions were done within and across regions and effect sizes were normalized (centered on the mean and normalized by 0.5 of the range) to determine the relative strength of individual ecophysiological drivers on NPP and NCP and how they changed as a function of water mass. Individual effect sizes are thus unit-less and can be interpreted the percent change in NPP or NCP that is associated with a percent change in the ecophysiological driver after accounting for weighted effects of other significant drivers.

5.4 RESULTS

5.4.1. Seascape and Oceanographic Context

Four seascapes were previously described (Chapter 2) that quantify the spatial differences in water mass biogeochemistry and assemblage in late summer, early autumn (Figure 5.1). These included a subarctic seascape (SA), characterized by cooler temperatures and high chl-a; a summer transition seascape (Su-TRAN) that identifies the region between the subarctic and subtropical fronts; an oligotrophic boundary seascape

(OB) that has moderately low chl-a and nitrogen to phosphorus ratios (Chapter 2) ; and a subtropical seascape that has persistently low chl-a (<0.07 ug l) . The ship's track crossed through all four seascapes, with longitudinal repeats within the same seascape occurring in the SA, Su-TRAN and OB seascapes (Figure 5.1).

Sea surface height (SSH) deviations revealed several potential eddies along 152 W (Figure 5.2a). Specifically, anomalously high SSH was found at 30°-31°N, ~34°N, and 37 °N. Sea surface temperatures (SST, Figure 5.2b) were ~ 12° C in the subarctic, rose quickly through the transition seascapes, and leveled at ~ 26° C around the OB: ST boundary. Sea surface salinity (SSS, Figure 5.2b) shifts followed a similar pattern with fresher (~32.1-32.4) water occurring in the subarctic and higher SSS (~35) in the subtropics.

pCO_2 patterns have been reported elsewhere (Lockwood et al., in press). pCO_2 was undersaturated in the subarctic and transition seascapes and supersaturated south of ~42 °N, the approximate location of the Su-TRAN: OB boundary (Figure 5.2). The undersaturation was most remarkable in the Su-TRAN seascape with pCO_2 ranging from 320-340 µatm.

5.4.2 FRRf: subdiurnal patterns

Across the study region, Fv/Fm increased toward the subtropics with minima of ~0.30 during midday in the subarctic and maxima of ~0.53 in the subtropics. (Table 5.2, Figure 5.3). Diurnal patterns of Fv/Fm exhibited the typical bimodal pattern of morning and

evening maxima (Figure 5.3) with noontime depressions associated with non-photochemical quenching and midnight depressions associated with the reduction of the plastiquinone pool (Behrenfeld et al., 2005). All seascapes exhibited nighttime depression of Fv/Fm with the exception of the Su-TRAN; the largest relative decrease occurred in the SA (~11%).

5.4.3 Spatial ecophysiology: seascape patterns

Dissolved inorganic nutrients, sea surface temperature, PAR, and chl-a spatial patterns tended to follow the latitudinal gradients (Table 5.2). Nutrient concentrations were highest in the subarctic with substantial concentrations of nitrate (6.64 ± 2.19 μM), phosphate (0.72 ± 0.26 μM) and silicate (11.17 ± 5.81 μM). In the Su-TRAN region, concentrations of major nutrients decreased to about half that of the subarctic with the exception of silicate (8.92 +/- 6.03 μM), which was highly spatially variable. In the OB and ST seascapes, surface nutrient concentrations were a factor of 10 less than the northern seascapes, with the exception of silicate. Salinity increased equatorward with 32.3 ± 0.1 north of the subarctic front, 32.4 ± 0.2 and 33.5 ± 0.5 across the Su-TRAN and OB regions, and reaching 35.2 ± 0.3 in the ST. SST also gradually increased equatorward with mean SST of 12.8 ± 0.8 °C in the subarctic and 15.3 ± 1.5 °C, 21.2 ± 0.9 °C, 25.5 ± 0.5 °C, in the Su-TRAN, OB and ST respectively. Mean of PAR also increased gradually from the SA (536 ± 161μE m^{-2} s^{-1}) to the ST (936 ± 25 μE m^{-2} s^{-1}) with variance of PAR decreasing equatorward. Finally, chl-a was highest and most variable in the SA (0.48 ± 0.16 μg l^{-1}) and decreased toward the ST (0.05 ± 0.01 μg l^{-1}).

Several indices exhibited spatial maxima within the Su-TRAN region. The functional cross section of PSII (σPSII) generally followed the interaction of chl-a with PAR (Table 5.1), with highest values occurring in Su-TRAN region (762 ± 207 m^{-1}), followed the SA, the OB and then the ST (502 ± 88.2 m^{-1}). While nanophytoplankton still dominated the percentage contribution and total biomass (57.7% and 0.23 µg chl-a, respectively) microphytoplankton were locally abundant in the Su-TRAN region with percentage contribution of biomass >30%. Pigment diversity was highest in the Su-TRAN (2.11 ± 0.11) and almost 20% lower in the subtropics (1.75 ± 0.14). NCP was highest, but also spatially variable, in the Su-TRAN seascape (2.80 ± 1.77. Finally, while discrete experiments revealed that NPP was highest in the subarctic and decreased slightly in the Su-TRAN region, spatially interpolated results revealed no difference between the two regions ($NPPp_{subarctic}$= 3.2 ± 1.6 mg C m^{-3} hr^{-1} = $NPPp_{Meso-BND}$=3.1 ± 1.9 mg C m^{-3} hr^{-1}).

5.4.4 Spatial ecophysiology: longitudinal patterns

With our cruise track, we were able to determine the longitudinal gradient for the SA, Su-TRAN and OB seascapes (Table 5.3). In the SA and Su-TRAN seascapes, SST, salinity, and PAR tended to increase toward the west with concomitant westward decreases in Fv/Fm, σPSII and biological O_2 saturation (Table 5.3). Longitudinal changes in NPPp were not apparent in the subarctic or Meso-BND, though a westward decrease in NPPp was apparent in the OB, corresponding to decreases in chl-a and increases in diversity and σPSII. Diversity also shifted across the SA (but not the Su-TRAN).

5.4.5 Ecophysiological constraints on NPP

Forcing of NPP across the entire study area was most strongly related to chl-a concentrations, then light availability and the functional cross section, and finally relatively weakly related to variable fluorescence (Table 5.4, Scaled effect sizes = 2.97 ± 0.08 > 1.27 ± 0.08 = 1.34 ± 0.12 > 0.23 ± 0.08 respectively, R^2=0.98, p<0.0001). However, the source of variation and forcing strength were different across seascapes, reflecting both physical and ecological drivers within water masses.

The strong effect of chl-a on NPP across the entire study area was likely driven by their strong correlation in the Su-TRAN zone. Here the scaled effect size of chl-a (3.25 ± 0.09) was more than double that of σPSII (1.33 ± 0.10), 3 times stronger than PAR (0.90 ± 0.11), 6 times that of salinity (0.51 ± 0.14) and >9 times stronger than Fv/Fm. (0.33 ± 0.11). Unlike for the basin scale pattern, SST had no effect on NPP after accounting for the influence of the other variables.

In the SA, increased NPP was also associated with moderate changes in chl-a (0.72 ± 0.04), but also decreased microphytoplankton abundance (-0.28 ± 0.06), cooler temperatures (-0.22 ± 0.06), and decreased temperature variability (-0.19 ± 0.04). These likely reflect an interaction with cooler, iron-replete shelf water and water column stratification associated with inputs of freshwater. The negative effect of microphytoplankton abundance indicates that extant NPP was likely driven by nano- and pico-phytoplankton in the SA seascape.

In the oligotrophic boundary seascape, increased NPP was associated with high relative abundance of microphytoplankton, low diversity, relatively cooler temperatures,

and small but highly significant effects associated with increased photosynthetic efficiency (Fv/Fm effect= 0.11+/- 0.008).

Spatial patterns of ecophysiological drivers of NPP in the subtropics were influenced by an eddy located between 30 and 31 N, 152 W and another less prominent along the same line at ~34 N. Excluding these eddies, patterns of NPP were largely driven by concomitant changes in σPSII and increased photosynthetic efficiency (0.33 ± 0.01 and 0.16 ± 0.01, respectively). When the eddy stations were included in the analyses, the influence of chl-a increased (no eddy chl-a effect=0.11 ± 0.006 < eddy included chl-a effect =0.62 ± 0.08) as did increases in percentage of nano-phytoplankton (0.58 ± 0.19). However, as chl-a increased the proportion of nanophytoplankton decreased, leading to a negative interaction between chl-a and percentage of nanophytoplankton (nanoB effect: -0.57 ± 0.19).

5.4.6 Ecophysiological constraints on NCP

Net community production was strongly associated with net primary production across the extent of our study area (Table 5.5, NPP effect: 2.86 ± 0.34). Salinity and light availability had the next strongest association with their strength being roughly equal and opposite with high salinity and low light associated with increased NCP. Light was likely not limiting during August and the sign of the PAR effect was likely an effect of colinearity with macronutrient availability. Across the entire region, salinity had a strong positive effect (1.18 ± 0.27) despite strong negative associations within the SA and Su-TRAN. Once latitudinal changes were accounted for by other variables, changes in

salinity were no longer associated with large-scale changes in evaporation but more locally weighted to nutrient delivery. After accounting for chemical and physical variables, NCP was also associated with higher biomass of smaller phytoplankton (percentage nano effect= 0.34 ± 0.22, microphytoplankton biomass effect 0.75 $^{+/-}$ 0.18) and higher diversity (0.75 ± 0.18).

NCP in the SA was associated with decreased NPP (-0.45 ± 0.18) and salinity (-0.85 ± 0.14). Across the Su-TRAN, NCP was strongly positively associated with NPP (1.3 ± 0.57), warmer temperatures (1.52 ± 0.06), decreased salinity (-2.23 ± 0.89) and increased pigment diversity (1.01 ± 0.33). After accounting for the negative effect of picoplankton abundance (-0.22 ± 0.06), NCP in the OB was also associated with increased NPP (0.2 ± 0.06). Increased NCP in the ST seascape was also associated with increased NPP (0.34 ± 0.08), as well as increased SST (0.27 ± 0.08), slightly higher salinity (0.17 ± 0.05), increased chl-a (0.31 ± 0.14) and microphytoplankton biomass (0.27 ± 0.14). Removing the eddy stations resulted in halving of the salinity effect (0.08 ± 0.03) and eliminating chl-a and microphytoplankton biomass effect.

5.4.7 Spatial coupling of NPP and NCP

Throughout our study region, NPP and NCP were strongly coupled (Figure 5.4 and Table 5.6: r=0.78, $F_{1, 146}$ =230, p<0.0001); however, there was variation in the strength, magnitude, and sign of the correlation within and across seascapes. In the subarctic, the relationship tended toward neutral or negative (Figure 5.4a and Table 5.6, r =-0.24 to -0.72); there was insufficient data to determine if there was longitudinal variability. In the

Su-TRAN, the NPP-NCP relationship was strongly positive (Figure 5.4b, Table 5.6: $r=0.7$, $F_{1, 39}=36.3$; $p<0.0001$), although NCP and NPP were more strongly coupled in the east ($r_{145N}=0.92 > r_{152N}=0.53$). Different slopes and coupling strengths between the two meridians led to a non-linear NPP: NCP relationship within the OB seascape (Figure 5.4c). In the subtropics, BPP and NCP were strongly spatially correlated ($r=0.68$ $F_{1, 45}=38$, $p<0.0001$) but data were insufficient to assess east-west variability

The biological pump- efficiency, magnitude, and community composition: On broad scales, export efficiency, as determined by the ratio of NCP to NPP (Dunne et al., 2005), was higher in the subtropics, reaching a low between 35-40 °N, and then increased to moderate levels (Figure 5.5a). NCP was generally low in the subtropics (with the exception of the eddy at 30 °N), through the TZCF (42 - 42.5 °N depending on longitude), and reached a peak between 45 and 46 °N. Concentrations of both fucoxanthin (FUCO) and 19 –hexanoyloxyfucoxanthin (19-HEX) were very low in the ST (Figure 5.5 b). North of 30 °N, increases in FUCO were apparent though were still relatively low. These increases were mostly apparent in mesoscale features that occurred at 30, 34, and 37 °N where FUCO: 19-HEX ratios exceeded 1:1. North of the OB:Su-TRAN boundary, the absolute concentration of FUCO and 19-hex both increased; however the increase of 19-HEX lagged the increase in FUCO. The lag resulted in a high ratio of the two pigments from 42.5-44 °N and a moderate ratio through 46 °N, which co-occurred with the highest FUCO concentrations in our study area. North of 46 °N, the concentrations of both pigments increased, albeit FUCO did so to a lesser degree, which resulted in a decreased ratio of the two pigments.

5.5 DISCUSSION

In this study, we utilized an objective, seascape framework to evaluate the role of different drivers of primary production and net community production across the NE Pacific. We evaluated these drivers in a systematic and quantitative fashion to lend inference to future modeling efforts and field campaigns. The combined approach integrated physiology, ecology, and biochemistry and allowed us to embed ecophysiological measurements into geochemical cycles. While this cruise represents a snapshot in time, the results taken in the context of the large spatial extent as well as additional modeling efforts (Lockwood et al., in press) provide insight into the functioning of this geochemically and ecologically important region. Specifically, it focuses our attention on emergent properties of the transition zone where the efficiency, magnitude, and speciation of the biological pump act in synergy to affect air-sea CO_2 exchange.

Excess nitrate transported into the iron-replete transition zone (Ayers and Lozier, 2010) may be the mechanism for high NPPp and high NCP found in the Su-TRAN seascape. The subarctic NE Pacific is a high-nitrate low chlorophyll region where iron limitation of phytoplankton abundance, NPP and NCP has been demonstrated with shipboard and in situ experiments (Boyd et al., 2004). Southward Ekman transport of excess nitrate has been suggested as a source of nutrients to the transition zone chlorophyll front (Ayers and Lozier, 2010), with peaks in transport occurring in the eastern subarctic boundary region in late summer. Episodic alleviation of Fe-limitation and subsequent nitrogen drawdown in the NE subarctic has been attributed to

atmospheric deposition of central Asian dust (Mahawold et al., 2009) or local glacial flour (Cruisias et al., 2011), advection of water from the continental shelf via eddies (Crawford et al., 2002; Lam et al., 2006), or deposition of volcanic ash (Hamme et al, 2010, Langmann et al., 2010). Indeed the latter may be evoked as the Kasotochi eruption resulted in increased primary and community productivity over much of the subarctic (Hamme et al., 2010). However, patterns at multiple scales suggest that a local source of new nutrients, including iron, may also be important in the Su-TRAN.

5.5.1 Physiology: fluorescence diagnostics

While we did not measure iron in surface waters or iron-uptake in phytoplankton, fluorescence patterns across and within seascapes suggest that the transition is not iron-limited, unlike the subarctic seascape. Decreases in Fv/Fm have been associated with iron-limitation such as the pattern seen broadly from the western to eastern subarctic Pacific (Suzuki et al., 2002) and across the subtropical-equatorial HNLC boundary (Behrenfeld et al. 2006). Across our study area, we were able to visualize a gradual shift in mean Fv/Fm through the transition seascape with low values associated with the Fe-limited subarctic and moderate values in the subtropical gyres. No seascape appeared to be particularly iron-stressed based on the nighttime depression of Fv/Fm (Behrenfeld et al., 2005); however, the SA seascape had the largest percentage decrease whereas the adjacent Su-TRAN had virtually no decrease.

5.5.2 Ecology: community structure and export

The role of phytoplankton diversity in primary and export production is poorly understood. Taxa with mineral ballasting, e.g. diatoms and some coccolithophores, may contribute disproportionately to export (Armstrong et al., 2002). It has also been suggested that all phytoplankton contribute to export production proportionally to their primary production (Richardson and Jackson, 2007); while larger phytoplankton may be ballasted, near-neutrally buoyant picoplankton can aggregate or be packaged in larger faecal matter. In the transition we saw both high concentrations of chl-a and relatively high contributions by microphytoplankton (Table 5.2 and 5.3), suggesting that export was likely driven by diatoms. Analysis of biomarker pigments supports this hypothesis, and that diatom abundances may be greater than that of coccolithophores.

Most analyses have focused on the mechanism of individual species or select taxonomic groups, not the emergent properties of plankton assemblages. Diversity can also play a role in carbon production and export by maximizing nutrient use efficiency (Ptanick et al., 2008) and by affecting the spatial and temporal coupling between autotrophic and heterotrophic processes in surface waters. In our study, we found that phytoplankton pigment diversity was an important correlate of NCP in the mesotrophic boundary seascape, which influenced patterns across the entire study region. However, while diversity, NPP, and NCP were coupled latitudinally, NPP appeared to lead NCP and diversity longitudinally. In typical bloom succession, high diversity and moderate NPP tend to follow lowest diversity and highest NPP (Margalef, 1967; Guillard and Kilham, 1978). However, we cannot resolve causality. High diversity can contribute to

export via increased nutrient use efficiency or be a result of export subsequent succession. The coupling of NPP, NCP and phytoplankton diversity in the transition region remains an active area of research.

In the subtropics, two eddies present at ~34° and 30° N exhibited local variability of community structure and local increases in NPP. Local increases in NCP also occurred, but only in the eddy at 30° N. While both features exhibited decreases in pico-phytoplankton and concomitant increases in nano- and micro-phytoplankton, the degree of change varied between the features. Diversity and micro-phytoplankton both increased at 30 °N, whereas at 34 °N, increases in diversity were not apparent nor was the increase in micro-phytoplankton as profound. Whether the differences are due to age or strength of the eddy is unknown.

5.5.3 Biogeochemical rates

High rates of NPP have been measured in the subarctic HNLC region at Station Papa during the fall, although these rates did not exceed 30 mg m^{-3} d^{-1} (Boyd and Harrison, 1999). During this cruise, mean NPP in the SA was >25% higher than previously measured with some areas exhibiting 2-fold higher NPP. NPP (as measured by 12 hour 14C incubations) at Station Aloha typically average 7 mg C m^{-3} d^{-1} in August and 6 mg C m^{-3} d^{-1} in September; we saw similar rates outside of eddies in the OB and ST seascapes. NPP across the transition was also high; however, placing in historical context is difficult due to the paucity of measurements in this region. On a seascape scale, average satellite-derived NPP in the transition region from 1998-2010 was generally higher than that of

adjacent seascapes (Chapter 2). This and other studies (Lockwood et al., in press) suggest that this region has persistently high NPP.

5.5.4 NCP spatial variability

Macroscale analyses of patterns of community structure and productivity (both primary and export production) have been all but absent in pelagic systems where both within ecosystem and cross-system comparison of pattern and mechanism has been hampered by lack of an objective definition of ecosystem boundaries (Chapter 2). Across all three legs, we see that NPP and NCP are strongly coupled. The slope, however, varies longitudinally with greater export per unit assimilation occurring toward the east (Figure 5.4). We interpret this not as changes in the efficiency of the system but rather an accumulative effect of maintained high NPP in this region. The high NPP associated with moderate NCP the western transition (152°W) suggests that there may be a source of new nutrients, including iron, to the west of our study region. Lockwood et al also report high zonal and meridional variability in NCP as well air-sea CO_2 flux at <5 km scales. They hypothesized that local frontal dynamics could have important impact on biogeochemical fluxes in this region.

5.5.5 Effectiveness of the biological pump.

In our study, we were able to link the role of physiological acclimation to carbon assimilation, carbon assimilation and assemblage to export production, and export

production to air-sea exchange. Given potential shifts in ecosystem functioning associated with ocean acidification, temperature, or expansion of oligotrophic boundaries, understanding how water masses respond and modulate perturbations at different scales becomes increasingly important. In the transition seascape, we see a large biologically driven shift in pCO_2 that appears to be not episodic (Chapter 2, Chapter 4; Lockwood et al. 2012) but a seasonally recurring function of the ecosystem. Both biomass and light capture capacity contributed to high NPP in the transition. However, while NPP and phytoplankton diversity contributed to NCP in the transition, NCP and NPP were associated with shifts in salinity. We interpret the salinity effect to be equivalent to nutrient availability on both gyre scale and local (10-100s km) scales. Previous researchers have documented effects on export due to temperature (Laws et al., 2000) and food web structure (Legendre et al., 2002; Dunne et al., 2005): here we see that nutrient inputs are likely stronger drivers of NPP and NCP. Importantly, NCP is strongly coupled to NPP in the transition seascape. This, the recurrence of high NPP, and the importance of biologically mediated air-sea exchange (Lockwood et al, in press; Howard et al., 2010) suggest that the North Pacific transition region should be a focus of future modeling and cruise-based investigations related to how the biological pump contributes to the ocean carbon sink under different climate forcing.

The efficacy of the biological pump in drawing down CO_2 depends on three things: the magnitude of the pump, the efficiency of the pump, and the chemical make-up of the pump. During our study, the magnitude of export was greatest where the particle export ratio was moderately high, leaving little assimilated carbon to be respired in the surface. Furthermore, pigment spatial succession suggests that the air-sea exchange

driven by DIC drawdown of the biological pump was not neutralized by calcification. Thus for the snapshot of the cruise, the triumvirate of factors related to the effectiveness of the biological pump contributed in synergy to the Su-TRAN role as a sink for atmospheric CO_2.

Conclusion: In this narrow but geochemically and ecologically important band, we see an example in the transition where processes that occur on timescales of <1 day, multiple days, and weeks are coherent. How the ecophysiological drivers outlined in this study vary on interannual scales remains to be assessed. The Arctic Oscillation drives the position of the westerlies that entrain iron-rich dust from central Asia to be deposited over the Pacific (Mahawold et al., 2009). However, the latitude as well as areal extent of the transition zone may be driven by interactions of the North Pacific Gyre Oscillation (Chapter 4, Di Lorenzo et al., 2008) and Pacific Decadal Oscillation (Chai et al., 2003). Furthermore, if projected decreases in NPP (Chapter 4; Polovina et al., 2011) are met with concomitant decreases in NCP as suggested by the relationships revealed in this study, then the loss of biologically-mediated atmospheric carbon sequestration will be profound. While more research is needed in this ecologically and geochemically important zone, we assert that the systematic seascape approach that we have employed and our subsequent results will inform future modeling and ship-based efforts that will illuminate the spatiotemporal variability of processes that contribute to the efficacy of the biological pump on interannual to climate scales.

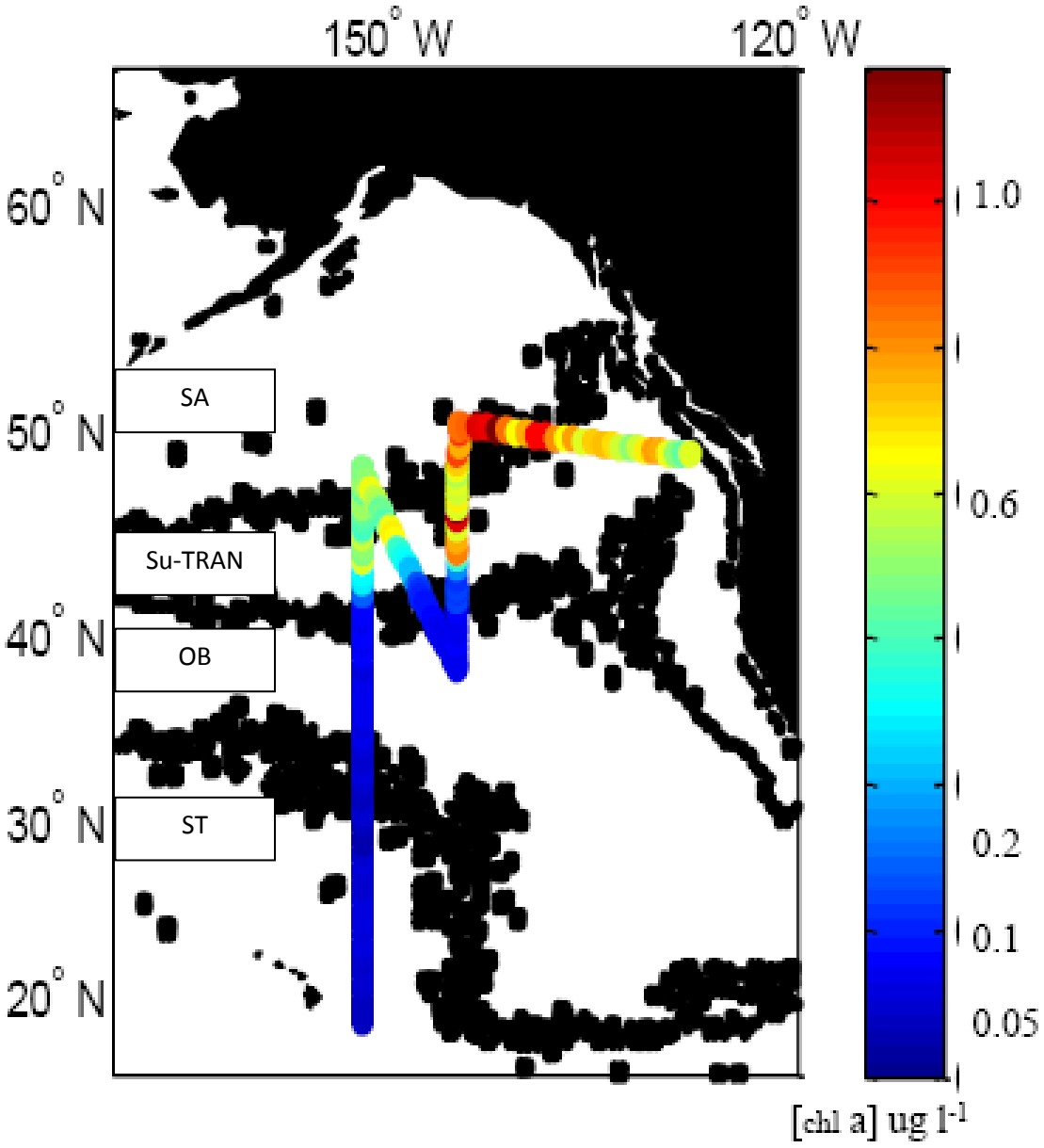

Figure 5.1. In situ chlorophyll a concentration across NE Pacific Seascapes. Seascape boundaries (black pixels) demarcate four objectively determined seascapes adetermined from monthly climatologies (1998-2010) of satellite derived chl-a, sea surface temperature and photosynthetically active radiation for August (Chapter 2). SA= subarctic; Su-TRAN= summer transition; OB= oligotrophic boundary; and ST= subtropic.

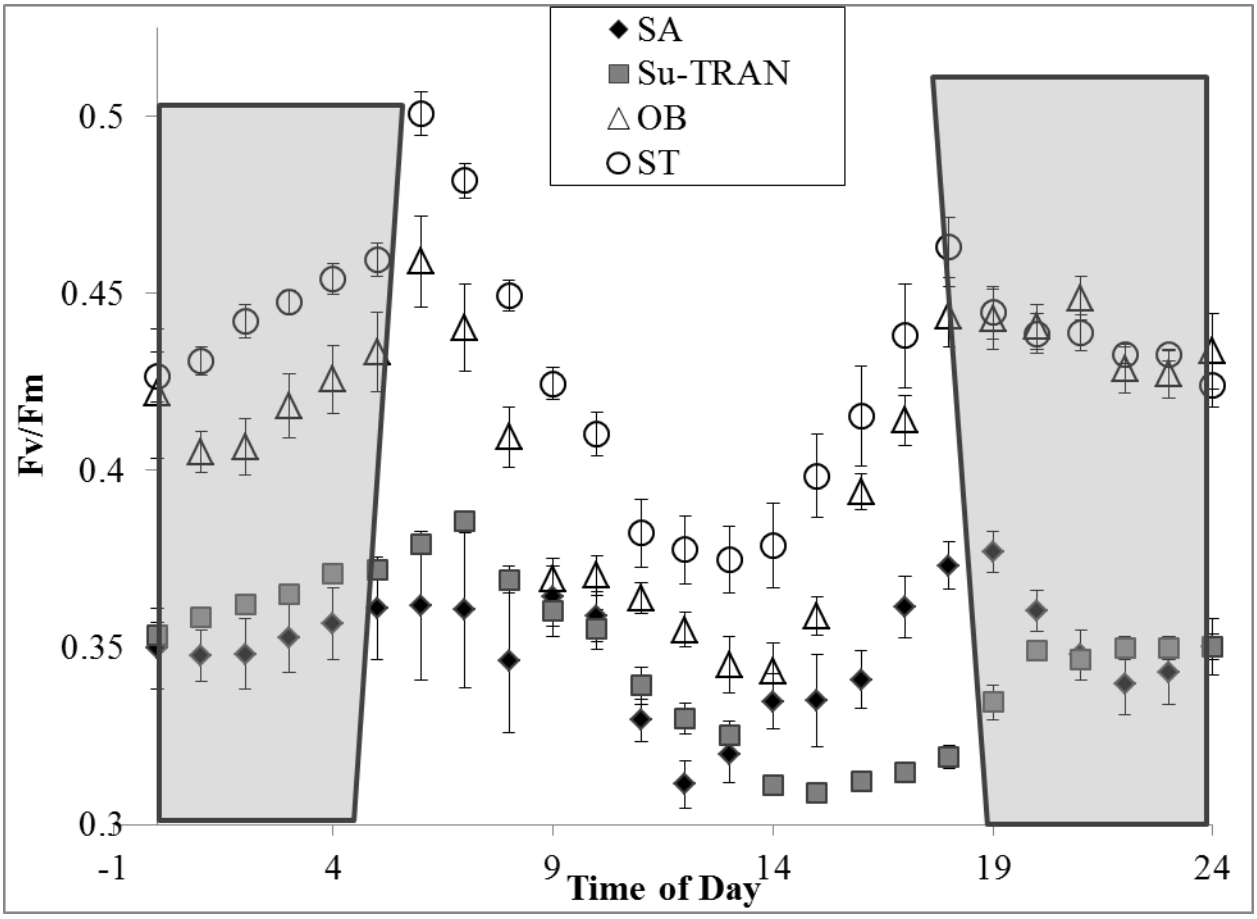

Figure 5.2. Macro-physiological trends (mean +/- SE) of variable fluorescence (Fv/Fm) for surface waters over ~ 3 weeks of August, early September for four objectively-defined seascapes in the northeastern Pacific. SA=>46.8 °N, Su-TRAN=~42 to 46.8 °N, OB=34-42 °N, ST=< 34 °N. Shading denotes approximate nighttime periods.

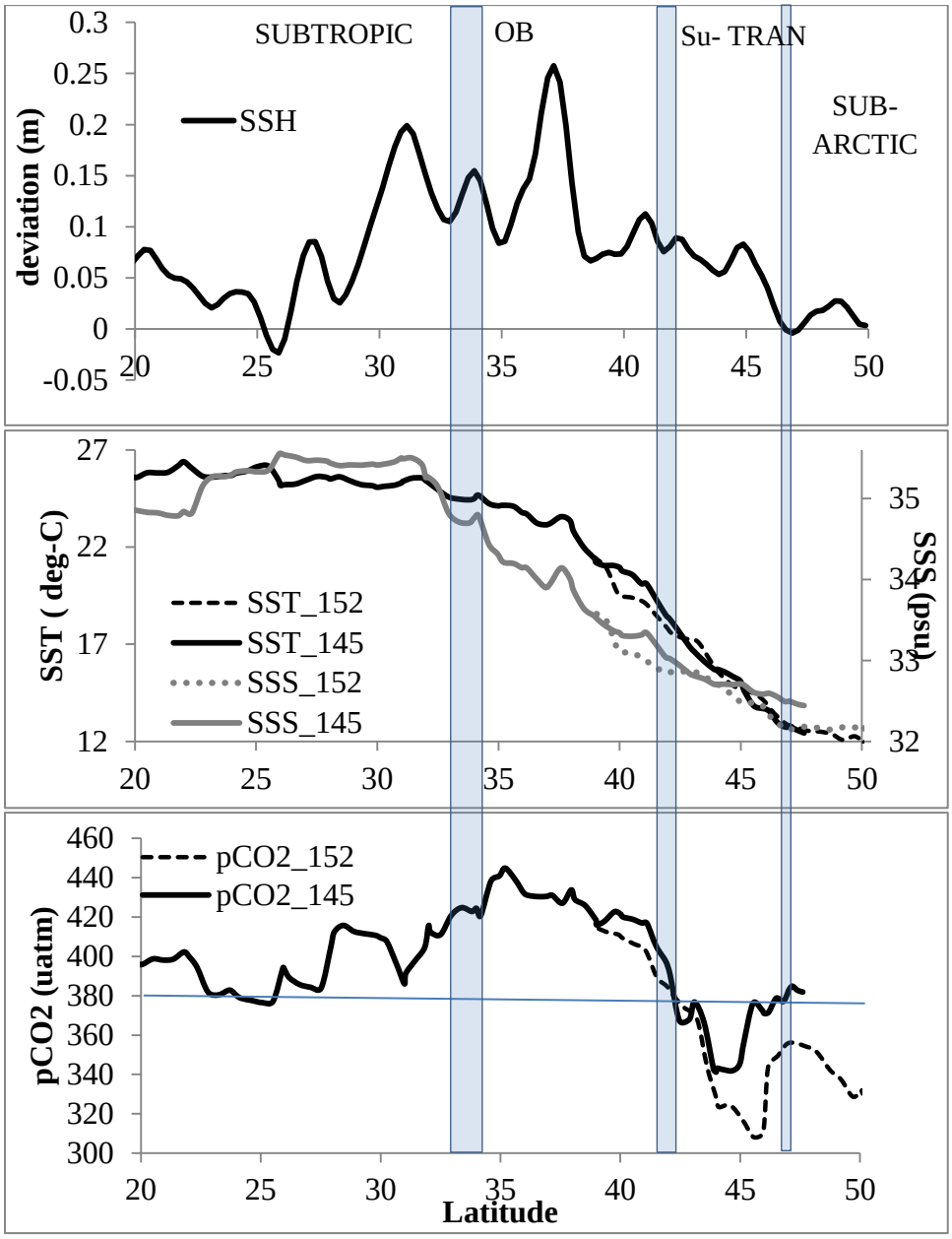

Figure 5.3. Oceanographic and geochemical context: Latitudinal variations of SSH, SST, Salinity and pCO2 along 152 °W (solid lines) and 145 °W (dashed lines, SSH not shown). Blue bars denote boundaries between seascapes as in Figure 1 and as defined by Chapter 2; bar width denotes general width of boundary. The large decreases of pCO2 seen between 47 and 42 °N is purportedly dominated by biological drawdown (Howard et al. 2010; Lockwood et al., in press).

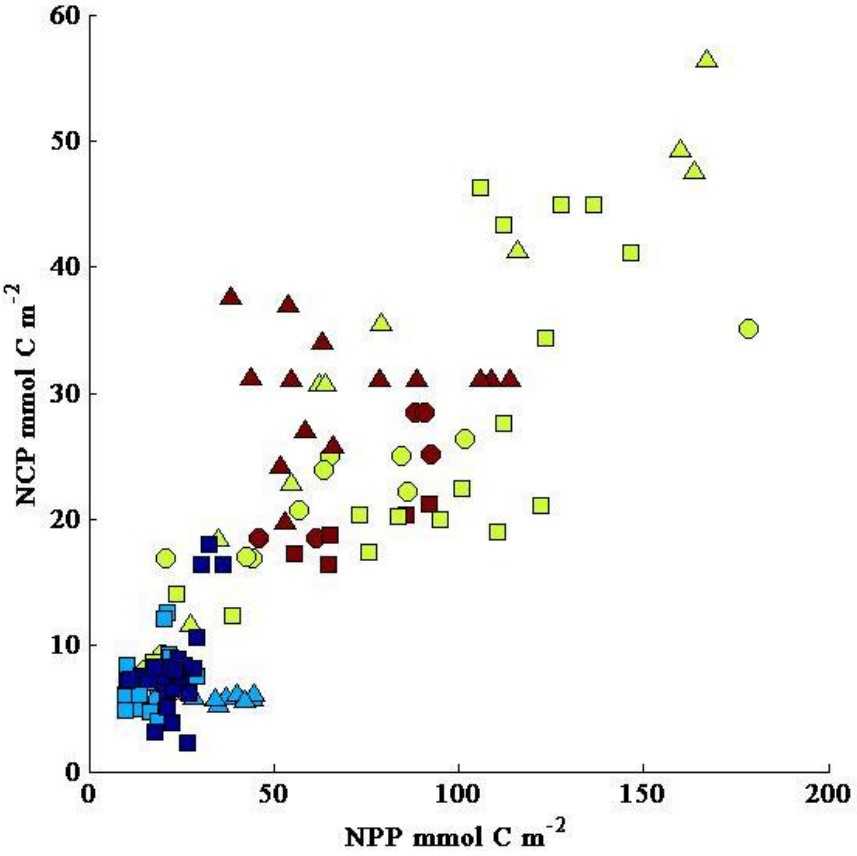

Figure 5.4. Relationship between Net Community Production (NCP) and Net Primary Productivity (NPP) across NE Pacific Seascapes. Color coding denotes seascapes: red=SA; light green=Su-TRAN; cyan=OB; dark blue=ST. Symbols denote specific lines where Squares=152 °W, triangles=145 °W and circles=rest of cruise track.

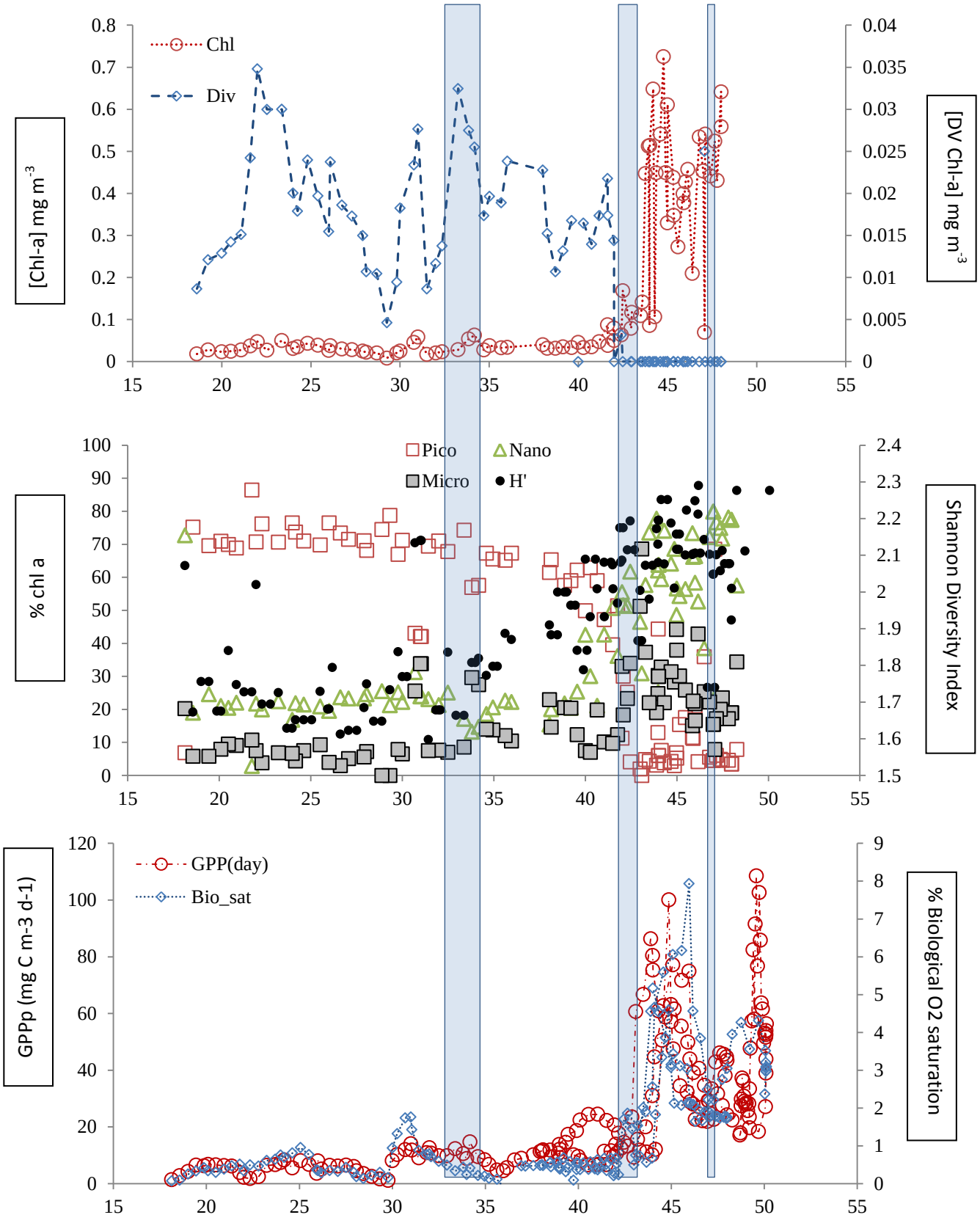
Chl
Div
[Chl-a] mg m-3
[DV Chl-a] mg m-3
Pico
Nano
Micro
H'
% chl a
Shannon Diversity Index
GPP(day)
Bio_sat
GPPp (mg C m-3 d-1)
% Biological O2 saturation

Figure 5. 5

Figure 5.5. Variation in phytoplankton community structure and biological rates in the NE Pacific. Blue bars denote boundaries between seascapes as in Figure 1 and as defined in Chapter 2; bar width denotes general width of boundary. Panel A shows the relative dominance of different groups based on the abundance of chl a and divinyl chl a. Panel B. Changes in functional diversity and the % contribution of pico, nano, and microphytoplankton to total chl a . Panel C shows the latitudinal variation in NPP and Biological O2 saturation, an index of net community production.

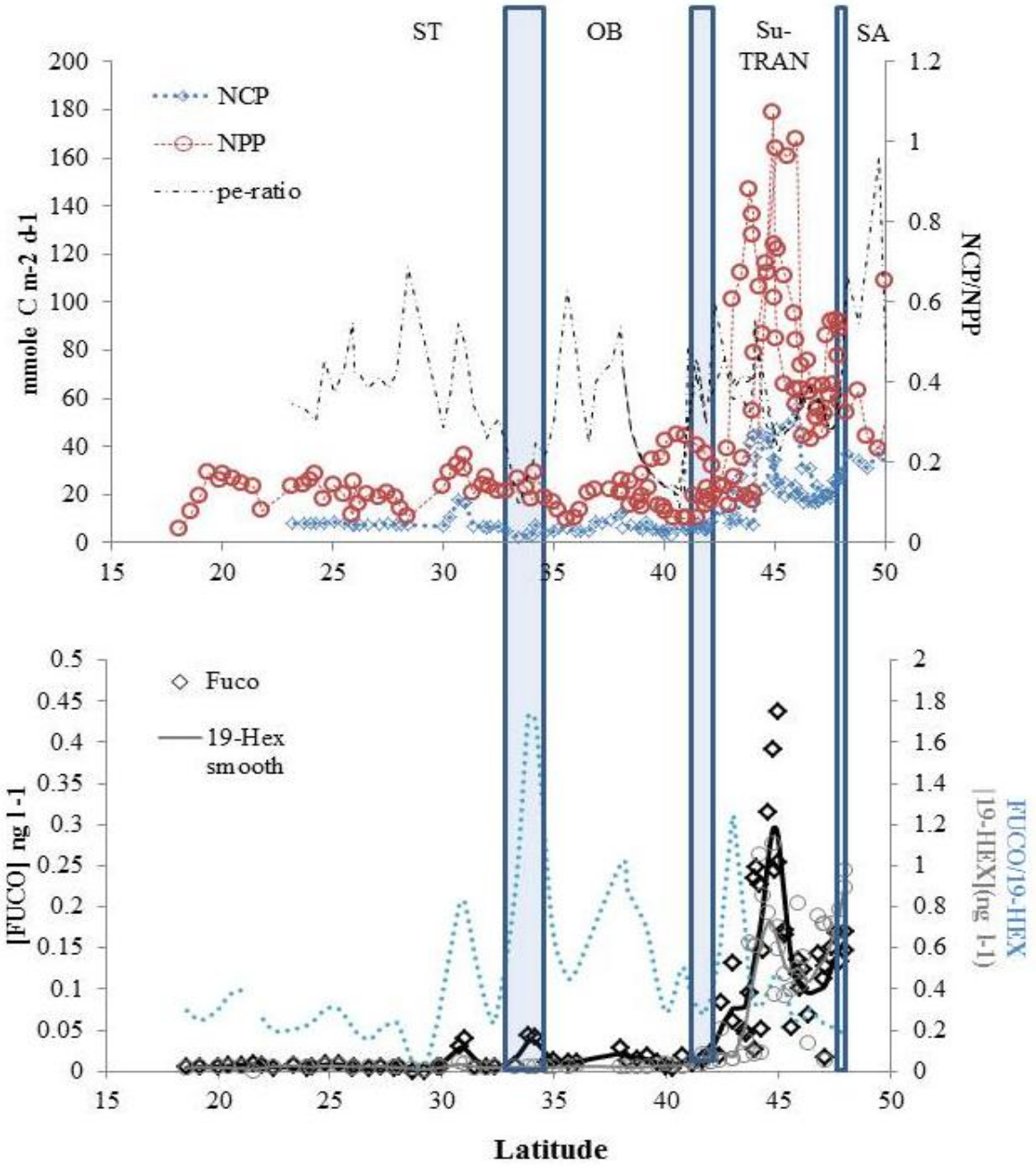

Figure 5.6. Relative contribution of magnitude, efficiency, and community structure to potential functioning of the biological pump . Panel 1. Latitudinal patterns of net primary production (NPP, red circle), community production (NCP, blue diamond) and export efficiency (pe-ratio: NCP/NPP, black dashed line). Blue pars denote boundaries between seascapes. Panel 2. Relative abundances of biomarker pigments for diatoms and haptophytes including coccolithophores showing fucoxanthin (FUCO, black triangle, black line), 19-hexanoylfucoxanthin (19-HEX, grey circles, grey line) and the ratio between FUCO and19-HEX (blue dotted line).

Table 5.1. Regression models used to spatially tune the NPP proxy from the FRRf ^{14}C relationship

Scale	F-stat (N)	p	Intercept (SE)	Slope (SE)	R^2
NE Pacific	115.0 (17)	<0.0001	0.292 (0.193)	1.062 (0.099)	0.88
>42.5 °N	55.1 (11)	<0.0001	0.211 (0.340)	1.088 (0.151)	0.85
<42 °N	17.1 (6)	0.0256	0.530 (0.314)	3.398(0.821)	0.81

Table 5.2. Summary of Chemical, Physical and Biological Properties within NE Pacific Seascape Surface Waters. Values are mean (+/- SE) within seascapes.

	SA	Su-TRAN	OB	ST
NO_3 (µM)	6.64 (2.19)	2.45 (2.77)	0.17 (0.27)	0.15 (0.07)
PO_4 (µM)	0.72 (0.26)	0.36 (0.30)	0.14 (0.07)	0.05 (0.06)
NO_2- (µM)	0.15 (0.05)	0.05 (0.04)	0.01 (0.02)	0.001 (0.004)
NH_4 (µM)	0.14 (0.15)	0.08 (0.08)	0.02 (0.04)	0.01 (0.02)
Silicate (µM)	11.17 (5.81)	8.92 (6.03)	3.89 (1.64)	2.85 (1.28)
SST (C)	12.81 (0.85)	15.34 (1.53)	21.19 (1.91)	25.49 (0.44)
Salinity (psu)	32.30 (0.13)	32.69 (0.16)	33.53 (0.46)	35.19 (0.30)
PAR (uE m-2 s-1)	536 (161)	656 (155)	853 (119)	936 (25)
Fv/Fm	0.35 (0.04)	0.36 (0.03)	0.41 (0.03)	0.43 (0.03)
s PSII	752 (192)	762 (207)	552 (95)	502 (88.2)
H' (HPLC)	2.07 (0.13)	2.11 (0.11)	1.96 (0.11)	1.75 (0.14)
%pico	10.74 (19.2)	11.75 (11.1)	58.65 (7.95)	66.93 (15.0)
%nano	69.92 (16.6)	57.71 (12.5)	26.56 (10.7)	23.07 (10.3)
%micro	19.20 (6.52)	30.32 (11.6)	14.69 (5.88)	9.93 (8.92)
Micro ug chl l^{-1}	0.08 (0.03)	0.11 (0.08)	0.01 (0.01)	0.01 (0.01)
Nano ug chl l^{-1}	0.31 (0.09)	0.23 (0.16)	0.02 (0.01)	0.01 (0.01)
Pico ug chl l^{-1}	0.04 (0.07)	0.04 (0.04)	0.04 (0.01)	0.03 (0.01)
Tchl-a ug l^{-1} (HPLC)	0.48 (0.16)	0.38 (0.20)	0.09 (0.05)	0.05 (0.01)
14C mg C m^{-3} hr^{-1}	2.53 (0.72)	2.05 (1.52)	0.80 (0.15)	0.77 (0.09)
NPP p mg C m^{-3} hr^{-1}	3.15 (1.60)	3.13 (1.88)	0.91 (0.41)	0.53 (0.26)
NPP p mg C m^{-3} d^{-1}	42.5 (21.7)	38.8 (23.4)	11.9 (5.46)	6.76 (3.32)
Biological Saturation	2.59 (0.83)	2.80 (1.77)	0.41 (0.17)	0.55 (0.39)

Table 5.3. Meridional gradient in selected physical, chemical and biological parameters. Difference between leg 4 (152 °W) and leg 2 (145°W) are shown for the subarctic, mesotrophic transition and oligotrophic transition seascapes. Significance is as a result of pooled variance t-tests: *p<0.05, **p<0.01, ***p<0.001. nb= insufficient data for comparison. Sample sizes ranged from 19-28 except for: NH_4 where sample size=6 for each seascape and for subarctic H' where sample size =6.

	SA	Su-TRAN	OB
SST (C)	0.50 (0.17)***	0.15 (0.56)	1.22 (0.47)*
Salinity (psu)	0.30 (0.01)***	0.14 (0.06) *	0.24 (0.09)*
PAR (uE m^{-2} s^{-1})	132 (83)	307 (31)***	-85 (61)
NH_4 (umol l^{-1})	nb	0.07 (0.06)	-0.10 (0.01)**
Fv/Fm	-0.03 (0.01)**	-0.05 (0.01)***	0.02 (0.01)*
σ_{PSII}	-90 (110)	-241 (73)**	214 (9)***
Chl a (ug l^{-1})	-0.01 (0.05)	0.07 (0.07)	-0.11 (0.01)***
H'	-0.21(.02)***	-0.02 (0.08)	0.11 (0.03)**
NPPp (mgC m^{-3} hr^{-1})	0.17 (0.45)	0.76 (0.66)	-0.83 (0.10)***
Biosat (% O_2 sat.)	-1.34 (0.25)***	-1.73 (0.66)*	-0.01 (0.05)

Table 5.4. Normalized effects of ecophysiological parameters on net primary production within and across Northeast Pacific seascapes. Effect sizes are derived from multiple linear regression analysis (see methods) and can be interpreted as percent change in response with percent change in parameter. Effect sizes are significant ($p<0.05$) unless othewise noted (NS).

Seascape	SA		Su-TRAN		OB		ST (with eddy)		ST (no eddy)		NE Pacific	
R^2	0.99		0.98		0.99		0.99		0.99**		0.98	
R^2 adj	0.98		0.98		0.99		0.98		0.98		0.98	
N	10		44		8		31		41		77	
	Effect	SE	Effect	SE	Effect	SE	Effect	SE	Effect	SE	Effect	SE
intercept	2.52	0.02	3.13	0.04	0.68	0.003	0.53	0.004	0.49	0.003	1.78	0.03
PAR			0.9	0.11			0.04	0.01	0.04	0.01	1.27	0.08
[chl]	0.72	0.04	3.25	0.09			0.62	0.08	0.11	0.006	2.97	0.08
s PSII			1.33	0.1			0.33	0.01	0.33	0.01	1.34	0.12
Fv/Fm			0.33	0.11	0.11	0.008	0.16	0.01	0.16	0.01	0.23	0.08
SST	-0.22	0.06			-0.28	0.012						
SST σ	-0.19	0.04										
salinity			0.51	0.14								
% pico												
% nano							0.58	0.19				
% micro					0.32	0.007					0.18 NS	0.08
picoB												
nanoB							-0.57	0.19				
microB	-0.28	0.06										
H' HPLC					-0.18	0.02						

Table 5.5. Normalized effect of ecophysiological parameters on net community production within and across NE Pacific seascapes. Effect sizes are derived from multiple linear regression analysis (see methods) and can be interpreted as percent change in response with percent change in parameter. Effect sizes are significant ($p<0.05$) unless othewise noted (NS).

Seascape	SA		Su-TRAN		OB		ST (with eddy)		ST (no eddy)		NE Pacific	
R^2	0.89		0.84		0.84		0.87		0.64		0.86	
R^2 adj	0.85		0.8		0.078		0.84		0.62		0.84	
N	17		25		8		31		41		74	
	Effect	SE	Effect	SE	Effect	SE	Effect	SE	Effect	SE	Effect	SE
intercept	2.29	0.07	2.48	0.13	0.31	0.02	0.56	0.03	0.44	0.03	1.38	0.07
GPP	-0.45	0.18	1.3	0.57	0.2	0.06	0.34	0.08	0.36	0.06	2.86	0.34
PAR	-0.18	0.17	-0.7 NS	0.39							-1.16	0.27
[chl]							0.31	0.14				
SST			1.52	0.6			0.27	0.08	0.28	0.05		
SST σ	0.17 NS	0.17									0.49	0.24
salinity	-0.85	0.14	-2.23	0.89			0.17	0.05	0.08	0.03	1.18	0.27
% pico					-0.22	0.06					0.34	0.22
% nano												
% micro												
picoB												
nanoB			1.00 NS	0.57								
microB							0.27	0.14			-0.78	0.38
H' HPLC			1.01	0.33							0.75	0.18

Table 5.6. Spatial relationships between NPP and NCP across and within NE Pacific seascapes. Correlation coefficients, r, sample size (N) and F-statistics are reported for the NPP:NCP relationship across the region and for individual legs denoted by their longitude.

	r	N	F	p
NE Pacific	**0.86**	**124**	**230**	**<0.0001**
152 °W	**0.90**	**68**	**195**	**<0.0001**
145 °W	**0.78**	**32**	**37.6**	**<0.0001**
SA	0.14	28	1.8	0.19
152 °W	**0.82**	**6**	**4.34**	**0.05**
145 °W	0.01	15	0.01	0.9
Su-TRAN	**0.85**	**40**	**36.3**	**<0.0001**
152 °W	**0.77**	**14**	**4.72**	**0.05**
145 °W	**0.96**	**11**	**105**	**<0.0001**
OB	0.15	33	0.79	0.38
152 °W	**0.44**	**20**	**4.3**	**0.05**
145 °W	0.33	9	0.28	0.68
ST	**0.58**	**46**	**13.1**	**<0.0001**

CHAPTER 6: General conclusion

6.1 General overview

In this dissertation, I applied the hierarchical patch mosaic paradigm of landscape ecology to the study of the seasonal and interannual variability of the North Pacific in order to facilitate comparative analysis between pelagic ecosystems and to provide spatiotemporal context for analyzing data from eulerian time-series studies. The dynamic, objectively-determined seascapes described within this dissertation offer improved hydrographic coherence compared to oceanic regions with subjectively defined and static boundaries (Chapter 2). These seascapes represent unique biogeochemical functioning (Chapter 2) and microbial communities (Chapter 3). They describe previously uncharacterized spatiotemporal variability, which can have important ramifications for the oceanographic context in which we place *in situ* observations (Chapter 4). Finally, they provide an objective extent by which to model important biogeochemical processes and compare ecosystem functioning (Chapter 5). Thus, the seascape concept may be a powerful tool for ecologists and oceanographers alike to characterize spatiotemporal variability and objectively compare the response of ocean ecosystems to environmental perturbations (Murakski et al., 2010). Here I revisit the major findings of this research and identify a few critical areas where questions remain.

6.2 Dynamic seascapes: biogeochemical modeling

Chapter 2 presents a rigorous test of the seascape concept at the seasonal scale. Novel methods of objectively describing hierarchy were presented in concert with rigorous

application of both signal processing and inferential statistics. Identified seascapes had different nutrient concentrations, ratios, and biophysical forcing of biogeochemical patterns. It is recognized that the multiple linear regression approach used to characterize biophysical forcing of pCO_2 maybe simplistic. However, the capacity of seascapes to limit non-hydrographical variability suggests that more sophisticated approaches (e.g. Hales et al., 2012) will be fruitful. Given the importance of the North Pacific transition seascape to global carbon cycles (Takahashi et al., 2009), it is critical to continue to investigate the relative influence of temperature-related solubility, convergence, and biological drawdown on air-sea CO_2 exchange and how they shift in time.

Based on the variable biogeochemical patterns observed between seascapes in Chapter 2 and verified explicitly in Chapter 3, seascapes are characterized by distinct microbial communities. Furthermore, because seascapes represent objective hierarchies, we were able to quantify the relative importance of environmental forcing on microbial communities at different scales. Importantly, while other chapters demonstrate the utility of the seascape concept for empirical modeling and *in situ* studies, Chapter 3 makes the case that the seascape, like the hierarchically organized landscape, may describe entities relevant to ecological theory.

6.3 Dynamic seascapes: ecology

Several questions central to ecology require that researchers have well-defined spatial extents. For example, understanding the underlying drivers of community, landscape/seascape or latitudinal scale patterns of species diversity requires explicit quantification of both sample size and extent of study area (Whitaker et al., 2001).

Understanding whether local environmental perturbations (habitat effects) or the large-scale, long-term legacy of historical differentiation in habitats (provincial effects) describe extant differences in planktonic species or functional group distributions (Martiney et al. 2006) also requires that the spatial extent of measurement be explicit as well as nested. At local scales, both environmental and ecological interactions may play a role in organizing the microbial community. However, whether the endogenous drivers of microbial community structure are associated with dispersal (Liebold and Norberg, 2004), top-down trophic (Steinberg et al., 2010), or bottom up forcing (Cullen et al., 1991) the seascape provides an objective extent over which to test these hypotheses with *in situ* measurements or modeling (Prowe et al., 2012).

6.4 Dynamic seascapes: global change

In Chapter 4, it was discovered that interannual shifts in the boundaries of a transition seascape and two distinct oligotrophic subtropical seascapes affect the variability observed at benchmark time series Station ALOHA on interannual scales. Encroachment by different seascapes on Station ALOHA resulted in shifts in phytoplankton abundances, dominance, and net primary production. Station ALOHA is ideally situated to measure the interannual oscillations of subtropical seascapes, which may facilitate modeling of how climate affects not only the subtropics, but also adjacent seascapes.

The extent (~6 million km^2) of subtropical expansion is borne almost entirely by the transition zone, resulting in a transfer of ~1.2 Pg C of total primary production between a system primed for export production and one dominated by the microbial loop.

As is discussed in Chapter 5, this shift may have repercussions on not only the extent of the transition seascape, but also on its role as sink for atmospheric carbon dioxide. In the transition seascape, high net primary production is recurring and is strongly coupled to high net community production or export of carbon from the mixed layer. Collaborative efforts (Lockwood et al., in press; Howard et al., 2010) have shown that export production dominates other processes in drawing down atmospheric CO_2. During the 2008 cruise, it was observed that the phytoplankton community shifted from dominance by smaller eukaryotes in the subarctic seascape to one dominated by diatoms in the transition seascape. The fixed organic carbon was not only ballasted for rapid sinking, but pigment biomarker analysis suggests that the associated mineral was diatom-derived silica rather than calcium carbonate.

6.5 Dynamic seascapes: future research

Seascapes are a useful construct for quantifying and comparing surface processes. However, how the seascape concept translates to processes at greater depths remains a challenge for future modeling efforts. In the subtropics, sunlight penetrates relatively deep (>100 m) into the ocean. The result is that there is a second community at the base of the euphotic zone that is less nutrient-depleted but may have sufficient light to photosynthesize (Venrick, 1988; Winn et al., 1995; Letelier et al., 2004). This deep chlorophyll maximum (DCM) community has seasonality and can be intermittently affected by vertical physical oscillations (Huissman et al., 2006) leading to shifts of 10s of meters of the DCM. The episodic alleviation of light and nutrient limitation can lead to

increased biomass, productivity and subsequent export production. During the University of Washington Student Cruise highlighted in Chapter 5, there was higher NPP at depths of 50-65 meters than at the surface in the region just south of the transition seascape's convergence with the subtropics (Kavanaugh unpubl.). While space and time were lacking to include these results in the dissertation, they highlight the fact that subsurface processes may be critical in some regions for injecting carbon below the seasonal mixed layer. Testing the coherence of seascapes throughout the water column is a logical next step and remains a goal for future research.

This dissertation provides a first step in understanding the seascape variability in the NE Pacific as well as modulation of primary and export production in a critical transition region. The multivariate seascape approach described here provides spatiotemporal context for *in situ* studies and allows objective comparisons of systems' responses to climatic forcing. Globally, several programs are currently afloat to monitor the ocean through cabled observatories (Ocean Observatories Initiative; http://www.oceanobservatories.org/), ship-based opportunities and Argo floats (Global Ocean Observing System; http://www.ioc-goos.org/) and deep water moorings (OceanSITES; http://www.oceansites.org/index.html). A truly integrated ocean observing system will utilize the insight gained from the increased resolution of *in situ* observations, refined ecosystem models as well as satellite remote sensing that will continue to provide greater spatiotemporal context. The results highlighted in this dissertation suggest that the pelagic seascape framework, through its capacity to scale both mechanism and context, may serve as an important and unifying component of such an observing system.

BIBLIOGRAPHY

Alvain, S., C. Moulin, Y. Dandonneau, and F. M. Bréon. 2005. Remote sensing of phytoplankton groups in case 1 waters from global SeaWiFS imagery. Deep Sea Research Part I: Oceanographic Research Papers **52**: 1989–2004

Anouar, F., F. Badran, and S. Thiria. 1998. Probabilistic self-organizing map and radial basis function networks. Neurocomputing **20**: 83–96

Armstrong, R. A., C. Lee, J. I. Hedges, S. Honjo, and S. G. Wakeham. 2001. A new, mechanistic model for organic carbon fluxes in the ocean based on the quantitative association of POC with ballast minerals. Deep Sea Research Part II: Topical Studies in Oceanography **49**: 219–236

Ayers, J. M., and M. S. Lozier. 2010. Physical controls on the seasonal migration of the North Pacific transition zone chlorophyll front. Journal of Geophysical Research **115**: C05001

Belgrano, A., M. Lima, and N. C. Stenseth. Non-linear dynamics in marine-phytoplankton population systems : Emergent properties of complex marine systems: a macroecological perspective. Marine ecology. Progress series **273**: 281–289.

Bidigaire, R. R., C. Fei, M. R. Landry, R. Lukas, C. C. S. Hannides, S. J. Christensen, D. M. Karl, S. Lei, and C. Yi. Subtropical ocean ecosystem structure changes forced by North Pacific climate variations. Journal of plankton research **31**: 1131–1139.

Brown, J. H. On the relationship between abundance and distribution of species. The American naturalist **124**: 255–279.

Barnes, C., X. Irigoien, J. A. A. De Oliveira, D. Maxwell, and S. Jennings. 2010. Predicting marine phytoplankton community size structure from empirical relationships with remotely sensed variables. Journal of Plankton Research **33**: 13–24

Barton, A. D., S. Dutkiewicz, G. Flierl, J. Bragg, and M. J. Follows. 2010a. Patterns of diversity in marine phytoplankton. Science (New York, N.Y.) **327**: 1509–11

Barton, A. D., S. Dutkiewicz, G. Flierl, J. Bragg, and M. J. Follows. 2010b. Patterns of Diversity in Marine Phytoplankton . Science **327** : 1509–1511

Beaugrand, G., P. C. Reid, and F. Ibañez. 2000. Biodiversity of North Atlantic and North Sea calanoid copepods . Marine Ecology Progress Series **204**: 299–303.

Behrenfeld, M. J., and P. G. Falkowski. 1997. A Consumer's Guide to Phytoplankton Primary Productivity Models. Limnology and Oceanography **42**: 1479–1491.

Behrenfeld, M. J., R. T. O/'Malley, D. A. Siegel, C. R. McClain, J. L. Sarmiento, G. C. Feldman, A. J. Milligan, P. G. Falkowski, R. M. Letelier, and E. S. Boss. 2006a. Climate-driven trends in contemporary ocean productivity. Nature **444**: 752–755.

Behrenfeld, M. J., R. T. O'Malley, D. a Siegel, C. R. McClain, J. L. Sarmiento, G. C. Feldman, A. J. Milligan, P. G. Falkowski, R. M. Letelier, and E. S. Boss. 2006b. Climate-driven trends in contemporary ocean productivity. Nature **444**: 752–5

Behrenfeld, M. J., J. T. Randerson, C. R. McClain, G. C. Feldman, S. O. Los, C. J. Tucker, P. G. Falkowski, C. B. Field, R. Frouin, W. E. Esaias, D. D. Kolber, and N. H. Pollack. 2001. Biospheric Primary Production During an ENSO Transition . Science **291** : 2594–2597

Behrenfeld, M. J., K. Worthington, R. M. Sherrell, F. P. Chavez, P. Strutton, M. McPhaden, and D. M. Shea. 2006c. Controls on tropical Pacific Ocean productivity revealed through nutrient stress diagnostics. Nature **442**: 1025–1028.

Bibby, T. S., Y. Zhang, and M. Chen. 2009. Biogeography of Photosynthetic Light-Harvesting Genes in Marine Phytoplankton. PLoS ONE **4**: e4601.

Bograd, S. J., D. G. Foley, F. B. Schwing, C. Wilson, R. M. Laurs, J. J. Polovina, E. A. Howell, and R. E. Brainard. 2004. On the seasonal and interannual migrations of the transition zone chlorophyll front. Geophys. Res. Lett. **31**: L17204

Bouvier, T., and P. A. Del Giorgio. 2007. Key role of selective viral-induced mortality in determining marine bacterial community composition. Environmental Microbiology **9**: 287–297.

Bowker, G. C., and S. L. Star. 2000. Sorting Things Out: Classification and Its Consequences (Google eBook), MIT Press.

Boyce, D. G., M. R. Lewis, and B. Worm. 2010. Global phytoplankton decline over the past century.

Bragg, J. G., S. Dutkiewicz, O. Jahn, M. J. Follows, and S. W. Chisholm. 2010. Modeling selective pressures on phytoplankton in the global ocean. R. DeSalle [ed.]. PloS one **5**: e9569

Brander, K. 2010. Impacts of climate change on fisheries. Journal of Marine Systems **79**: 389–402

Breitbarth, E., A. Oschlies, and J. Laroche. 2007. Physiological constraints on the global distribution of Trichodesmium ? effect of temperature on diazotrophy. Biogeosciences (BG), 4(1), 53-61

Brickley, P. J., and A. C. Thomas. 2004. Satellite-measured seasonal and inter-annual chlorophyll variability in the Northeast Pacific and Coastal Gulf of Alaska. Deep Sea Research Part II: Topical Studies in Oceanography **51**: 229–245

Brix, H., N. Gruber, D. M. Karl, and N. R. Bates. 2006. On the relationships between primary, net community, and export production in subtropical gyres.

Brown, J. H. 1995. Macroecology / James H. Brown.

Cole, J. J. Communication between terrestrial and marine ecologists : loud, sometimes abrasive, but healthy and occasionally useful : Bridging the gap between aquatic and terrestrial ecology. Marine ecology. Progress series **304**: 272–274.

Campbell, L., H. Liu, H. A. Nolla, and D. Vaulot. 1997. Annual variability of phytoplankton and bacteria in the subtropical North Pacific Ocean at Station ALOHA during the 1991–1994 ENSO event. Deep Sea Research Part I: Oceanographic Research Papers **44**: 167–192

Campbell, L., and D. Vaulot. 1993. Photosynthetic picoplankton community structure in the subtropical North Pacific Ocean near Hawaii (station ALOHA). Deep Sea Research Part I: Oceanographic Research Papers **40**: 2043–2060

Carr, M.-E., M. A. M. Friedrichs, M. Schmeltz, M. N. Aita, D. Antoine, K. R. Arrigo, I. Asanuma, O. Aumont, R. Barber, M. Behrenfeld, R. Bidigare, E. T. Buitenhuis, J. Campbell, A. Ciotti, H. Dierssen, M. Dowell, J. Dunne, W. Esaias, B. Gentili, W. Gregg, S. Groom, N. Hoepffner, J. Ishizakas, T. Kameda, C. Le Quere, S. Lohrenz, J. Marra, F. Melino, K. Moore, A. Morel, T. E. Reddy, J. Ryan, M. Scardi, T. Smyth, K. Turpie, G. Tilstone, K. Watersa, and Y. Yamanaka. 2008. A comparison of global estimates of marine primary production from ocean color. Deep Sea Research II 53.5-7 (2006): 741-770.

Carrascal, L. M., I. Galván, and O. Gordo. 2009. Partial least squares regression as an alternative to current regression methods used in ecology. Oikos **118**: 681–690

Cermeño, P., C. de Vargas, F. Abrantes, and P. G. Falkowski. 2010a. Phytoplankton biogeography and community stability in the ocean. H.H. Bruun [ed.]. PloS one **5**: e10037

Cermeño, P., C. de Vargas, F. Abrantes, and P. G. Falkowski. 2010b. Phytoplankton Biogeography and Community Stability in the Ocean. PLoS ONE **5**: e10037.

Chai, F., M. Jiang, R. Barber, R. Dugdale, and Y. Chao. 2003. Interdecadal Variation of the Transition Zone Chlorophyll Front: A Physical-Biological Model Simulation between 1960 and 1990. Journal of Oceanography **59**: 461–475

Chavez, F. P., M. Messié, and J. T. Pennington. 2011. Marine primary production in relation to climate variability and change. Annual review of marine science **3**: 227–60.

Clements, F. E. 1936. Nature and Structure of the Climax. Journal of Ecology **24**: 252–284 CR – Copyright © 1936 British Ecolog.

Corno, G., D. M. Karl, M. J. Church, R. M. Letelier, R. Lukas, R. R. Bidigare, and M. R. Abbott. 2007. Impact of climate forcing on ecosystem processes in the North Pacific Subtropical Gyre. J. Geophys. Res. **112**: C04021

Corno, G., R. M. Letelier, M. R. Abbott, and D. M. Karl. 2006. Assessing primary production variability in the North Pacific Subtropical Gyre: A comparison of fast repetition rate fluorometry and 14C measurements. Journal of Phycology **42**: 51–60

Crusius, J., A. W. Schroth, S. Gass, C. M. Moy, R. C. Levy, and M. Gatica. 2011. Glacial flour dust storms in the Gulf of Alaska: Hydrologic and meteorological controls and their importance as a source of bioavailable iron. Geophys. Res. Lett. **38**: L06602

Cullen, J. J. 1991. Hypotheses to Explain High-Nutrient Conditions in the Open Sea. Limnology and Oceanography **36**: 1578–1599.

Deutsch, C., N. Gruber, R. M. Key, J. L. Samiento, and A. Ganachaud. Denitrification and N2 fixation in the Pacific Ocean. Global biogeochemical cycles **15**: 483–506.

Dandonneau, Y., Y. Montel, J. Blanchot, J. Giraudeau, and J. Neveux. 2006. Temporal variability in phytoplankton pigments, picoplankton and coccolithophores along a transect through the North Atlantic and tropical southwestern Pacific. Deep Sea Research Part I: Oceanographic Research Papers **53**: 689–712

DiTullio, G. R., and E. A. Laws. 1991. Impact of an atmospheric-oceanic disturbance on phytoplankton community dynamics in the North Pacific Central Gyre. Deep Sea Research Part A. Oceanographic Research Papers **38**: 1305–1329

Doney, S. C., V. J. Fabry, R. A. Feely, and J. A. Kleypas. 2009. Ocean Acidification: The Other CO 2 Problem. Annual Review of Marine Science **1**: 169–192

Doney, S. C., M. Ruckelshaus, J. Emmett Duffy, J. P. Barry, F. Chan, C. A. English, H. M. Galindo, J. M. Grebmeier, A. B. Hollowed, N. Knowlton, J. Polovina, N. N. Rabalais, W. J. Sydeman, and L. D. Talley. 2012. Climate Change Impacts on Marine Ecosystems. Annual Review of Marine Science **4**: 11–37

Dore, J. E., R. Lukas, D. W. Sadler, M. J. Church, and D. M. Karl. 2009. Physical and biogeochemical modulation of ocean acidification in the central North Pacific. Proceedings of the National Academy of Sciences of the United States of America **106**: 12235–40

Duarte, C. M., and A. Regaudie de Gioux. 2009. Thresholds of gross primary production for the metabolic balance of marine planktonic communities.

Dunne, J. P., R. A. Armstrong, and J. L. Sarmiento. 2009. Empirical and mechanistic models for the particle export ratio.

Eiler, A., D. H. Hayakawa, and M. S. Rappé. 2011. Non-random assembly of bacterioplankton communities in the subtropical north pacific ocean. Frontiers in microbiology **2**: 140

Emerson, S., P. Quay, D. Karl, C. Winn, L. Tupas, and M. Landry. 1997. Experimental determination of the organic carbon flux from open-ocean surface waters. Nature **389**: 951–954.

Evans, W., P. G. Strutton, and F. P. Chavez. 2009. Impact of tropical instability waves on nutrient and chlorophyll distributions in the equatorial Pacific. Deep Sea Research Part I: Oceanographic Research Papers **56**: 178–188

Fenchel, T., and B. J. Finlay. 2004. The Ubiquity of Small Species: Patterns of Local and Global Diversity. BioScience **54**: 777

Falkowski, P. G., R. T. Barber, and V. Smetacek. 1998. Biogeochemical Controls and Feedbacks on Ocean Primary Production . Science **281** : 200–206

Falkowski, P. G., T. G. Owens, A. C. Ley, and D. C. Mauzerall. 1981. Effects of Growth Irradiance Levels on the Ratio of Reaction Centers in Two Species of Marine Phytoplankton.. Plant Physiology **68**: 969–973

Falkowski, P., R. J. Scholes, E. Boyle, J. Canadell, D. Canfield, J. Elser, N. Gruber, K. Hibbard, P. Högberg, S. Linder, F. T. Mackenzie, B. Moore III, T. Pedersen, Y. Rosenthal, S. Seitzinger, V. Smetacek, and W. Steffen. 2000. The Global Carbon Cycle: A Test of Our Knowledge of Earth as a System . Science **290** : 291–296

Feely, R. A., S. C. Doney, and S. R. Cooley. 2009. Ocean acidification : present conditions and future changes.

Field, C. B., M. J. Behrenfeld, J. T. Randerson, and P. Falkowski. 1998. Primary Production of the Biosphere: Integrating Terrestrial and Oceanic Components . Science **281** : 237–240

Follows, M. J., S. Dutkiewicz, S. Grant, and S. W. Chisholm. 2007. Emergent Biogeography of Microbial Communities in a Model Ocean. Science **315** : 1843–1846

Forman, R. T. T. 1995. Some general principles of landscape and regional ecology. Landscape Ecology **10**: 133–142

Forman, R. T. T., and M. Godron. 1981. Patches and Structural Components for a Landscape Ecology. BioScience **31**: 733–740.

Fortin, M.-J., and M. R. T. Dale. 2005. Spatial Analysis: A Guide for Ecologists, Cambridge University Press.

Freeland, H. 2007. A short history of Ocean Station Papa and Line P. Progress In Oceanography **75**: 120–125

Friedrich, T., and A. Oschlies. 2009. Neural network-based estimates of North Atlantic surface pCO 2 from satellite data: A methodological study. Journal of Geophysical Research **114**: C03020

Fuhrman, J. A., I. Hewson, M. S. Schwalbach, J. A. Steele, M. V. Brown, and S. Naeem. 2006. Annually reoccurring bacterial communities are predictable from ocean conditions. Proceedings of the National Academy of Sciences of the United States of America **103**: 13104–9

Gregg, W. W., N. W. Casey, and C. R. McClain. Recent trends in global ocean chlorophyll. Geophysical research letters **32**: L03606.1–L03606.5.

Gasol, J. M., P. A. del Giorgio, and C. M. Duarte. 1997. Biomass Distribution in Marine Planktonic Communities. Limnology and Oceanography **42**: 1353–1363.

Ghil, M., and A. W. Robertson. 2001. Circulation Model Development, Elsevier.

Giovannoni, S. J., and K. L. Vergin. 2012. Seasonality in Ocean Microbial Communities . Science **335** : 671–676

Gleason, H. A. 1926. The Individualistic Concept of the Plant Association. Bulletin of the Torrey Botanical Club **53**: 7–26

Gomez-Pereira, P. R., B. M. Fuchs, C. Alonso, M. J. Oliver, J. E. E. van Beusekom, and R. Amann. 2010. Distinct flavobacterial communities in contrasting water masses of the North Atlantic Ocean. ISME J **4**: 472–487.

Gruber, N. 2011. Warming up, turning sour, losing breath: ocean biogeochemistry under global change. Philosophical transactions. Series A, Mathematical, physical, and engineering sciences **369**: 1980–96

Howard, E., S. Emerson, S. Bushinskey, and C. Stump. The role of net community production in air-sea carbon fluxes at the North Pacific subarctic-subtropical boundary region. Limnology and oceanography **55**: 2585–2596.

Hales, B., P. G. Strutton, M. Saraceno, R. Letelier, T. Takahashi, R. Feely, C. Sabine, and F. Chavez. 2012. Satellite-based prediction of pCO2 in coastal waters of the eastern North Pacific. Progress in Oceanography, **103**: 1-15

Hardman-Mountford, N. J., T. Hirata, K. A. Richardson, and J. Aiken. 2008. An objective methodology for the classification of ecological pattern into biomes and provinces for the pelagic ocean. Remote Sensing of Environment **112**: 3341–3352.

Hare, S. R., S. Minobe, W. S. Wooster, and S. McKinnell. 2000. An introduction to the PICES symposium on the nature and impacts of North Pacific climate regime shifts. Progress In Oceanography **47**: 99–102

Harrison, P. 2002. Station Papa Time Series: Insights into Ecosystem Dynamics. Journal of Oceanography **58**: 259–264

Hebel, D. V., and D. M. Karl. 2001. Seasonal, interannual and decadal variations in particulate matter concentrations and composition in the subtropical North Pacific Ocean. Deep Sea Research Part II: Topical Studies in Oceanography **48**: 1669–1695

Hill, P., J. Heywood, R. Holland, D. Purdie, B. Fuchs, and M. Zubkov. 2012. Internal and External Influences on Near-Surface Microbial Community Structure in the Vicinity of the Cape Verde Islands. Microbial Ecology **63**: 139–148

Hooker, S. B., N. W. Rees, and J. Aiken. 2000. An objective methodology for identifying oceanic provinces. Progress In Oceanography **45**: 313–338

Hsieh, C., S. M. Glaser, A. J. Lucas, and G. Sugihara. 2005. Distinguishing random environmental fluctuations from ecological catastrophes for the North Pacific Ocean. Nature **435**: 336–340.

Huisman, J., N. N. Pham Thi, D. M. Karl, and B. Sommeijer. 2006. Reduced mixing generates oscillations and chaos in the oceanic deep chlorophyll maximum. Nature **439**: 322–325.

Huisman, J., and F. J. Weissing. 1999. Biodiversity of plankton by species oscillations and chaos. Nature **402**: 407–410.

Jain, A. K., R. C. Dubes, and C. C. Chen. 1987. Bootstrap techniques for error estimation. IEEE Transactions on Pattern Analysis and Machine Intelligence **9**: 628–633

Jassby, A. D., and T. Platt. 1976. Mathematical Formulation of the Relationship Between Photosynthesis and Light for Phytoplankton. Limnology and Oceanography **21**: 540–547.

Ji, R., M. Edwards, D. L. Mackas, J. A. Runge, and A. C. Thomas. 2010. Marine plankton phenology and life history in a changing climate: current research and future directions. Journal of plankton research **32**: 1355–1368

Juranek, L. W., P. D. Quay, R. A. Feely, D. Lockwood, D. M. Karl, and M. J. Church. 2012. Biological production in the NE Pacific and its influence on air-sea CO2 flux: Evidence from dissolved oxygen isotopes and O2/Ar. J. Geophys. Res. **117**: C05022

Karl, D. M. 1999. A sea of change: Biogeochemical variability in the North Pacific subtropical gyre. Ecosystems, 2(3), 181-214

Karl, D. M., R. R. Bidigare, and R. M. Letelier. 2001. Long-term changes in plankton community structure and productivity in the North Pacific Subtropical Gyre: The domain shift hypothesis. Deep Sea Research Part II: Topical Studies in Oceanography **48**: 1449–1470.

Karl, D. M., M. J. Church, J. E. Dore, R. M. Letelier, and C. Mahaffey. 2012. Predictable and efficient carbon sequestration in the North Pacific Ocean supported by symbiotic nitrogen fixation. Proceedings of the National Academy of Sciences of the United States of America **109**: 1842–9

Karl, D. M. and R. M. Letelier. 2009. Seascape microbial ecology: Habitat structure, biodiversity and ecosystem function. In: S. A. Levin (Ed.), Guide to Ecology, Princeton University Press, Princeton, New Jersey, pp. 488–500

Karl, D. M., R. Letelier, D. Hebel, L. Tupas, J. Dore, J. Christian, and C. Winn. 1995. Ecosystem changes in the North Pacific subtropical gyre attributed to the 1991-92 El Nino. Nature **373**: 230–234.

Karl, D. M., and R. Lukas. 1996. The Hawaii Ocean Time-series (HOT) program: Background, rationale and field implementation. Deep Sea Research Part II: Topical Studies in Oceanography **43**: 129–156

Kolber, Z. S., O. Prášil, and P. G. Falkowski. 1998. Measurements of variable chlorophyll fluorescence using fast repetition rate techniques: defining methodology and experimental protocols. Biochimica et Biophysica Acta (BBA) - Bioenergetics **1367**: 88–106

Kotliar, N. B., and J. A. Wiens. 1990. Multiple Scales of Patchiness and Patch Structure: A Hierarchical Framework for the Study of Heterogeneity. Oikos **59**: 253–260.

De La Rocha, C. L., and U. Passow. 2007. Factors influencing the sinking of POC and the efficiency of the biological carbon pump. Deep Sea Research Part II: Topical Studies in Oceanography **54**: 639–658

Lachkar, Z., and N. Gruber. 2012. A comparative study of biological production in eastern boundary upwelling systems using an artificial neural network. Biogeosciences **9**: 293–308

Langmann, B., K. Zakšek, M. Hort, and S. Duggen. 2010. Volcanic ash as fertiliser for the surface ocean.2010 Atmospheric Chemistry and Physics **10.8**: 3891-3899

Laws, E. A., P. G. Falkowski, W. O. Smith Jr., H. Ducklow, and J. J. McCarthy. 2000. Temperature effects on export production in the open ocean. Global Biogeochem. Cycles **14**: 1231–1246

Lee, S., and J. A. Fuhrman. 1987. Relationships between Biovolume and Biomass of Naturally Derived Marine Bacterioplankton. Appl. Envir. Microbiol. **53**: 1298–1303.

Legendre, L. 2002. Fluxes of carbon in the upper ocean: regulation by food-web control nodes . Marine Ecology Progress Series **242**: 95–109.

Leibold, M. A., M. Holyoak, N. Mouquet, P. Amarasekare, J. M. Chase, M. F. Hoopes, R. D. Holt, J. B. Shurin, R. Law, D. Tilman, M. Loreau, and A. Gonzalez. 2004. The metacommunity concept: a framework for multi-scale community ecology. Ecology Letters **7**: 601–613

Leibold, M. A., and J. Norberg. 2004. Biodiversity in Metacommunities: Plankton as Complex Adaptive Systems? Limnology and Oceanography **49**: 1278–1289.

Letelier, R. M., D. M. Karl, M. R. Abbott, P. Flament, M. Freilich, R. Lukas, and T. Strub. 2000. Role of late winter mesoscale events in the biogeochemical variability of the upper water column of the North Pacific Subtropical Gyre. Journal of Geophysical Research **105**: 28723–28739

Levin, S. A. 1974. Dispersion and Population Interactions. The American Naturalist **108**: 207

Levin, S. A. 1976. Population dynamic models in heterogeneous environments. Annual Review of Ecology and Systematics **7**: 287–310

Levin, S. A., and J. Lubchenco. 2008. Resilience, robustness, and marine ecosystem-based management. Bioscience **58**: 27–32 ST

Levin, S. A., and R. T. Paine. 1974. Disturbance, patch formation, and community structure. Proceedings of the National Academy of Sciences of the United States of America **71**: 2744–2747

Levin, S. A., and M. Whitfield. 1994. Patchiness in Marine and Terrestrial Systems: From Individuals to Populations [and Discussion]. Philosophical Transactions of the Royal Society B: Biological Sciences **343**: 99–103

Li, W. K. W. 2009. From cytometry to macroecology: a quarter century quest in microbial oceanography. Aquatic Microbial Ecology **57**: 239–251 ST – From cytometry to macroecology: a qu

Li, W. K. W., W. G. Harrison, and E. J. H. Head. 2006. Coherent assembly of phytoplankton communities in diverse temperate ocean ecosystems. Proceedings. Biological sciences / The Royal Society **273**: 1953–60

Lidicker, W. Z. 2008. Levels of organization in biology: on the nature and nomenclature of ecology's fourth level. Biological Reviews **83**: 71–78 ST

Litzow, M. A., and L. Ciannelli. 2007. Oscillating trophic control induces community reorganization in a marine ecosystem. Ecology Letters **10**: 1124–1134

Liu, J. W., M. G. Weinbauer, C. Maier, M. H. Dai, and J. P. Gattuso. 2010. Effect of ocean acidification on microbial diversity and on microbe-driven biogeochemistry and ecosystem functioning. Aquatic Microbial Ecology **61**: 291–305

Lomas, M. W., D. K. Steinberg, T. Dickey, C. A. Carlson, N. B. Nelson, R. H. Condon, and N. R. Bates. 2010. Increased ocean carbon export in the Sargasso Sea linked to climate variability is countered by its enhanced mesopelagic attenuation. Biogeosciences **7**: 57–70 ST – Increased ocean carbon export in the S.

Longhurst, A. R. 2007. Ecological Geography of the Sea (Google eBook), Academic Press.

Longhurst, A., S. Sathyendranath, T. Platt, and C. Caverhill. 1995. An estimate of global primary production in the ocean from satellite radiometer data. Journal of Plankton Research **17**: 1245–1271

Lopez-Urrutia, A., E. San Martin, R. P. Harris, and X. Irigoien. 2006. Scaling the metabolic balance of the oceans. Proceedings of the National Academy of Sciences of the United States of America **103**: 8739–8744

Di Lorenzo, E., N. Schneider, K. M. Cobb, P. J. S. Franks, K. Chhak, A. J. Miller, J. C. McWilliams, S. J. Bograd, H. Arango, E. Curchitser, T. M. Powell, and P. Rivi&#xfffd;re. 2008. North Pacific Gyre Oscillation links ocean climate and ecosystem change. Geophys. Res. Lett. **35**: L08607

Lubchenco, J., and L. E. Petes. 2010. The Interconnected Biosphere: Science at the Ocean's Tipping Points. Oceanography **23**: 115–129

Lukas, R., and F. Santiago-Mandujano. 2008. Interannual to Interdecadal Salinity Variations Observed Near Hawaii: Local and Remote Forcing by Surface Freshwater Fluxes. Oceanography **21**: 46–55 ST

Maarel, E. 1990a. Ecotones and ecoclines are different. Journal of Vegetation Science **1**: 135–138

Maarel, E. van der. 1990b. Ecotones and Ecoclines Are Different. Journal of Vegetation Science **1**: 135–138

MacFayden, A. 1984. Advances in Ecological Research, Volume 14 (Google eBook), Academic Press.

MacIntyre, H. L., T. M. Kana, T. Anning, and R. J. Geider. 2002. Photoacclimation of photosynthesis irradiance response curves and photosynthetic pigments in microalgae and cyanobacteria. Journal of Phycology **38**: 17–38

Mahowald, N. M., S. Engelstaedter, C. Luo, A. Sealy, P. Artaxo, C. Benitez-Nelson, S. Bonnet, Y. Chen, P. Y. Chuang, D. D. Cohen, F. Dulac, B. Herut, A. M. Johansen, N. Kubilay, R. Losno, W. Maenhaut, A. Paytan, J. A. Prospero, L. M. Shank, and R. L. Siefert. 2009. Atmospheric Iron Deposition: Global Distribution, Variability, and Human Perturbations. Annual Review of Marine Science 1:245–278

Maldonado, M. T., P. W. Boyd, P. J. Harrison, and N. M. Price. 1999. Co-limitation of phytoplankton growth by light and Fe during winter in the NE subarctic Pacific Ocean. Deep-Sea Research Part Ii-Topical Studies in Oceanography **46**: 2475–2485

Malfatti, F., and F. Azam. 2009. Atomic force microscopy reveals microscale networks and possible symbioses among pelagic marine bacteria. Aquatic Microbial Ecology **58**: 1–14

Mantua, N. J., S. R. Hare, Y. Zhang, J. M. Wallace, and R. C. Francis. 1997. A Pacific interdecadal climate oscillation with impacts on salmon production. Bulletin of the American Meteorological Society **78**: 1069–1079

Margalef, R. 1978. Life-forms of phytoplankton as survival alternatives in an unstable environment. Oceanologica Acta **1**: 493–509 ST

Martiny, J. B. H., B. J. M. Bohannan, J. H. Brown, R. K. Colwell, J. A. Fuhrman, J. L. Green, M. C. Horner-Devine, M. Kane, J. A. Krumins, C. R. Kuske, P. J. Morin, S. Naeem, L. Ovreas, A. L. Reysenbach, V. H. Smith, and J. T. Staley. 2006. Microbial biogeography: putting microorganisms on the map. Nature Reviews Microbiology **4**: 102–112

McGarigal, K., S. Tagil, and S. A. Cushman. 2009. Surface metrics: an alternative to patch metrics for the quantification of landscape structure. Landscape Ecology **24**: 433–450

Miller, C. B., B. W. Frost, P. A. Wheeler, M. R. Landry, N. Welschmeyer, and T. M. Powell. 1991. Ecological dynamics in the subarctic Pacific, a possibly iron-limited ecosystem. Limnology and Oceanography **36**: 1600–1615

Mitchell, J. G., and L. Seuront. 2008. Towards a seascape topology II: Zipf analysis of one-dimensional patterns. Journal of Marine Systems **69**: 328–338

Mitchell, J. G., H. Yamazaki, L. Seuront, F. Wolk, and H. Li. 2008. Phytoplankton patch patterns: Seascape anatomy in a turbulent ocean. Journal of Marine Systems **69**: 247–253

Moisander, P. H., R. A. Beinart, I. Hewson, A. E. White, K. S. Johnson, C. A. Carlson, J. P. Montoya, and J. P. Zehr. 2010. Unicellular Cyanobacterial Distributions Broaden the Oceanic N-2 Fixation Domain. Science **327**: 1512–1514

Monahan, A. H., and K. L. Denman. 2004. Impacts of atmospheric variability on a coupled upper-ocean/ecosystem model of the subarctic Northeast Pacific. Global Biogeochemical Cycles **18**

Moore, C. M., S. Seeyave, A. E. Hickman, J. T. Allen, M. I. Lucas, H. Planquette, R. T. Pollard, and A. J. Poulton. 2007. Iron-light interactions during the CROZet natural iron bloom and EXport experiment (CROZEX) I: Phytoplankton growth and photophysiology. Deep-Sea Research Part Ii-Topical Studies in Oceanography **54**: 2045–2065

Moore, J. K., S. C. Doney, and K. C.-G. Lindsay. 2004. Upper ocean ecosystem dynamics and iron cycling in a global three-dimensional model. Global Biogeochemical Cycles **18 :** 4028.

Mouquet, N., T. E. Miller, T. Daufresne, and J. M. Kneitel. 2006. Consequences of varying regional heterogeneity in source-sink metacommunities. Oikos **113**: 481–488.

Mulholland, M. R., S. Floge, E. J. Carpenter, and D. G. Capone. 2002. Phosphorus dynamics in cultures and natural populations of Trichodesmium spp. Marine Ecology-Progress Series **239**: 45–55

Murawski, S. A., J. H. Steele, P. Taylor, M. J. Fogarty, M. P. Sissenwine, M. Ford, and C. Suchman. 2010. Why compare marine ecosystems? Ices Journal of Marine Science **67**: 1–9

Oliver, M. J., and A. J. Irwin. 2008. Objective global ocean biogeographic provinces. Geophysical Research Letters **35** 15 (2008): L15601.

O'Neill, R. V., R. H. Gardner, and M. G. Turner. 1992. A hierarchical neutral model for landscape analysis. Landscape Ecology **7**: 55–61

Partensky, F., Blanchot, J., & Vaulot, D. (1999). Differential distribution and ecology of Prochlorococcus and Synechococcus in oceanic waters: a review. Bulletin de l'Institut océanographique, Monaco Special 457-476

Pauly, D., R. Watson, and J. Alder. 2005. Global trends in world fisheries: impacts on marine ecosystems and food security. Philosophical Transactions of the Royal Society B-Biological Sciences **360**: 5–12

Platt, T., and S. Sathyendranath. 1999. Spatial structure of pelagic ecosystem processes in the global ocean. Ecosystems **2**: 384–394 .

Platt, T., and S. Sathyendranath. 2008. Ecological indicators for the pelagic zone of the ocean from remote sensing. Remote Sensing of Environment **112**: 3426–3436

Platt, T., S. Sathyendranath, M. H. Forget, G. N. White, C. Caverhill, H. Bouman, E. Devred, and S. Son. 2008. Operational estimation of primary production at large geographical scales. Remote Sensing of Environment **112**: 3437–3448

Polovina, J. J., J. P. Dunne, P. A. Woodworth, and E. A. Howell. Projected expansion of the subtropical biome and contraction of the temperate and equatorial upwelling biomes in the North Pacific under global warming. ICES Journal of Marine Science: Journal du Conseil 68.6: 986-995

Polovina, J. J., E. A. Howell, and M. Abecassis. 2008. Ocean's least productive waters are expanding. Geophysical Research Letters **35**

Polovina, J. J., E. Howell, D. R. Kobayashi, and M. P. Seki. 2001. The transition zone chlorophyll front, a dynamic global feature defining migration and forage habitat for marine resources. Progress in Oceanography **49**: 469–483

Polovina, J. J., G. T. Mitchum, and G. T. Evans. 1995. Decadal and basin-scale variation in mixed layer depth and the impact on biological production in the Central and North Pacific, 1960-88. Deep-Sea Research Part I-Oceanographic Research Papers **42**: 1701–1716

Polovina, J., I. Uchida, G. Balazs, E. A. Howell, D. Parker, and P. Dutton. 2006. The Kuroshio Extension Bifurcation Region: A pelagic hotspot for juvenile loggerhead sea turtles. Deep-Sea Research Part Ii-Topical Studies in Oceanography **53**: 326–339

Ptacnik, R., A. G. Solimini, T. Andersen, T. Tamminen, P. Brettum, L. Lepisto, E. Willen, and S. Rekolainen. 2008. Diversity predicts stability and resource use efficiency in natural phytoplankton communities. Proceedings of the National Academy of Sciences of the United States of America **105**: 5134–5138

Reuer, M. K., B. A. Barnett, M. L. Bender, P. G. Falkowski, and M. B. Hendricks. 2007. New estimates of Southern Ocean biological production rates from O2/Ar ratios and the triple isotope composition of O2. Deep Sea Research Part I: Oceanographic Research Papers **54**: 951–974

Ribalet, F., A. Marchetti, K. A. Hubbard, K. Brown, C. A. Durkin, R. Morales, M. Robert, J. E. Swalwell, P. D. Tortell, and E. V. Armbrust. 2010. Unveiling a phytoplankton hotspot at a narrow boundary between coastal and offshore waters. Proceedings of the National Academy of Sciences of the United States of America **107**: 16571–16576

Richardson, A. ., C. Risien, and F. . Shillington. 2003. Using self-organizing maps to identify patterns in satellite imagery. Progress In Oceanography **59**: 223–239

Richardson, T. L., and G. A. Jackson. 2007. Small phytoplankton and carbon export from the surface ocean. Science **315**: 838–840

Ross, on, R. Geider, E. Berdalet, M. Artigas, and J. Piera. 2011a. Modelling the effect of vertical mixing on bottle incubations for determining in situ phytoplankton dynamics. I. Growth rates. Marine Ecology Progress Series **435**: 13–31

Ross, O. N., and R. J. Geider. 2009. New cell-based model of photosynthesis and photo-acclimation: accumulation and mobilisation of energy reserves in phytoplankton. Marine Ecology-Progress Series **383**: 53–71 ST – New cell–based model of photosynthesis

Ross, O. N., R. J. Geider, and J. Piera. 2011b. Modelling the effect of vertical mixing on bottle incubations for determining in situ phytoplankton dynamics. II. Primary production. Marine Ecology-Progress Series **435**: 33–45

Saba, V. S., M. A. M. Friedrichs, M.-E. Carr, D. Antoine, R. A. Armstrong, I. Asanuma, O. Aumont, N. R. Bates, M. J. Behrenfeld, V. Bennington, L. Bopp, J. Bruggeman, E. T. Buitenhuis, M. J. Church, A. M. Ciotti, S. C. Doney, M. Dowell, J. P. Dunne, S. Dutkiewicz, W. Gregg, N. Hoepffner, K. J. W. Hyde, J. Ishizaka, T. Kameda, D. M. Karl, I. D. Lima, M. W. Lomas, J. Marra, G. A. McKinley, F. Melin, J. K. Moore, A. Morel, J. O'Reilly, B. Salihoglu, M. Scardi, T. J. Smyth, S. Tang, J. Tjiputra, J. Uitz, M. Vichi, K. Waters, T. K. Westberry, and A. Yool. 2010. Challenges of modeling depth-integrated marine primary productivity over multiple decades : a case study at BATS and HOT.

Sakamoto, C. M. 2004. Influence of Rossby waves on nutrient dynamics and the plankton community structure in the North Pacific subtropical gyre. Journal of Geophysical Research **109**: C05032

Saraceno, M., C. Provost, and M. Lebbah. 2006. Biophysical regions identification using an artificial neuronal network: A case study in the South Western Atlantic. Advances in Space Research. **37**: 793–805

Sarmiento, J. L., R. Slater, R. Barber, L. Bopp, S. C. Doney, A. C. Hirst, J. Kleypas, R. Matear, U. Mikolajewicz, P. Monfray, V. Soldatov, S. A. Spall, and R. Stouffer. 2004. Response of ocean ecosystems to climate warming. Global Biogeochemical Cycles **18 (3) GB3003**

Schneider, S. H., and R. E. Dickinson. 1974. Climate modeling. Reviews of Geophysics **12**: 447 -493.

Schoch, G. C., B. A. Menge, G. Allison, M. Kavanaugh, S. A. Thompson, and S. A. Wood. 2006. Fifteen Degrees of Separation: Latitudinal Gradients of Rocky Intertidal Biota along the California Current. Limnology and Oceanography **51**: 2564–2585.

Serret, P., E. Fernandez, and C. Robinson. 2002. BIOGEOGRAPHIC DIFFERENCES IN THE NET ECOSYSTEM METABOLISM OF THE OPEN OCEAN. Ecology **83**: 3225–3234

Serret, P., E. Fernandez, C. Robinson, E. M. S. Woodward, and V. Perez. 2006. Local production does not control the balance between plankton photosynthesis and respiration in the open Atlantic Ocean. Deep-Sea Research Part Ii-Topical Studies in Oceanography **53**: 1611–1628

Serret, P., C. Robinson, E. Fernandez, E. Teira, and G. Tilstone. 2001. Latitudinal variation of the balance between plankton photosynthesis and respiration in the eastern Atlantic Ocean. Limnology and Oceanography **46**: 1642–1652

Sheridan, C. C., and M. R. Landry. 2004. A 9-year increasing trend in mesozooplankton biomass at the Hawaii Ocean Time-Series Station ALOHA. Ices Journal of Marine Science **61**: 457–463

Sherr, E. B., B. F. Sherr, and K. Longnecker. 2006. Distribution of bacterial abundance and cell-specific nucleic acid content in the Northeast Pacific Ocean. Deep Sea Research Part I: Oceanographic Research Papers **53**: 713–725

Sherr, E. B., B. F. Sherr, and P. A. Wheeler. 2005. Distribution of coccoid cyanobacteria and small eukaryotic phytoplankton in the upwelling ecosystem off the Oregon coast during 2001 and 2002. Deep Sea Research Part II: Topical Studies in Oceanography **52**: 317–330

Sherr, E. B., B. F. Sherr, P. A. Wheeler, and K. Thompson. 2003. Temporal and spatial variation in stocks of autotrophic and heterotrophic microbes in the upper water column of the central Arctic Ocean. Deep Sea Research Part I: Oceanographic Research Papers **50**: 557–571

Sherr, E., and B. Sherr. 1988. Role of Microbes in Pelagic Food Webs: A Revised Concept. Limnology and Oceanography **33**: 1225–1227

Siegel, D. A., T. K. Westberry, M. C. O'Brien, N. B. Nelson, A. F. Michaels, J. R. Morrison, A. Scott, E. A. Caporelli, J. C. Sorensen, S. Maritorena, S. A. Garver, E. A. Brody, J. Ubante, and M. A. Hammer. 2001. Bio-optical modeling of primary production on regional scales: the Bermuda BioOptics project. Deep-Sea Research Part Ii-Topical Studies in Oceanography **48**: 1865–1896

Siegenthaler, U., and J. L. Sarmiento. 1993. Atmospheric carbon dioxide and the ocean. Nature **365**: 119–125

Signorini, S. R., and C. R. McClain. 2012. Subtropical gyre variability as seen from satellites. Remote Sensing Letters **3**: 471–479

Somerville, M. 1850. Physical geography (Google eBook), Lea & Blanchard.

Steele, J. H. 1991. Can ecological theory cross the land-sea boundary? Journal of Theoretical Biology **153**: 425–436

Steele, J. H., and E. W. Henderson. 1992. A SIMPLE-MODEL FOR PLANKTON PATCHINESS. Journal of Plankton Research **14**: 1397–1403

Steinberg, D. K., M. W. Lomas, and J. S. Cope. 2012. Long-term increase in mesozooplankton biomass in the Sargasso Sea: Linkage to climate and implications for food web dynamics and biogeochemical cycling. Global Biogeochemical Cycles **26**: GB1004

Suggett, D. J., H. L. MacIntyre, T. M. Kana, and R. J. Geider. 2009a. Comparing electron transport with gas exchange: parameterising exchange rates between alternative photosynthetic currencies for eukaryotic phytoplankton. Aquatic Microbial Ecology **56**: 147–162

Suggett, D. J., C. M. Moore, A. E. Hickman, and R. J. Geider. 2009b. Interpretation of fast repetition rate (FRR) fluorescence: signatures of phytoplankton community structure versus physiological state. Marine Ecology-Progress Series **376**: 1–19

Suzuki, K., H. Liu, T. Saino, H. Obata, M. Takano, K. Okamura, Y. Sohrin, and Y. Fujishima. 2002. East-West Gradients in the Photosynthetic Potential of Phytoplankton and Iron Concentration in the Subarctic Pacific Ocean during Early Summer. Limnology and Oceanography **47**: 1581–1594.

Sverdrup, H. U. 1953. On Conditions for the Vernal Blooming of Phytoplankton. ICES Journal of Marine Science **18**: 287–295

Sverdrup, H. U., M. W. Johnson, and R. H. Fleming. 1942. The oceans, their physics, chemistry, and general biology. Vol. 1087. New York: Prentice-Hall

Takahashi, T., S. C. Sutherland, C. Sweeney, A. Poisson, N. Metzl, B. Tilbrook, N. Bates, R. Wanninkhof, R. A. Feely, C. Sabine, J. Olafsson, and Y. Nojiri. 2002. Global sea-air CO2 flux based on climatological surface ocean pCO(2), and seasonal biological and temperature effects. Deep-Sea Research Part Ii-Topical Studies in Oceanography **49**: 1601–1622 ST – Global sea–air CO2 flux based on c.

Takahashi, T., S. C. Sutherland, R. Wanninkhof, C. Sweeney, R. A. Feely, D. W. Chipman, B. Hales, G. Friederich, F. Chavez, C. Sabine, A. Watson, D. C. E. Bakker, U. Schuster, N. Metzl, H. Yoshikawa-Inoue, M. Ishii, T. Midorikawa, Y. Nojiri, A. Kortzinger, T. Steinhoff, M. Hoppema, J. Olafsson, T. S. Arnarson, B. Tilbrook, T. Johannessen, A. Olsen, R. Bellerby, C. S. Wong, B. Delille, N. R. Bates, and H. J. W. de Baar. 2009. Climatological mean and decadal change in surface ocean pCO(2), and net sea-air CO2 flux over the global oceans. Deep-Sea Research Part Ii-Topical Studies in Oceanography **56**: 554–577

Thierstein, H. R., & Young, J. R. (Eds.). (2004). Coccolithophores: from molecular processes to global impact. Springer.

Thyssen, M., G. A. Tarran, M. V. Zubkov, R. J. Holland, G. Gregori, P. H. Burkill, and M. Denis. 2007. The emergence of automated high-frequency flow cytometry: revealing temporal and spatial phytoplankton variability. Journal of Plankton Research **30**: 333–343

Tortell, P. D., and M. C. Long. 2009. Spatial and temporal variability of biogenic gases during the Southern Ocean spring bloom. Geophysical Research Letters **36** (**1), L01603**

Turner, M. G. 2005. Landscape ecology: What is the state of the science? Annual Review of Ecology Evolution and Systematics **36**: 319–344

Turner, M. G., R. H. Gardner, and R. V. O'Neill. 2001. Landscape Ecology in Theory and Practice: Pattern and Process (Google eBook), Springer.

Turner, W., S. Spector, N. Gardiner, M. Fladeland, E. Sterling, and M. Steininger. 2003. Remote sensing for biodiversity science and conservation. Trends in Ecology & Evolution **18**: 306–314

Uitz, J., H. Claustre, A. Morel, and S. B. Hooker. 2006. Vertical distribution of phytoplankton communities in open ocean: An assessment based on surface chlorophyll. Journal of Geophysical Research **111**

Venrick, E. L. 1974. The Distribution and Significance of Richelia intracellularis Schmidt in the North Pacific Central Gyre. Limnology and Oceanography **19**: 437–445.

Weber, T. S., and C. Deutsch. 2010. Ocean nutrient ratios governed by plankton biogeography. Nature **467**: 550–4

Werner, D. 1977. The Biology of Diatoms, University of California Press.

Westberry, T., M. J. Behrenfeld, D. A. Siegel, and E. Boss. 2008. Carbon-based primary productivity modeling with vertically resolved photoacclimation. Global Biogeochemical Cycles **22**: GB2024

White, A. E., Y. H. Spitz, and R. M. Letelier. 2007. What factors are driving summer phytoplankton blooms in the North Pacific Subtropical Gyre? Journal of Geophysical Research **112**: 1–11

Whitney, F. A., W. R. Crawford, and P. J. Harrison. 2005. Physical processes that enhance nutrient transport and primary productivity in the coastal and open ocean of the subarctic NE Pacific. Deep Sea Research Part II: Topical Studies in Oceanography **52**: 681–706

Whittaker, R. J., K. J. Willis, and R. Field. 2001. Scale and species richness: towards a general, hierarchical theory of species diversity. Journal of Biogeography **28**: 453–470

Wiens, J. A. 1976. Population Responses to Patchy Environments. Annual Review of Ecology and Systematics **7**: 81–120

Williams, P. J.le B., Bowers, C. M. Duarte, S. Agusti, P. A. del Giorgio, and Cole. 1999. Regional Carbon Imbalances in the Oceans. Science **284**: 1735b–1735

Wilson, C., and D. Adamec. 2001. Correlations between surface chlorophyll and sea surface height in the tropical Pacific during the 1997–1999 El Niño—Southern Oscillation event. Journal of Geophysical Research **106**: 31175–31188

Wilson, C., T. A. Villareal, N. Maximenko, S. J. Bograd, J. P. Montoya, and C. A. Schoenbaechler. 2008. Biological and physical forcings of late summer chlorophyll blooms at 30°N in the oligotrophic Pacific. Journal of Marine Systems **69**: 164–176

Winn, C., D. Hebel, R. Letelier, D. Bird, and D. Karl. 1990. Variability in biogeochemical fluxes in the oligotrophic central pacific: Results of the Hawaii Ocean Time-series Program. EOS, Transactions, American Geophysical Union; (United States) **71:2**.

Wu, J. 1999. Hierarchy and scaling: Extrapolating information along a scaling ladder.

Wu, J., and R. Hobbs. 2002. Key issues and research priorities in landscape ecology: An idiosyncratic synthesis. Landscape Ecology **17**: 355–365

Wu, J., and O. L. Loucks. 1995. From Balance of Nature to Hierarchical Patch Dynamics: A Paradigm Shift in Ecology. The Quarterly Review of Biology **70**: 439–466.

Yentsch, C. M., P. K. Horan, K. Muirhead, Q. Dortch, E. Haugen, L. Legendre, L. S. Murphy, M. J. Perry, D. A. Phinney, S. A. Pomponi, R. W. Spinrad, M. Wood, C. S. Yentsch, and B. J. Zahuranec. 1983. Flow Cytometry and Cell Sorting: A Technique for Analysis and Sorting of Aquatic Particles. Limnology and Oceanography **28**: 1275–1280

Zapata, M., S. W. Jeffrey, S. W. Wright, F. Rodríguez, and J. L. Garrido. 2004. Photosynthetic pigments in 37 species (65 strains) of Haptophyta: implications for oceanography and chemotaxonomy . Marine Ecology Progress Series **270**: 83–102.

Zhang, Y., J. M. Wallace, and D. S. Battisti. 1997. ENSO-like Interdecadal Variability: 1900–93. Journal of Climate **10**: 1004–1020

Zubkov, M. V., M. A. Sleigh, and P. H. Burkill. 2000. Assaying picoplankton distribution by flow cytometry of underway samples collected along a meridional transect across the Atlantic Ocean. Aquatic Microbial Ecology, **21(1),** 13-20.

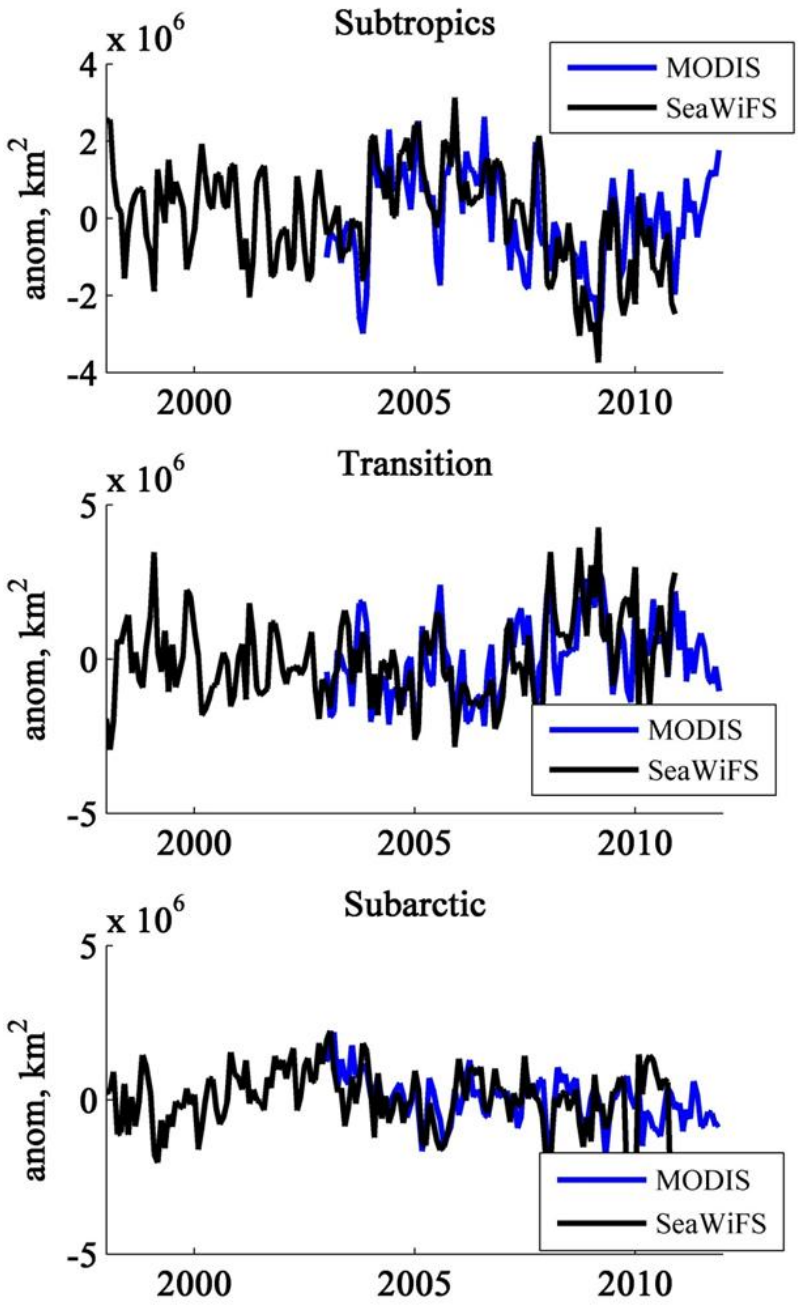

Figure A.1. Variation in interannual extents of seascapes determined from different satellite sensors. Blue: MODIS-Aqua sea surface temperature (SST), photosynthetically active radiation (PAR) and chl-a used to classify seascapes. Black: AVHRR SST, SeaWiFS PAR and SeaWiFS chl-a used to classify seascapes. SeaWiFS data record extended from 1998-2010; MODIS data recorded extends from 2002 through 2011.

Table A1. The chl-a and Fm' relationship across water masses with different assemblages: sensitivity, slope and skill. Local regression relationships were to interpolate chl-a based on dominant taxa in Chapter 5. Prokaryotic dominant waters were determined by the relative abundance of divinyl chl-a measured by high performance liquid chromatography (HPLC).

Scale	Method	Assemblage	Intercept (SE)	Slope (SE)	R^2
NE Pacific	HPLC	Mixed	0.0529 (0.014)	0.00049 (0.00003)	0.81
>42.5 °N	HPLC	Eukaryotic dominant	0.062 (0.047)	0.000536 (0.000067)	0.72
<42 °N	HPLC	Prokaryotic dominant	0.034(0.0048)	0.00093(0.00020)	0.43